Theses and Dissertations

May 2019

Anthropogenically Driven Changes to Shallow Groundwater in Southeastern Wisconsin and Its Effects on the Aquifer Microbial Communities

Madeline Jean Salo
University of Wisconsin-Milwaukee

ANTHROPOGENICALLY DRIVEN CHANGES TO SHALLOW GROUNDWATER IN

SOUTHEASTERN WISCONSIN AND ITS EFFECTS ON THE AQUIFER MICROBIAL

COMMUNITIES

by

Madeline J. Salo

A Thesis Submitted in

Partial Fulfillment of the

Requirements for the Degree of

Master of Science

in Geosciences

at

The University of Wisconsin-Milwaukee

May 2019

ABSTRACT
ANTHROPOGENICALLY DRIVEN CHANGES TO SHALLOW GROUNDWATER IN
SOUTHEASTERN WISCONSIN AND ITS EFFECTS ON THE AQUIFER

by

Madeline J. Salo

The University of Wisconsin-Milwaukee, 2019
Under the Supervision of Professor Timothy J. Grundl

This study investigates if, and to what extent, the microbial community present in the shallow groundwater of southeastern Wisconsin is affected by the influx of treated municipal wastewater effluent. The primary study area consisted of three wells located in the shallow sand and gravel aquifer along the upper Fox River in Waukesha, Wisconsin. One well is located roughly 1500 feet from the river and pumps pristine groundwater. Two riverbank inducement wells are located within 200 feet of the river and pump a mixture of groundwater and river water that contains effluent from three upstream wastewater treatment plants. Water from all three wells was analyzed for geochemical composition (major ions, nutrients, dissolved gases and dissolved organic carbon) and microbial community composition (16S rRNA gene composition, 16S rRNA activity and metagenomic sequencing). Geochemical and microbial community data were combined to identify thermodynamically feasible metabolic pathways capable of being carried out by the microbial consortia. Geochemical results show the riverbank inducement wells differ from the pristine well in thermodynamic capabilities. Microbial results show differences in the microbial consortia present in the pristine well and the riverbank inducement wells. Microbial community taxa identified with known subsurface microorganisms, recently discovered microorganisms from the CPR and DPANN superphyla, and unclassified unknown organisms.

To my cousin Parker Jack Haire,

(who would have never read this)

for giving me 21 years of memories that I will never forget.

I love you.

TABLE OF CONTENTS

LIST OF FIGURES

LIST OF TABLES

LIST OF EQUATIONS

LIST OF ABBREVIATIONS

$\Delta G°$	Gibbs free energy
$\Delta G°_f$	Standard free energy of formation
ΔG_r	Gibbs free energy of reaction
ASV	Amplicon sequence variants
ATP	Adenosine triphosphate
C	Concentration
CPR	Candidate phyla radiation
D_c	Diffusion coefficient
DNA	Deoxyribonucleic acid
DPANN phylum	Diapherotrites, Parvarchaeota, Aenigmarchaeota, Nanoarchaeota, Nanohaloarchaea
DOC	Dissolved organic carbon
EPA	Environmental Protection Agency
FEF	Free energy flux
ID	Identification
K_{eq}	Equilibrium constant
NA	Not analyzed
ND	Non-detect
Q	Reaction quotient
R	Universal gas constant
r	Radius of the microbial cell
RBI	Riverbank inducement
RNA	Ribonucleic acid
SRP	Spectrophotometer
T	Temperature
TDP	Total dissolved phosphorous
U	Enzyme unit, the amount of the enzyme that produces a certain amount of enzymatic activity or the amount that catalyzes the conversion of 1 micromole of substrate per minute
WDNR	Wisconsin Department of Natural Resources
WWTP	Wastewater treatment plant

LIST OF UNITS

°C	degree Celsius
°K	degree Kelvin
μL	Microliter
mL	Milliliter
L	Liter
μg	Microgram
mg/L	Milligram per liter
ppm	Parts per million
ppb	Parts per billion
μm	Micron
μmol	Micromole
μmol/L	Micromole per liter
pCi/L	Picocuries per liter
mEq/kg	Milliequivalents per kilogram
kJ mol^{-1}	Kilojoules per mole
J °K^{-1}mol^{-1}	joules per degree Kelvin per mole
kJ cell^{-1} s^{-1}	kilojoules per cell per second
U/μL	Enzyme unit per microliter

ACKNOWLEDGMENTS

First and foremost, I thank my advisor, Dr. Timothy Grundl, for challenging me and helping me build a strong knowledge base and set of skills professionally and academically. I also thank him for his enthusiasm, humor, and unwavering project commitment and support. I owe my success to him. I thank Patrick Anderson for his mentoring and assistance on water analyses and data interpretation at the School of Freshwater Sciences. I thank Ryan Newton and Natalie Gayner for their commitment and support to the microbial portion of this study. I thank my family and friends who tolerated my busy schedule and made the journey interesting and enjoyable. Lastly, I am forever grateful for the love and support from my partner, Zachary M. Richmond.

Chapter 1: Introduction

Groundwater is a significant source of drinking water in Wisconsin. Many communities in eastern Wisconsin rely on the deep aquifer, and the demand for water over time has made aquifer depletion a critical issue. Along with decreasing water levels, the deep aquifer also contains radium concentrations that exceed federal regulations. Shallow groundwater wells have been placed close to the Fox River to mitigate the issues described above. These wells are termed riverbank inducement (RBI) wells.

RBI wells create a more sustainable water supply because RBI wells induce water to flow from the river to the aquifer. The aquifer's recharge is augmented, and it lessens the extent of drawdown. The shallow groundwater also does not contain dissolved radium like the deep aquifer. In addition, water is recycled locally when RBI wells are located downstream of wastewater treatment plants (WWTP). The treated water being discharged from the WWTP originated from the RBI wells, and some of it will be pulled back toward the same RBI wells once it travels downstream, which increases sustainability. However, the close interaction between groundwater and surface water bodies has potential negative effects on the previously pristine aquifer.

An existing monitoring network is located in southeastern Wisconsin. The monitoring network has been studied long-term and an extensive geochemical database has been created and maintained since 2005. The primary study area in the monitoring network is a RBI well field located in the city of Waukesha, Wisconsin. Two RBI wells are located within 200 feet of the river and pump a mixture of groundwater and river water that contains effluent from three upstream WWTPs. A third well is located roughly 1500 feet from the river and pumps pristine groundwater. The Wisconsin Department of

Natural Resources (WDNR) unique well numbers for the RBI wells are RL255 and RL256, and the unique well number for the pristine well is WK947; the common names for the wells are Well 11, Well 12, and Well 13, respectively.

The previously pristine aquifer is now being impacted through the mixing of previously pristine groundwater with river water due to the RBI wells. Microorganisms are native to deep subsurface ecosystems, and it is known that they drive most geochemical reactions within aquifers. This study investigates if, and to what extent, the microbial community present in the shallow groundwater of southeastern Wisconsin is affected by the influx of treated municipal wastewater effluent. The information collected in this study will combine geochemical and microbial community data in groundwater and shed light on how microbial communities behave in impacted aquifers.

1.1 History of the City of Waukesha

Many communities in southeastern Wisconsin and northeastern Illinois tap into the deep sandstone aquifer. Because of the many communities relying on the aquifer, and slow recharge rates in certain areas, long-term data shows that the aquifer is being depleted. In Waukesha County, a thick shale layer limits recharge from getting into the aquifer, and by the mid-2000s groundwater heads in Waukesha had dropped by 450 feet (Gaumnitz et al., 2004). By 2006, the deepest cone of depression in the region lay under the city of Waukesha, Wisconsin (Cape and Grundl, 2006).

Furthermore, many communities relying on the deep aquifer must treat the water due to radium concentrations exceeding federal regulations. The U.S. Environmental Protection Agency (EPA) has set a limit of 5 picocuries per liter (pCi/L) and in 2006, radium concentrations three times the EPA limit were reported in 42 communities that

use the deep aquifer (McCoy, 2016). Because of aquifer depletion and radium contamination, Waukesha city officials decided the deep aquifer was no longer a sustainable resource. Waukesha applied for a diversion under the Great Lakes Compact to switch their water supply from the deep aquifer to Lake Michigan. The diversion was approved in June 2016, and it is expected that Waukesha will change its water supply within the next few years.

In the meantime, the city is utilizing the shallow groundwater wells, or RBI wells, to mitigate aquifer depletion and radium contamination. The RBI wells in Waukesha are located close to the Fox River to augment aquifer recharge by inducing water to flow from the river to the aquifer and lessen drawdown. Furthermore, radium contamination is being addressed through the mixing of radium-free shallow groundwater with radium-tainted water from the deep aquifer. Waukesha Water Utility is also removing radium by hydrous manganese oxide treatment (Waukesha Water Utility, 2014).

Chapter 2: Setting

2.1 Study Area

The Fox River watershed is expansive; the watershed spans southeastern Wisconsin and northeastern Illinois totaling 2,658 square miles (Figure 1). The headwaters of the Fox River watershed are in Colgate, Wisconsin, near Waukesha, and its confluence with the Illinois River is located in Ottawa, Illinois. The Fox River itself is 223 miles long and 32 WWTPs discharge into the river. The portion of the watershed residing in Wisconsin is termed the Upper Fox River watershed and accounts for 938 square miles of the total area.

The topography of the main study in Waukesha, Wisconsin is primarily composed of glacial features. The Wisconsin Glaciation is the most recent period of the Ice Age, which ended approximately 10,000 years ago. Near the end of the Wisconsin Glaciation, glacial till and glacial outwash sediments were deposited and various glacial features such as moraines, drumlins, kames, and outwash plains characterize the period. A series of ridges were formed in what is known today as southeastern Wisconsin from two ice lobes, and today the ridges create a gently rolling landscape. Depressions formed by large chunks of melting ice are also located among the ridges. In Waukesha County, elevation ranges from 700 to 900 feet above mean sea level.
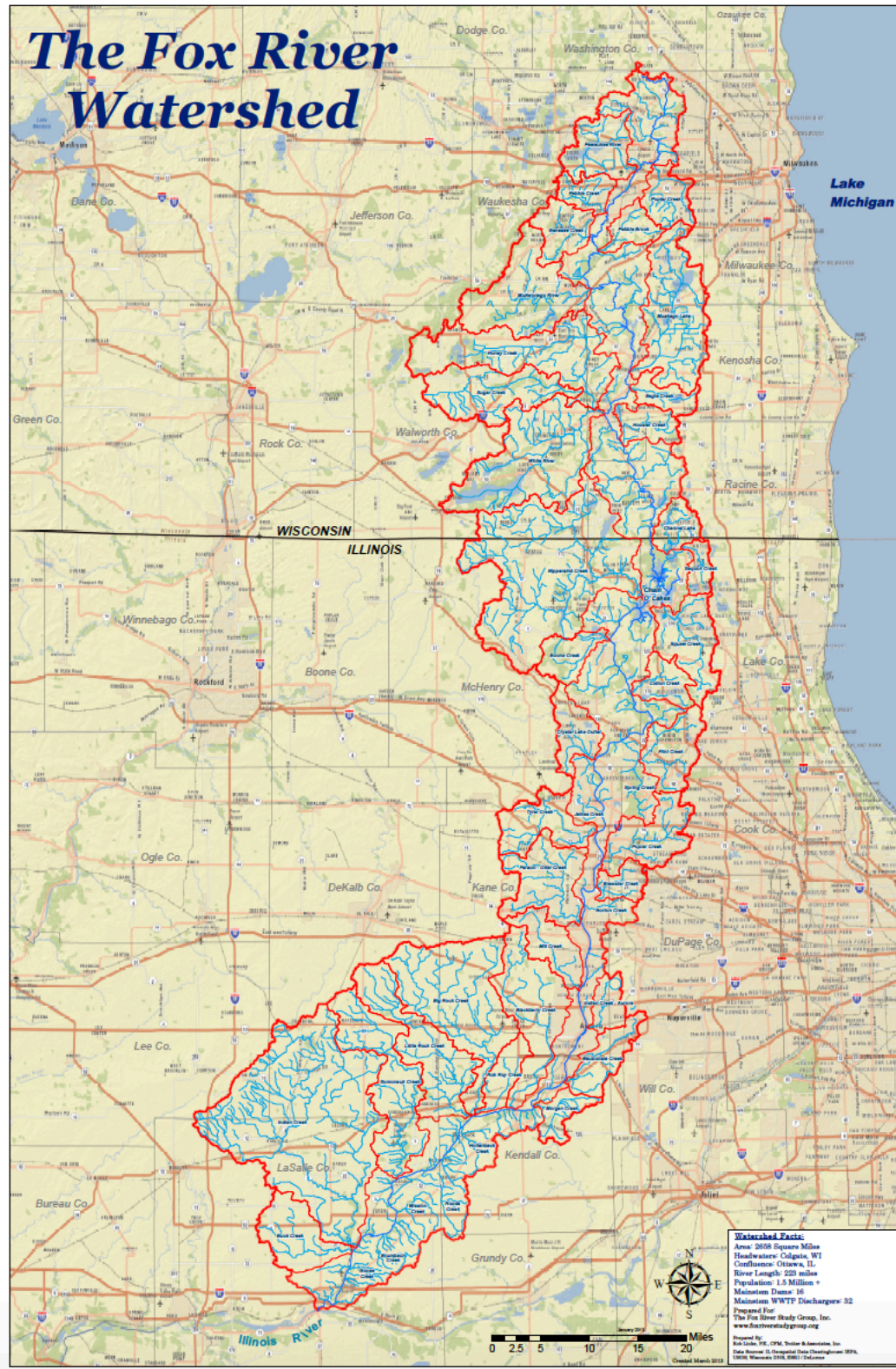
Figure 1. Map of the Fox River Watershed (Fox River Study Group, Inc. 2018).

2.2 Climate and Precipitation

The National Oceanic and Atmospheric Administration National Climatic Data Center reports an average annual temperature of 6.94°Celsius and an average annual precipitation of 0.84 meters for Waukesha WI Station USC00478937 between 2002 and 2013. Most of the precipitation occurs in the summer and the least amount of precipitation occurs in the winter.

2.3 Regional Geology

Waukesha County is situated east of the Wisconsin Arch in the Michigan Basin. Preglacial and glacial erosion shaped bedrock topography in the County. Bedrock dips eastward at a rate of approximately 10 feet per mile. From bottom to top, the bedrock units generally consist of Precambrian igneous and metamorphic rocks; Cambrian sandstone, Ordovician dolomite, sandstone, and shale; and Silurian dolomite (Waukeshacounty.gov). Throughout most of the County, the uppermost bedrock unit is composed of Silurian deposits that overlays an impervious layer of Maquoketa shale.

2.4 Hydrostratigraphy

The hydrostratigraphy of the Waukesha County consists of several units that influence flow and chemical dynamics of groundwater in southeastern Wisconsin. Regional hydrostratigraphy is shown in Figure 2 and the following information is based on Klump et al. (2008). The deep aquifer is composed of Cambrian and Ordovician deposits underlying the Sinnippee Group and Maquoketa Formation. The Cambrian and Ordovician deposits form the Cambrian-Ordovician Aquifer System and it underlies the Maquoketa Aquitard. The units act together as a regional confining aquitard and that has vertical hydraulic conductivities 1.5×10^{-6} m/d. A shallow, unconfined aquifer overlay the

regional aquitard and it is composed of dolomite from the Silurian and Devonian Periods

with a layer of glacial deposits from the Pleistocene Era. These units form the Quaternary

and Silurian Aquifers. All the bedrock units thicken and dip eastward, and confined

conditions are present in the deep aquifer creating lateral groundwater flow toward Lake

Michigan. The Maquoketa Aquitard thins westward where its confining capability

diminishes. West of the Maquoketa Formation boundary, the Sinnippee Group no longer

acts as an aquitard because the bedrock unit has been highly weathered. Because of this,

the shallow sandstone aquifer and the deep aquifer are hydraulically connected, and

recharge occurs exclusively in this area (Figure 3).

Stratigraphic Nomenclature		Hydraulic conductivity Kh(m/d)	Lithology and Generalized Hydrostratigraphy	
Group	Formation			
Quaternary	(undifferentiated)	0.06–3.0		Quaternary and Silurian Aquifers: sand and gravel, till, dolomite
Devonian	(undifferentiated)	9		
Silurian	(undifferentiated)	0.3–1.2		
	Maquoketa	9×10^{-5}–0.09		Maquoketa Aquitard: shale and dolomite
Sinnippee	Galena	0.012–0.09		
	Platteville			
Ancell	Glenwood	0.36–1.8		Cambrian-Ordovician Aquifer System: sandstone and dolomite with interbedded shale and siltstone (leaky aquitards)
	St. Peter			
Prarie du Chien	(undifferentiated)			
Trempeleau	Jordan	0.07–0.7		
	St. Lawrence			
Tunnel City	(undifferentiated)			
Elk Mound	Wonewoc	0.7–2.6		
	Eau Claire	0.18–1.1		
	Mt Simon	0.36–1.8		
Precambrian	impermeable			Precambrian: igneous and metamorphic

Figure 2. Generalized hydrostratigraphic column for southeast Wisconsin (Klump et al., 2008).
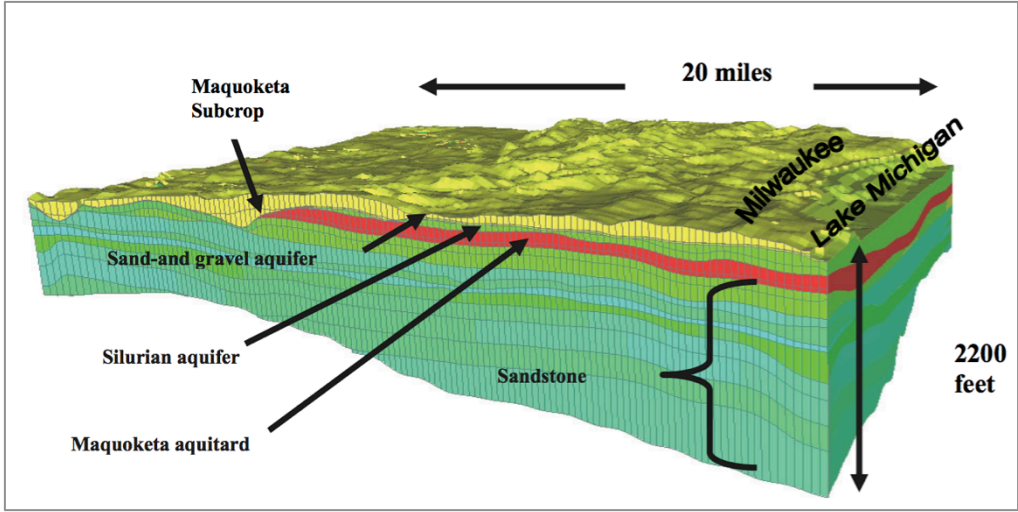
Figure 3. Cross section showing general hydrogeology of southeast Wisconsin (Waukeshacounty.gov).

Chapter 3: Study Parameters

Physical parameters included alkalinity, pH, specific conductivity, and temperature. Geochemical parameters included dissolved gases, dissolved organic carbon (DOC), major ions, and nutrients. Microbial parameters included 16S rRNA gene community composition, 16S rRNA activity, and metagenomic sequencing. Ribosomal RNA (rRNA) mediates protein synthesis as part of the ribosome. Throughout evolutionary history, rRNA has remained highly conserved and it is found in all known living organisms. In microorganisms, there are variable regions specific to different taxa within the conserved regions of the rRNA gene, making it a good molecular marker to target and identify phylogeny and taxonomy. The hypervariable v4 region was targeted in this study to capture both archaeal and bacterial microorganisms (Parada, Needham, and Fuhrman, 2016; Walters et al., 2016). Microbial community composition data indicated which microorganisms were present in the shallow groundwater wells and in what abundance. The data essentially indicates "who" was there, "who" contributed to the activity of the system, and how environmental conditions impacted community structure. Community compositions were determined using microbial 16S rRNA gene sequencing. 16S rRNA activity data indicated "who" was active and in what ratio to 16S genetic abundance, while metagenomic sequencing indicated the genetic potential.

Chapter 4: Previous Research

4.1 Previous Fox River Studies

Previous studies have been conducted on the monitoring network used in this study, and geochemistry data has been collected at each site in the monitoring network for over a decade. Thorp (2013) used the monitoring network to investigate the occurrence of Fox River water entering Well 11 and Well 12 through geochemical analysis, quantified the extent of anthropogenic influence on the aquifer using geochemical modeling, and discriminated between sources of contamination using trace element and stable isotope analysis. Most recently, Fields-Sommers (2015) used the monitoring network to define recharge mechanisms of induced water from the Fox River coming into the RBI wells through hydrogen and oxygen isotopes, as well as geochemical tracers to locate the source of salt influx in the RBI wells, she also continued the overall geochemistry tracking of the monitoring network to maintain a long-term database.

Thorp (2013) predicted major ions would level off after an initial breakthrough; however, major ion analysis from Fields-Sommers (2015) showed that sodium and chloride levels in both RBI wells continued rising (Figures 4 and 5). A stepwise increase was especially visible in Well 11. Feinstein et al. (2010) successfully predicted the first rise would occur with an increase in pumpage, because of more water being induced to flow towards the RBI wells. Approximately four years after the RBI wells became operational, the pumpage dropped and the first plateau occurred. A second rise occurred as pumpage increased again, approximately six to ten years after the RBI wells became operational. The sodium and chloride concentrations leveled off in a second plateau in

early 2014 due to a decrease in pumpage. The overall trend of sodium and chloride in both RBI wells is influenced heavily by the amount of pumpage, indicating anthropogenic activities in the form of WWTP effluent are affecting the wells.
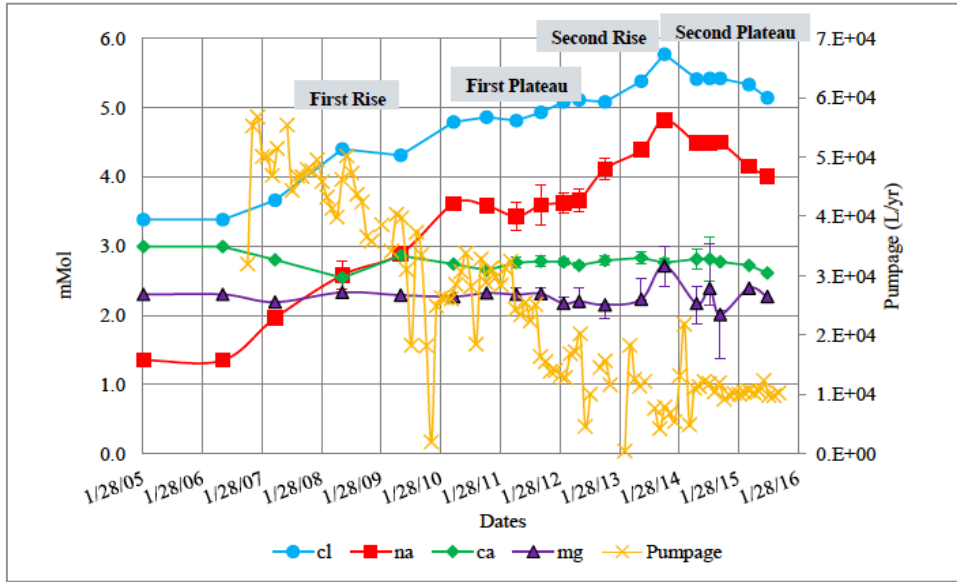
Figure 4. Major ion chemistry in Well 11 from 2005 through 2015 (Fields-Sommers, 2015).
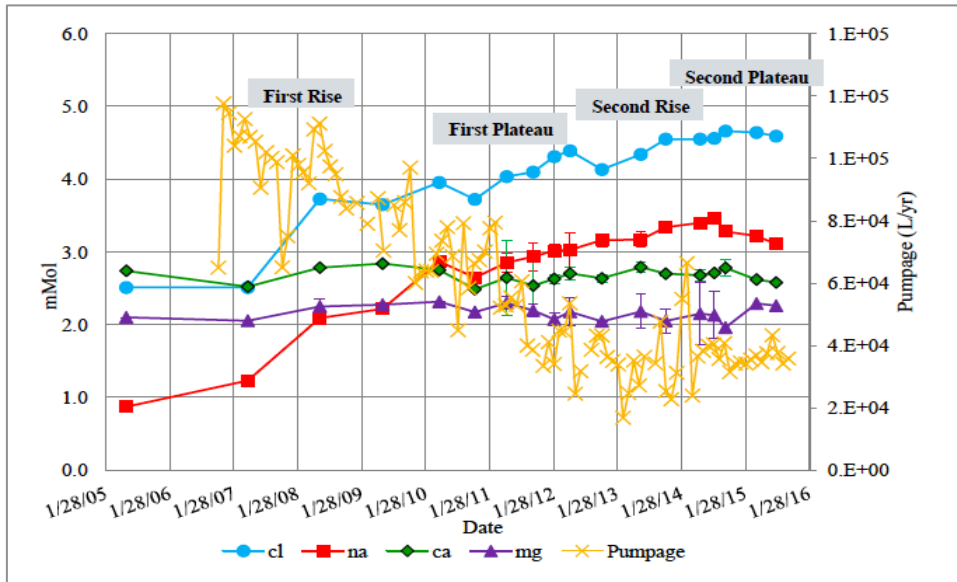
Figure 5. Major ion chemistry in Well 12 from 2005 through 2015 (fields-Sommers, 2015).

Unlike both RBI wells, the major ion chemistry of the pristine well remained constant over time regardless of the amount of pumpage (Figure 6). Sodium concentrations ranged

from 2.1-2.5 mMol/L while chloride concentrations ranged from 1.5-1.7 mMol/L throughout the wells operational period, 2010 through 2016. The current study extends the data from 2016 through 2018. The major ion results from Well 13 show the well has no hydrologic connection to the Fox River, and only pumps pristine groundwater.
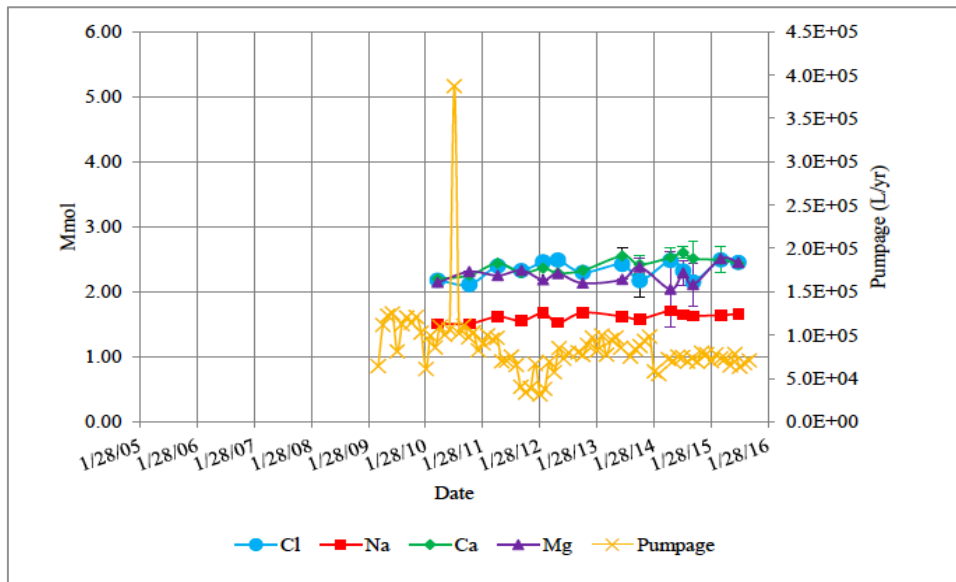
Figure 6. Major ion chemistry in Well 13 from 2009 through 2015 (Fields-Sommers, 2015).

Thorp (2013) discriminated between the sources of contamination entering the RBI wells. The Fox River water entering the wellfield is enriched in sodium chloride. Natural and anthropogenic sources of salt, such as seawater and WWTP effluent can be distinguished through the boron/chloride ratio (Vengosh et al., 13 1991). Figure 7 shows the comparison between end member waters to a mixing line of pristine well water to seawater. The red is composed of three end member waters. The yellow square point is an average of 50 WWTP samples, the green circle point is an average of Fox River water, and the red circle point is pristine well water. The blue line represents a mixing line of pristine well water and seawater. The red square points and the yellow triangle points

12

represent the RBI wells. The RBI wells plot against the end member line, indicating that the salt in the water of the RBI wells is WWTP effluent dominated.
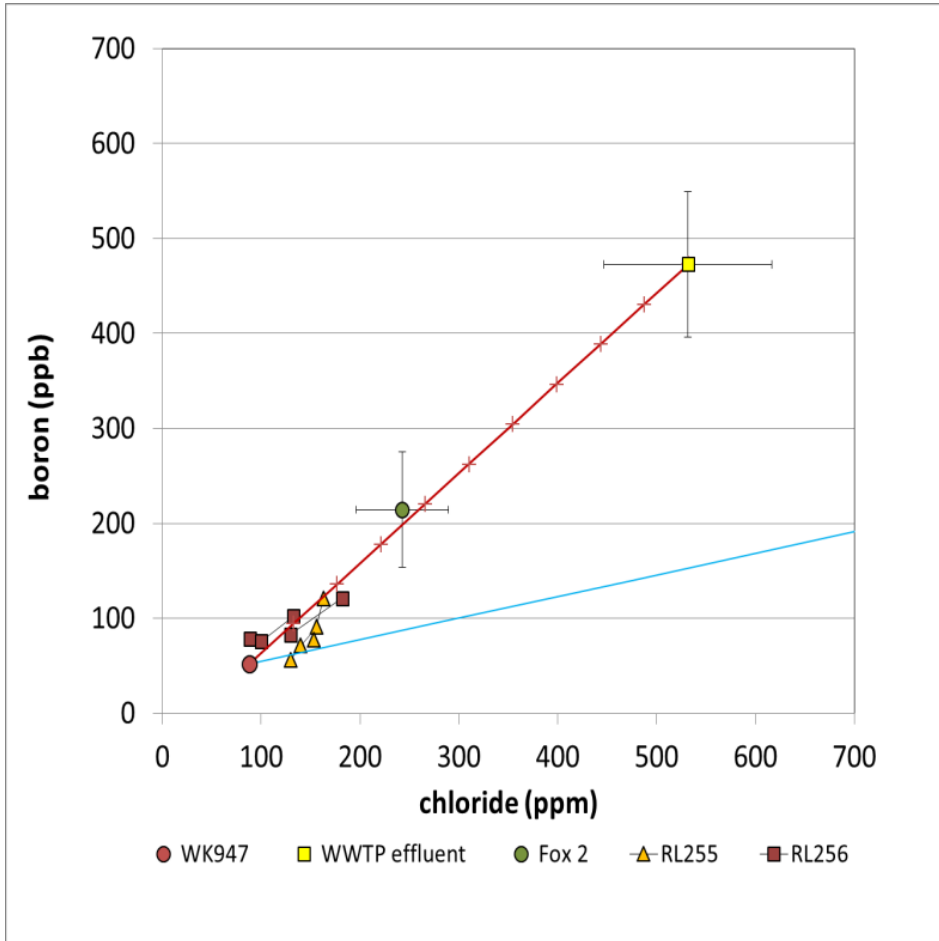
Figure 7. RBI wells pumping a mix of pristine groundwater and WWTP effluent (Thorp, 2013).

4.2 Previous Microbiology Studies

Geochemistry data collected from the monitoring network was combined with microbial community data sets to identify thermodynamically feasible metabolic pathways capable of being carried out by the microbial consortia. As the microbiology field has grown, the number of metagenomic data sets that represent sequences from a wide range of microbial communities has increased (Delmont et al., 2012). The data identified potential metabolic pathways and geochemical reactions being carried out by

the microbial consortia. Previous studies have successfully used metagenomics to study the functional capabilities of microorganisms in aquifers (Lisle, 2014). For example, Smith et al. (2012) examined the extent of variation between the composition and function of microbial communities in two aquifer systems. Lin et al. (2012) and Luef et al. (2015) also completed studies using metagenomics to study groundwater. Amend and Shock (2012) formulated 370 possible reactions that are related to microbial metabolism in environmental systems. Lisle (2014) looked at the 370 possible reactions laid out by Amend and Shock (2012) and identified five energetically favorable reactions in the Floridian aquifer system located in southern Florida. Lisle determined which biogeochemical reactions were favored in the Floridian aquifer from thermodynamic principles to calculate free energy yields. The biogeochemical reactions most likely to proceed were determined by calculating the Gibbs free energy for each specific well in the study. The free energy yields of redox reactions driven by microbial activity were applied to constrain the list of the possible biogeochemical reactions to those that were relevant to the study environment. A similar approach was used to combine the geochemical and metagenomic data in this study. This study used similar techniques, but it differed from the previously mentioned studies by comparing microbial communities from pristine and impacted wells.

Previously unknown microorganisms were discovered in groundwater recently, which expanded the tree of life (Hug et al., 2016). Many of the previously unknown organisms were discovered using 16S rRNA gene sequencing and genome sequences deriving from the anoxic subsurface. The recently discovered microorganisms largely make up the Diapherotrites, Parvarchaeota, Aenigmarchaeota, Nanoarchaeota,

Nanohaloarchaea (DPANN) phylum and candidate phyla radiation (CPR) in the new tree of life (Castelle et al., 2015b; Eme and Ford Doolittle, 2015; Hug et al., 2016; Liu et al., 2018; Rinke et al., 2013). The Banfield Lab at University of California, Berkeley, found the recently discovered radiations. Jill Banfield has pioneered the groundwater microbial field and the newly discovered radiations expanded the tree of life (especially bacteria) by approximately 40% in the last few years and the sequences and organisms originated from groundwater.

Chapter 5: Relevance and Research Objective

RBI wells in southeastern Wisconsin are pumping 40-60% Fox River water that contains significant amounts of WWTP effluent. There is a need to understand how shallow groundwater aquifers are being impacted by anthropogenic activities. Shallow aquifers are important sources of water for municipal uses like drinking water, agriculture, and industry. Microorganisms are also known to be key players in biogeochemical reactions that influence water quality and treatment processes. The purpose of the proposed research is to investigate if, and to what extent the microbial community present in the shallow groundwater of southeastern Wisconsin is affected by the influx of treated municipal wastewater effluent. This study combined two graduate students' research by merging geochemical analysis and microbial analyses to obtain a more complete picture of a valuable freshwater resource. The change in microbial community composition and genetic functional potential between pristine and impacted groundwater sites will be characterized to better understand the impact of anthropogenic activities on native microbial communities. The specific objective of this study is outlined below:

1. Define differences in the microbial communities and the functional reactivity between pristine and contaminated portions of a shallow sand and gravel aquifer.

    i. Collect groundwater samples from a shallow sand and gravel aquifer and analyze them for microbial community genetic/physiological potential and composition. Samples will be collected from a pristine portion of the aquifer and a portion impacted with treated WWTP effluent.

ii. Collect geochemical data on the same samples and calculate free energy

yields to determine energetically favorable reactions present in the system.

iii. Assess differences in the microbial communities and geochemical

reactivities of the pristine and contaminated locations.

Chapter 6: Methods

6.1 Monitoring Network

This study was conducted in southeastern Wisconsin on an existing monitoring network consisting of 18 sites. The sites are in the Root, Menomonee, and Fox River watersheds in Waukesha and Milwaukee County, Wisconsin. The monitoring network is composed of seven high capacity wells, seven river locations, one artesian spring, and three WWTPs. Three high capacity wells are operated by the City of Brookfield (IZ385, IZ386, and EM275) and one high capacity well (SV631) is in St. Martin's of Tours Parish in Franklin, Wisconsin. Four river sites are located on the Fox River (Fox 0-3), and the three remaining river sites are located on the Root River, Sussex Creek, and Underwood Creek. Hygeia Spring, the artesian spring, is in Big Bend, Wisconsin. The three WWTPs are in Brookfield, Sussex, and Waukesha, Wisconsin. The primary study area is in a well field near the upper Fox River in Waukesha, Wisconsin. The City of Waukesha operates three high capacity wells in the shallow sand and gravel aquifer. Two RBI wells, Well 11 and Well 12, are located 225 feet and 83 feet, respectively, from the riverbank. The background well, Well 13, is located 1,500 feet from the riverbank. See Figure 8 for detailed locations. The two RBI wells are pumping as much as 50% river water, which contains treated wastewater effluent from the three WWTPs, and the background well is pumping pristine groundwater. All three of the wells are screened in a shallow gravel layer at depths ranging from 60 to 150 feet.
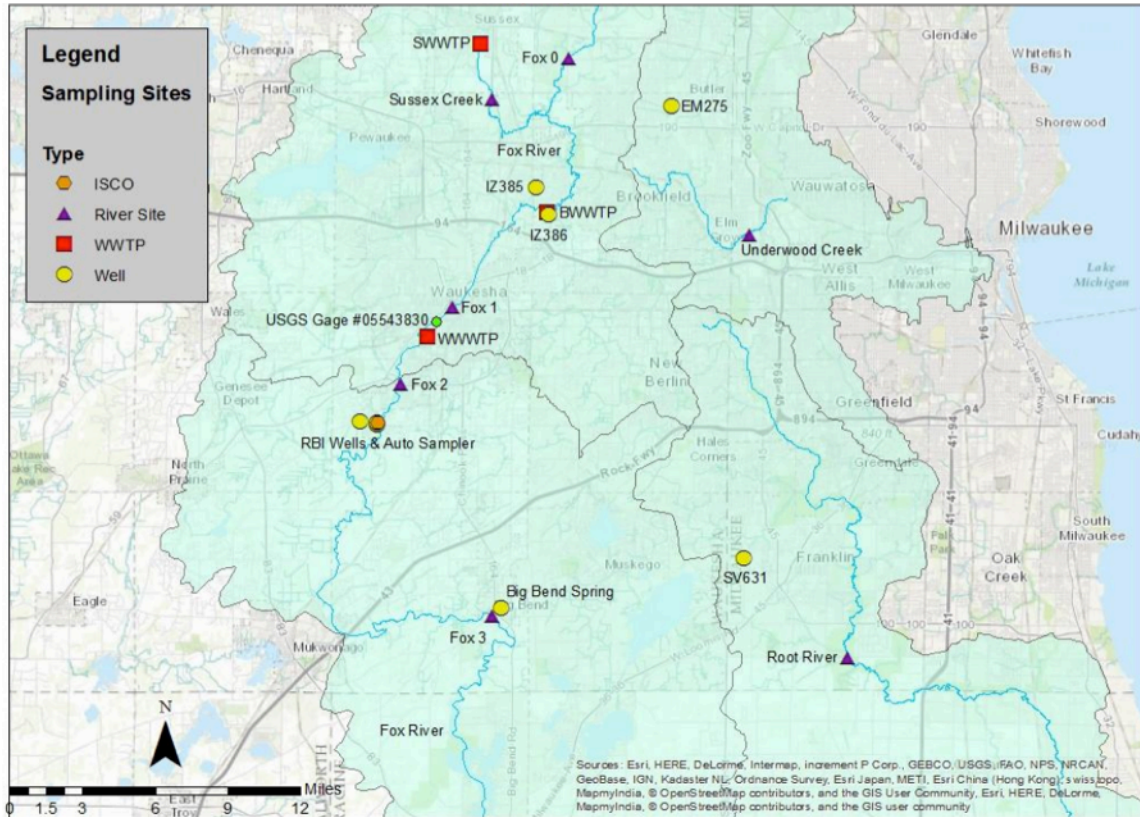
Figure 8. Map of monitoring network, with light green indicating the watersheds of the sampling sites (Fields-Sommers, 2015).

The monitoring network was sampled in the spring, summer, and fall over a 14-month period. Sampling of river sites was conducted during baseflow conditions when the aquifer has the most influence over surface water. Baseflow conditions were determined by USGS stream gage on Fox River at Waukesha, Wisconsin (gage # 05543830). The gaging station is located less than a mile downstream from Fox 1. Water from each site was analyzed for geochemical composition (major ions, nutrients, dissolved gases and DOC), and water from the primary study area was also analyzed for microbial community composition (16S rRNA gene composition, 16S rRNA activity).

6.2 Field Methods and Equipment

At river sites, and the artesian spring, a Teflon bailer was used to collect water at equal intervals across the river. The water was combined to create a representative

19

sample of the entire site. For well sampling, water was collected using a flow-through chamber that was connected to the well sampling port through tubing. Wells were purged for a minimum of 10 minutes prior to sampling to ensure the sample was representative of native groundwater. At each WWTP a 24-hour composite sample was taken by staff and refrigerated in a 1 liter (L) Nalgene bottle with as little air as possible to reduce oxygen exposure. The WWTP samples were picked up the following day.

Nitrile gloves were used in sample preparation and during sampling. All sample bottles, syringes, and filter holders were washed in an acid bath composed of 90% distilled water and 10% hydrochloric acid for a minimum of 12 hours before use. Sampling equipment was single use and disposed of after use to prevent cross contamination. Tubing used at each well was not replaced, but was thoroughly cleaned while the wells were purged.

Water samples were filtered using 0.2 micron (μm) regenerated cellulose filters. Filtering took place in the field using 60 milliliter (mL) plastic syringes. Two Nalgene 250 mL bottles were filled with filtered water for major ion analysis. The bottle designated for cation analysis received 1 mL of trace metal nitric acid for preservation. At the primary study area, a 250 mL Nalgene bottle was filled with filtered water for nutrient (nitrate, nitrite, ammonium, and phosphate) and DOC analysis. Major ion samples were refrigerated until analysis, while nutrient and DOC samples were frozen.

Hydrogen gas was sampled following microseeps gas stripping cell instructions from Pace Analytical (Appendix A). Groundwater was pumped through a cell at a rate of over 300 mL/minute for 10 minutes. The cell contained air after 10 minutes it was

determined to be at equilibrium. When the equilibrium time was up, 15 mL sample of gas was withdrawn from the cell. The sample was then sent to Pace Analytical for analysis.

The physical parameters (dissolved oxygen, electrical conductivity, and temperature) were measured at each site except the WWTPs. Dissolved oxygen was measured using YSI Model 52 oxygen meter with high sensitivity electrode membrane that was calibrated to the current barometric pressure before sampling, and a CHEMetrics colormetric ampoule kit for low oxygen (K-7501) was used to replicate the dissolved oxygen measurement. Electrical conductivity was measured using a YSI Pro30 Conductivity Meter. Temperature readings were given on each YSI meter. For river sites, the meter probes were placed as far off the riverbank as possible to ensure the most accurate measurement. In the artesian spring, the meters were put directly into the outflow pipe. In the well houses, the meters were situated in the flow-through chamber.

Chemical parameters that are subject to rapid change (alkalinity, ferrous iron, and pH) were measured in the field at each site except the WWTPs. Prior to the summer of 2017, alkalinity was measured by taking a 50 mL water sample and titrating it to 4.5 pH using 0.2 Normal hydrochloric acid. The total acid added was determined by the mass difference between the original 50 mL sample and the mass of the sample post titration, using an Ohaus SP402 portable scale. After the summer of 2017, a Hach digital titrator was used in place of the scale. Alkalinity that could not be measured in the field was estimated by charge balance with the major ions. Ferrous iron was measured using a CHEMetrics colormetric ampoule kit (K-6210). pH was measured using an Accumet 1002 pH meter by Fisher Scientific and calibrated to pH of 4.0 and 7.0.

21

Microbial RNA and DNA for 16S rRNA gene sequencing were obtained by collecting 2-3 L water samples from each well house in the Waukesha well field. Water was filtered in the field using an in-line filtration system. Water was filtered sequentially through 3 μm, 0.2 μm and 0.1 μm polycarbonate filters with a diameter of 47 mL. Filter papers were stored in sterile 2 mL tubes. To minimize the fast degradation/alteration rate of RNA, tubes were flash frozen by being placed in liquid nitrogen immediately after filtration. One mL of 3 μm filtrate and 0.2 μm filtrate was collected and fixed with formalin for cell enumeration using DAPI fluorescent stain and microscopy. Water samples were stored in an -80°C freezer until extraction processing.

Microbial genomic DNA for shotgun metagenomic sequencing was obtained by collecting 20 L water samples from each well house in the Waukesha well field. Water was filtered sequentially at the School of Freshwater Sciences using an in-line filtration system through 3 μm, 0.2 μm and 0.1 μm polycarbonate filters with a diameter of 142 mL. Filter papers were stored in sterile whirl pak bags in an -80°C freezer until extraction.

6.3 Laboratory Methods

All analyses were conducted at the University of Wisconsin - Milwaukee School of Freshwater Sciences. Major ion samples were analyzed on an ion chromatograph and atomic absorption spectrometer for anions and cations, respectively. Anion analytes, chloride (Cl^-), nitrate (NO_3^-), phosphate (PO_4^-), and sulfate (SO_4^{2-}), were analyzed using ion chromatography on a DIONEX ICS-1000 IC System with Chromeleon version 6.80 SR7 workstation software. Cation analytes, calcium (Ca^{2+}), sodium (Na^+), magnesium (Mg^{2+}), and potassium (K^+), were analyzed using atomic absorption spectroscopy on a

SOLAAR with version 11.02 workstation software. Calibrations were performed at the beginning of each analytical run to account for drift. Ion concentrations were calculated independently of the previously mentioned software using calibration curves constructed from chemical standards (See Appendix B).

Nutrient samples were analyzed on an ion chromatograph, AutoAnalyzer, and spectrophotometer for nitrate (NO_3^-), nitrite (NO_2^-) and ammonium (NH_4^+), and total dissolved phosphorous, respectively. Nutrient samples were analyzed using multiple methods. Nitrate was analyzed on an ion chromatograph following the same methods used to analyze major ions. Nitrogen species, nitrite and ammonium, were measured using the molybdenum blue method on an AutoAnalyzer. Total dissolved phosphorus was measured on a spectrophotometer using the molybdate method after photo-oxidation was used to break down dissolved organic phosphorus compounds into orthophosphate.

DOC was analyzed using the high temperature combustion method by converting inorganic carbon to dissolved carbon dioxide, after which it was purged from the sample. The remaining organic carbon was oxidized to carbon dioxide, which was detected by the instrument and correlated to total organic carbon.

Staff in the Bootsma and Klump lab at the School of Freshwater Sciences analyzed dissolved carbon dioxide and methane, respectively. Pace Analytical analyzed hydrogen gas.

Natalie Gaynor at the School of Freshwater Sciences analyzed microbial data using the following methods. Filter papers were used for DNA and RNA extraction. The 0.2 μm and 0.1 μm pore size filter papers were cut within their collection tubes using sterilized small dissection scissors. DNA and RNA were simultaneously extracted from

the same sample using Qiagen's AllPrep Powerviral DNA/RNA kit. Zirconian beads

were added to the sample tubes after cutting the filters into small pieces and vortexed in a

bead beater for 2.5 minutes, then the samples were placed on ice for 5 minutes. The

process was repeated for a total of 2 bead beating (Smith et al., 2012) steps. The

extraction process followed manufacturer's instructions except for elution in three

volumes up to 100 microliters (μL). Extracted DNA and RNA were stored in sample

tubes and placed in an -80°C freezer.

Promega's RQ1 RNase-Free DNase (Cat #M6101) kit for DNase Treatment of

RNA Samples Prior to RT-PCR was used. Promega's DNase protocol called for 1-8 μL

of RNA sample in elution buffer. The full 8 μL of sample was used due to the

groundwater samples being from low biomass systems with low nucleic acid yields. A

total of 16 μL of RNA sample was used per sample per DNase treatment in order to have

enough for two reactions (one positive with reverse transcriptase, and one negative

without reverse transcriptase) in subsequent steps in the RT-PCR. One μL of DNase (the

protocol called for 1 unit or μL per 1 μg of RNA), and 2 μL of Buffer were used in the 16

μL sample reactions.

RNA was reverse transcribed using the Promega's GoScript™ Reverse

Transcription System. The reverse primer 806Rb for the v4 16S rRNA gene region was

used in the cDNA synthesis (806 μm Rb – GGACTACNVGGGTWTCTAAT). 8.5 μL of

DNase treated RNA was used with 1.5 μL of primer for each reaction. Each sample had

two reactions: one positive reaction including the reverse transcriptase and one negative

reaction without the reverse transcriptase. The two reactions were used to ensure the

DNAase treatment worked correctly and no carryover-over of initial DNA remained in the RNA/cDNA sample for the subsequent 16S rRNA gene PCR.

Polymerase Chain Reaction (PCR) was used to target and amplify the v4 16S rRNA gene region in the DNA and cDNA samples using Invitrogen's™ Platinum™ Taq DNA Polymerase. Forward and reverse primers 515Fb and 806Rb with Illumina adapters were used, as shown below:

515Fb-illumina –

TCGTCGGCAGCGTCAGATGTGTATAAGAGACAGGTGYCAGCMGCCGCGGTAA

806Rb-illumina –

GTCTCGTGGGCTCGGAGATGTGTATAAGAGACAGGGACTACNVGGGTWTCTAAT

Reactions were run in triplicate for each sample and then pooled prior to cleanup with the AMPure Bead cleanup system. One PCR reaction out of the three triplicates for each sample was screened using gel electrophoresis to verify amplification and DNA fragment size. A modified reconditioned/nested PCR protocol was used when one normal PCR (25 µL reaction volume, 1 µL template, 30 cycles) was not sufficient for sample amplification. In the reconditioned PCR, two consecutive PCR's were carried out. The first PCR had a smaller reaction volume and shorter cycle period, however, 1 µL of template was still used (15 µL reaction volume, 1 µL template, 10 cycles). Then 1 µL of the reconditioned PCR was used as a template in the full PCR (25 µL reaction volume, 1 µL of template, 30 cycles). Negative control reaction components, volumes, and concentrations are described below.

Table 1. Negative control reaction components, concentrations, and volumes.

Master Mix of PCR Components	Working Concentration	Normal PCR	Reconditioned PCR
Reaction Volume	-	25	15
PCR Cycles	-	30	10
10x Buffer for Platinum Taq	10x	2.5 μL	1.5 μL
F Primer	5 μm stock	1 μL	0.6 μL
R Primer	5 μm stock	1 μL	0.6 μL
50 mM MgSO$_4$	50 μm	1 μL	0.6 μL
10 mM dNTP Mix	10 mm	0.5 μL	0.3 μL
Platinum Taq Polymerase	5 U/μL	0.1 μL	0.06 μL

Table 2. PCR thermocycler conditions.

PCR Thermocycler Conditions			
1	Initial denaturation	94°C	5 minutes
2	Denature	94°C	30 seconds
3	Anneal	50°C	45 seconds
4	Extend	72°C	60 seconds
Repeat 2 – 4 30x, or 10x for first reconditioned PCR step			
5	Final Extension	72°C	2 minutes
6	Hold	10°C	Hold

Sequencing was performed on the Illumina MiSeq at the Great Lakes Genomics Center (GLGC). An extraction blank was run as a negative control and a mock community was sequenced as a positive control for quality control and processing. Data was processed in-house through GLGC support (Aurash Mohaimani). Data was further processed through Mothur (Schloss et al., 2009), DADA2 (Callahan et al., 2016), and SILVA classification (Quast et al., 2013). R and RStudio was used to visualize and statistically analyze (Willis, 2017) processed data along with the vegan package in R (Oksanen, 2005; Oksanen et al., 2013).

6.4 Thermodynamic Calculations

Seven groundwater samples were collected from each shallow groundwater well (Well 11, Well 12, Well 13) over a 14-month period spanning from November 2016

through January 2018 and analyzed for common groundwater constituents for biogeochemical analyses. The constituents were averaged between the seven samples to create a composite sample representative of the groundwater in each well (Table 3). Sulfide and ferrous iron were not detected in any shallow groundwater wells, however, Chemet kits were used to perform the measurements, and so the detection limits for the Chemet kits were used in thermodynamic analyses to account for minuscule concentrations of the constituents.

Table 3. Composite water quality data for three shallow groundwater wells with respective standard deviations from November 2016 through January 2018.

Parameter	Units	RBI Well 11	RBI Well 12	Pristine Well 13
Temperature	°C	10.42 ± 1	10.61 ± 0.2	10.5 ± 0.1
pH		6.98 ± 0.1	6.99 ± 0.2	7.06 ± 0.6
Calcium	mg/L	93.12 ± 30	90.48 ± 20	83.71 ± 10
Chloride	mg/L	218.48 ± 60	201.28 ± 60	97.24 ± 30
Magnesium	mg/L	54.93 ± 2	53.32 ± 2	56.71 ± 4
Potassium	mg/L	3.3 ± 0.8	3.16 ± 0.5	2.56 ± 0.5
Sodium	mg/L	101.43 ± 5	81.1 ± 3	39.79 ± 2
Dissolved oxygen	mg/L	0.18 ± 0.3	0.15 ± 0.2	0.14 ± 0.2
Ferrous Iron	mg/L	0.1	0.1	0.1
Ammonium	mg/L	0.001	0.07	0.03
Nitrate	mg/L	1.49 ± 1	0.3 ± 0.7	1.74 ± 1
Nitrite	mg/L	0.05	0.003	0.04
Sulfate	mg/L	64.11 ± 20	68.17 ± 10	96.9 ± 10
Sulfide	mg/L	0.1	0.1	0.1
Total dissolved phosphorus	mg/L	0.002	0.004	0.003
Dissolved organic carbon	mg/L	0.49 ± 0.3	0.93 ± 0.3	0.65 ± 0.4
Bicarbonate	mg/L	420.68 ± 200	462.25 ± 100	411.26 ± 100
Hydrogen	μmol/L	0.002	0.005	0.004
Methane	μmol/L	0.007	0.417 ± 0.2	0.043

Free energy calculations were performed with 22 biogeochemical reactions to access the potential metabolic pathways being carried out by the microbial consortia. The reactions include the groundwater constituents measured in this study and are commonly driven by microorganisms in groundwater systems (Davidson et al., 2011; Lisle, 2014) (Table 4).

Table 4. Balanced biogeochemical reactions.

Reaction Number	Reaction
1	$CH_4 + SO_4^{2-} \rightarrow H_2O + HCO_3^- + HS^-$
2	$Acetate + NO_3^- + H_2O \rightarrow 2HCO_3^- + NH_3$
3	$4H_2 + 1.6NO_3^- + 1.6H^+ \rightarrow 0.8N_2 + 4.8H_2O$
4	$Acetate + 1.6NO_3^- + 0.6H^+ \rightarrow 2HCO_3^- + 0.8H_2O + 0.8N_2$
5	$4H_2 + NO_3^- + H^+ \rightarrow NH_3 + 3H_2O$
6	$Acetate + SO_4^{2-} \rightarrow 2HCO_3^- + HS^-$
7	$4H_2 + H^+ + SO_4^{2-} \rightarrow HS^- + 4H_2O$
8	$4Acetate + 4H_2O \rightarrow 4CH_4 + 4HCO_3^-$
9	$4H_2 + H^+ + HCO_3^- \rightarrow CH_4 + 3H_2O$
10	$4H_2 + H^+ + 2HCO_3^- \rightarrow Acetate + 4H_2O$
11	$Acetate + 8Fe(OH)_3 + 15H^+ \rightarrow 8Fe_2^+ + 20H_2O + 2HCO_3^-$
12	$HS^- + 8Fe(OH)_3 + 15H^+ \rightarrow SO_4^{2-} + 8Fe^{2+} + 20H_2O$
13	$4H_2 + 2O_2 \rightarrow 4H_2O$
14	$Acetate + 2O_2 \rightarrow 2HCO_3^- + H^+$
15	$CH_4 + 2O_2 \rightarrow HCO_3^- + H^+ + H_2O$
16	$HS^- + 2O_2 \rightarrow SO_4^{2-} + H^+$
17	$(^4/_3)NH_3 + 2O_2 \rightarrow (^4/_3)NO_2^- + (^4/_3)H^+ + (^4/_3)H_2O$
18	$H_2S + 4NO_3^- \rightarrow SO_4^{2-} + 4NO_2^- + 2H^+$
19	$3H_2S + 4NO_2^- + 2H^+ + 4H_2O \rightarrow 3SO_4^{2-} + 4NH_4^+$
20	$(^4/_3)NH_4^+ + 2O_2 \rightarrow (^4/_3)NO_2^- + (^8/_3)H^+ + (^4/_3)H_2O$
21	$4NO_2^- + 2O_2 \rightarrow 4NO_3^-$
22	$8Fe^{2+} + 2O_2 + 20H_2O \rightarrow 8Fe(OH_3) + 16H^+$

The activities of each constituent were used in the free energy calculations expressed by:

$$a[A] + b[B] \rightleftarrows c[C] + d[D] \tag{1}$$

where A, B represent the activities of the reactants while C, D represent the activities of the products, and a, b, c, d are the stoichiometric constants from the balanced equations respective to the corresponding activities. The activity of each groundwater constituent was calculated using PHREEQC version 3.1.7.9213 (Parkhurst and Appelo, 2005) with the wateqf.dat database derived from WATEQ4F (Ball and Nordstrom, 1991).

The standard Gibbs free energies ($\Delta G°$, joules per mole) were calculated for the balanced reactions using the following equation:

$$\Delta G° = \sum \Delta G°_f \, (\text{products}) - \Delta G°_f \, (\text{reactants}) \tag{2}$$

where $\Delta G°_f$ (joules per mole) represents the values for the standard free energy of formation of the products and reactants in each reaction. The Amend and Shock (2011) values of $\Delta G°_f$ were used to calculate $\Delta G°$.

The equilibrium constant (K_{eq}) for all 22 reactions was calculated using the $\Delta G°$ values and solving for K_{eq}:

$$K_{eq} = e^{-(\Delta G°/RT)} \tag{3}$$

where R is the universal gas constant (8.3145 joules per degree Kelvin per mole (J °K^{-1}mol^{-1}), and T is temperature (°K).

Free energy values under in situ conditions (ΔG_r) were calculated using the $\Delta G°$ values for each reaction, groundwater temperatures (Table 3), and activities of the reactants and products (Appendix B), demonstrated by the following equations:

$$\Delta G_r = \Delta G° + RT\ln Q \tag{4}$$

where

$$Q = [C]^c \, [D]^d \, / \, [A]^a \, [B]^b \tag{5}$$

Free energy flux (FEF, kilojoules per cell per second) is the amount of energy a microbial cell can potentially generate from performing each reaction assuming that the reaction proceeds until one reactant (the limiting reactant) is fully consumed. The FEF was calculated by the following equation:

$$FEF = 4\pi * r * D_c * C * \Delta G_r \tag{6}$$

where r (micrometers) is the radius of the microbial cell, D_c (meters squared per second) is the diffusion coefficient of the limiting reactant, C (moles per cubic meter) is the

concentration of the limiting reactant, and ΔG_r (kilojoules per cell per second) is the free energy of reaction under in situ conditions for each reaction.

Free energy calculations were related to the 22 reactions (Table 4) based on the relationship of free energy yields for the production of adenosine triphosphate (ATP) (Schink, 1997; Thauer et al., 1977). Three assumptions were made to relate the free energy calculations to ATP production or microbial activity. The first assumption was conservation of energy occurs during the electron transport process for all reactions. The second assumption was the conversion of energy to ATP proceeds with maximum efficiency, creating a minimum free energy yield for ATP production, which is commonly set at –20 kilojoules per mole (kJ mol^{-1}) of limiting reactant for ΔG_r. The final assumption was the maximum rate that energy could be gained is dependent on diffusion rates (Onstott, 2005), and that deep subsurface microorganisms are immobile. Only reactions whose ΔG_r were less than –20 kJ mol^{-1} were considered to be energetically favorable.

Chapter 7: Results and Discussion

7.1 Geochemical Analyses

For the composited groundwater sample representative of Well 11 the pH was neutral (6.98) and the temperature low (10.42°C). For the composited sample representative of Well 12, the pH was neutral (6.99) and the temperature low (10.61°C). The geochemical results show slightly higher levels of metabolic gases, in particular methane and hydrogen, higher levels of ammonia and total dissolved phosphate, and lower levels of nitrate in RBI wells. For the composited sample representative of pristine groundwater (Well 13), the pH was neutral (7.06), the temperature low (10.5°C), with low levels of metabolic gases, chloride (97.24 mg/L), and sodium (39.79 mg/L), and high sulfate levels (96.9 mg/L) compared to the RBI wells (Well 11 and Well 12).

Piper diagrams were created for each shallow groundwater well (Figures 9-11). The samples plotted on the Piper diagrams were used to create a composite sample representative of the groundwater in each well used in the thermodynamic calculations. The diagrams are a graphical representation of the chemistry for groundwater samples collected at each well. On the diagrams, each dot represents a different sample, and as the color of the dot gets lighter, it indicates a more recent sample. The samples were collected after the previous study by Fields-Sommers (2015).

As shown on the bottom left ternary plot for each diagram, there is generally no change between samples, indicating calcium and magnesium remain steady over time, as reported by Fields-Sommers (2015). The bottom right ternary plots for the RBI wells show a chloride increase over time, as seen in the previous study. In addition,

concentrations are much higher compared to the pristine well. All wells are near calcite

saturation (SI = -0.10 ± 0.02).
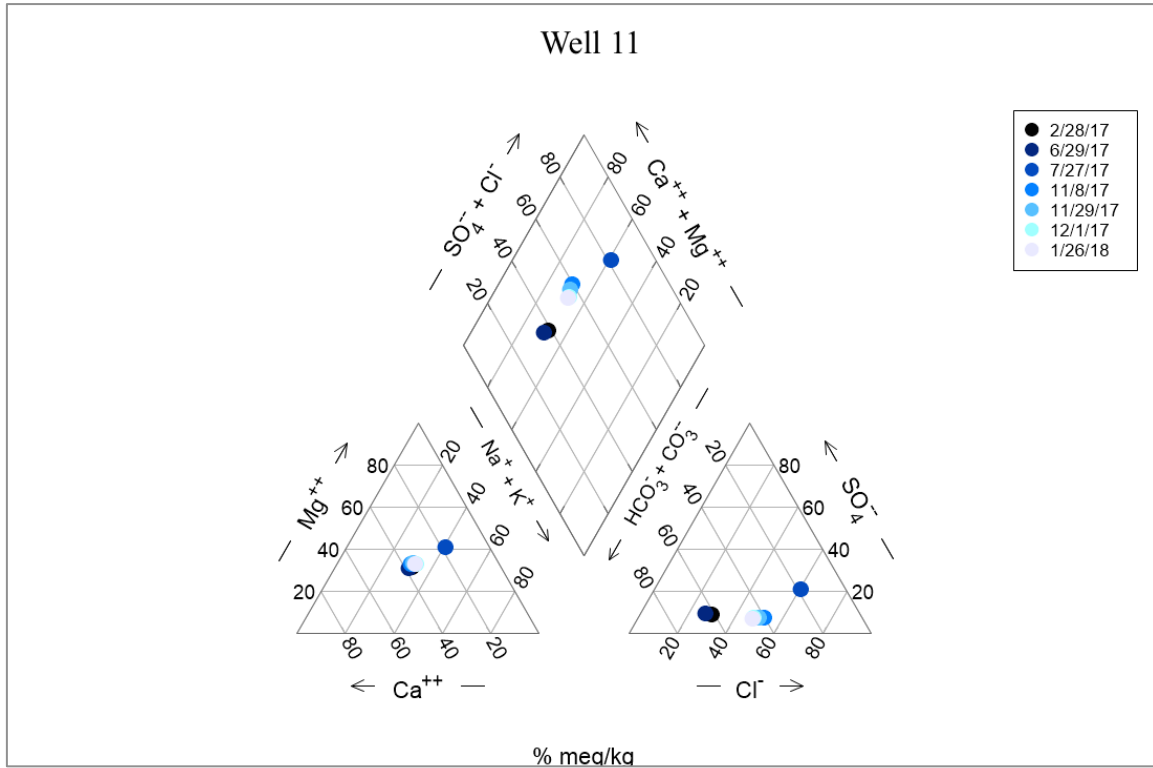
Figure 9. Piper diagram for Well 11.
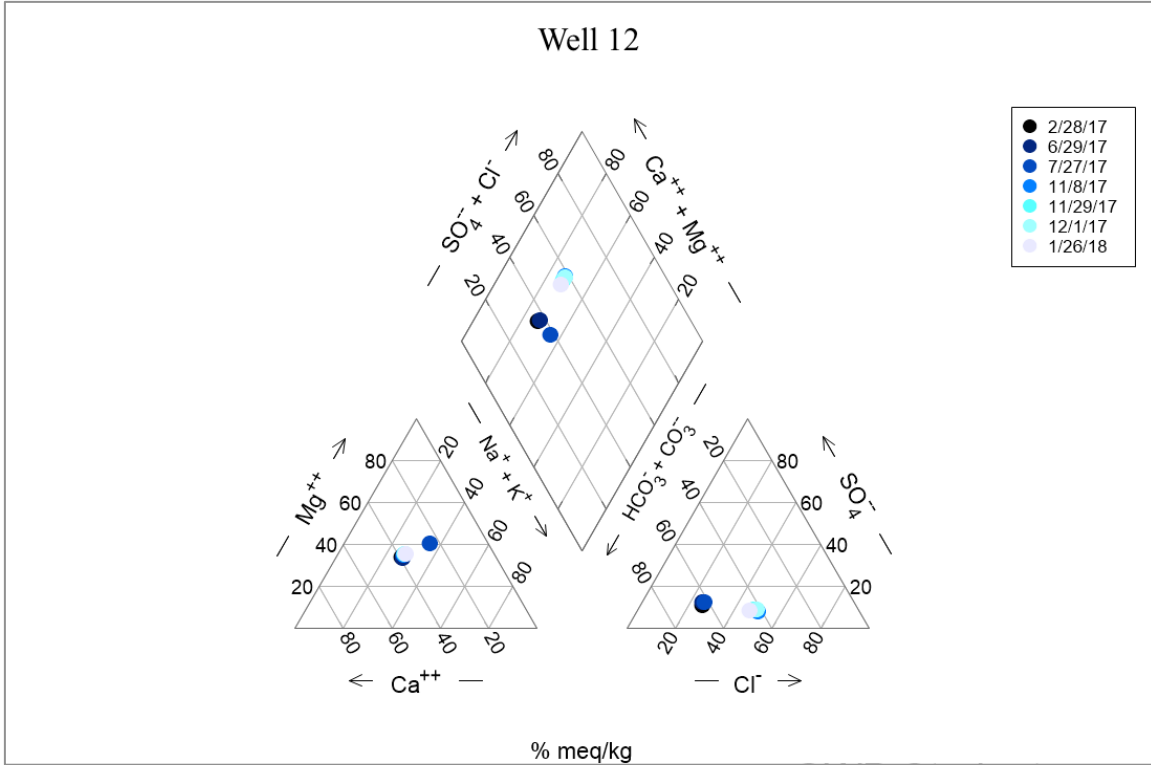
Figure 10. Piper diagram for Well 12.
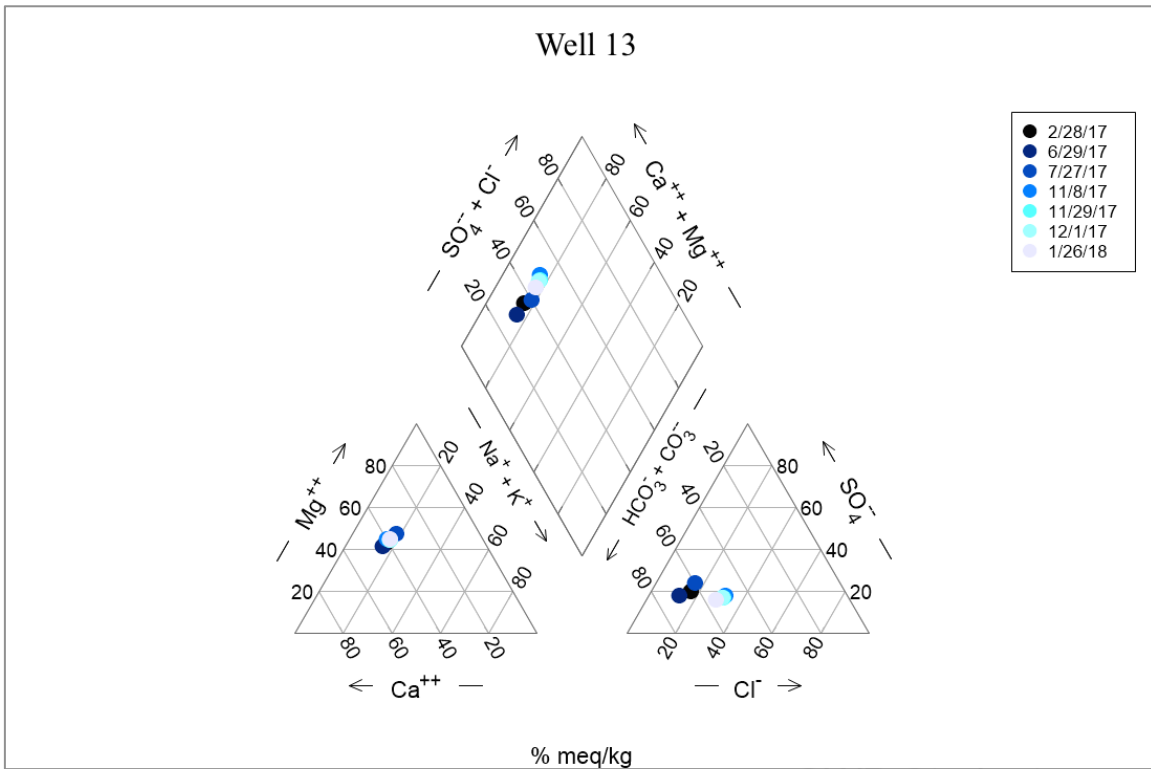
Figure 11. Piper diagram for Well 13.

7.2 Thermodynamic Analyses

The biogeochemical reactions most likely to proceed for each shallow groundwater well were calculated using the geochemistry of the groundwater and thermodynamic analyses. Amend and Shock (2001) formulated 370 possible reactions that are related to microbial metabolism in the environment. Approximately 200 out of the 370 reactions were redox reactions. Free energy yields of the redox reactions were used to constrain the list of most probable biogeochemical reactions. The geochemical data from this study (Table 3) were used to determine which biogeochemical reactions (Table 4) were applicable to the groundwater in this study.

Sulfide and ferrous iron were not detected in any shallow groundwater wells. Chemet kits were used to perform these measurements, therefore, the detection limits for the Chemet kits were used in thermodynamic analyses. The ΔG_r and FEF values are maximum estimates for reactions involving sulfide and ferrous iron. The ΔG_r of all reactions in Table 4 were normalized to 8 moles of electrons transferred per reaction.

Table 5. The free energy of reaction and free energy flux for a set of biogeochemical reactions.
[Free energy of the reaction (ΔG_r), kilojoules per mole (kJ mol^{-1}); Free energy flux (FEF), kilojoules per cell per second (kJ cell^{-1} s^{-1})]

Redox Reaction	RBI Well 11		RBI Well 12		Pristine Well 13	
	ΔG_r	FEF	ΔG_r	FEF	ΔG_r	FEF
1. $CH_4 + SO_4^{2-} \rightarrow H_2O + HCO_3^- + HS^-$	5	2×10^{-19}	-29	-7.6×10^{-17}	-1	-1.8×10^{-19}
2. Acetate + NO_3^- + $H_2O \rightarrow 2HCO_3^- + NH_3$	-496	-2.6×10^{-14}	-498	-4.9×10^{-14}	-490	-4.9×10^{-14}
3. $4H_2 + 1.6NO_3^- + 1.6H^+ \rightarrow 0.8N_2 + 4.8H_2O$	-	-	-	-	-	-
4. Acetate + $1.6NO_3^-$ + $0.6H^+ \rightarrow 2HCO_3^- + 0.8H_2O + 0.8N_2$	-	-	-	-	-	-
5. $4H_2 + NO_3^- + H^+ \rightarrow NH_3 + 3H_2O$	-482	-3.03×10^{-18}	-477	-7.53×10^{-18}	8.09×10^{39}	91.89

Redox Reaction	RBI Well 11		RBI Well 12		Pristine Well 13	
	ΔG_r	FEF	ΔG_r	FEF	ΔG_r	FEF
6. Acetate + $SO_4^{2-} \rightarrow$ $2HCO_3^- + HS^-$	-55	-2.9 x 10^{-15}	-56	-5.5 x 10^{-15}	-57	-5.7 x 10^{-15}
7. $4H_2 + H^+ + SO_4^{2-} \rightarrow$ $HS^- + 4H_2O$	30	1.9 x 10^{-19}	21	3.3 x 10^{-19}	23	2.9 x 10^{-19}
8. $4Acetate + 4H_2O \rightarrow$ $4CH_4 + 4HCO_3^-$	-237	-1.3 x 10^{-14}	-203	-2.0 x 10^{-14}	-226	-2.2 x 10^{-14}
9. $4H_2 + H^+ + HCO_3^-$ $\rightarrow CH_4 + 3H_2O$	25	1.6 x 10^{-19}	26	4.1 x 10^{-19}	23	2.9 x 10^{-19}
10. $4H_2 + H^+ +$ $2HCO_3^- \rightarrow$ Acetate + $4H_2O$	84	5.3 x 10^{-19}	77	1.2 x 10^{-18}	80	1.0 x 10^{-18}
11. Acetate + $8Fe(OH)_3 + 15H^+ \rightarrow$ $8Fe_2^+ + 20H_2O +$ $2HCO_3^-$	-409	-3.0 x 10^{-16}	-957	-6.9 x 10^{-16}	-413	-2.5 x 10^{-16}
12. $HS^- + 8Fe(OH)_3 +$ $15H^+ \rightarrow SO_4^{2-} + 8Fe^{2+}$ $+ 20H_2O$	-354	-2.6 x 10^{-16}	-363	-2.6 x 10^{-16}	-356	-2.2 x 10^{-16}
13. $4H_2 + 2O_2 \rightarrow$ $4H_2O$	-740	-4.7 x 10^{-18}	-704	-1.1 x 10^{-17}	-702	-8.8 x 10^{-18}
14. Acetate + $2O_2 \rightarrow$ $2HCO_3^- + H^+$	-781	-2.8 x 10^{-14}	-781	-2.3 x 10^{-14}	-782	-2.2 x 10^{-14}
15. $CH_4 + 2O_2 \rightarrow$ $HCO_3^- + H^+ + H_2O$	-722	-3.2 x 10^{-17}	-730	-1.9 x 10^{-15}	-725	-2.0 x 10^{-16}
16. $HS^- + 2O_2 \rightarrow SO_4^{2-}$ $+ H^+$	-726	-6.1 x 10^{-15}	-725	-6.2 x 10^{-15}	-725	-6.7 x 10^{-15}
17. $(^4/_3)NH_3 + 2O_2 \rightarrow$ $(^4/_3)NO_2^- + (^4/_3)H^+ +$ $(^4/_3)H_2O$	-341	-2.5 x 10^{-19}	-370	-1.9 x 10^{-17}	-360	-9.5 x 10^{-18}
18. $H_2S + 4NO_3^- \rightarrow$ $SO_4^{2-} + 4NO_2^- + 2H^+$	-471	-5.2 x 10^{-15}	-504	-5.5 x 10^{-15}	-496	-5.0 x 10^{-15}
19. $3H_2S + 4NO_2^- +$ $2H^+ + 4H_2O \rightarrow 3SO_4^{2-}$ $+ 4NH_4^+$	-1340	-9.9 x 10^{-16}	-1251	-9 x 10^{-16}	-1280	-7.8 x 10^{-16}
20. $(^4/_3)NH_4^+ + 2O_2 \rightarrow$ $(^4/_3)NO_2^- + (^8/_3)H^+ +$ $(^4/_3)H_2O$	-226	-1.0 x 10^{-16}	-251	-7.8 x 10^{-15}	-241	-3.2 x 10^{-15}
21. $4NO_2^- + 2O_2 \rightarrow$ $4NO_3^-$	-248	-5.6 x 10^{-15}	-213	-2.9 x 10^{-16}	-221	-4.0 x 10^{-15}
22. $8Fe^{2+} + 2O_2 +$ $20H_2O \rightarrow 8Fe(OH)_3 +$ $16H^+$	-372	-2.7 x 10^{-15}	-362	-2.5 x 10^{-15}	-369	-2.6 x 10^{-15}

The ΔG_r and FEF values for heterotrophic reactions (Reactions 1, 2, 4, 6, 11, 14, and 15 in Table 5) in all shallow groundwater wells ranged from -957 to 5 kJ mol^{-1} and -1.8 x 10^{-19} to 2 x 10^{-19} kJ cell^{-1} s^{-1}, respectively.

Autotrophic nitrate reducing reactions yielded ΔG_r and FEF values ranging from -2288 to -396 kJ mol^{-1} and -6.2 x 10^{-18} and -1.4 x 10-^{15} kJ cell^{-1} s^{-1}, respectively (Reactions 3, 5, and 19 in Table 5).

The autotrophic iron reducing reaction (Reaction 12 in Table 5) yielded ΔG_r and FEF values ranging from -363 to -354 kJ mol^{-1} and -2.6 x 10^{-16} to -2.2 x 10^{-16} kJ cell^{-1} s^{-1}, respectively, while the autotrophic sulfate reducing reaction (Reaction 7 in Table 5) yielded values ranging from 21 to 30 kJ mol^{-1} and 1.9 x 10^{-19} to 3.3 x 10^{-16} kJ cell^{-1} s^{-1}, respectively.

Methanogenesis from hydrogen and carbon dioxide (Reaction 9 in Table 5) yielded ΔG_r and FEF values ranging from 23 to 25 kJ mol^{-1} and 1.6 x 10^{-19} to 4.1 x 10^{-19} kJ cell^{-1} s^{-1}, respectively, while acetogenesis from hydrogen and carbon dioxide (Reaction 10 in Table 5) yielded values ranging from 77 to 84 kJ mol^{-1} and 5.3 x 10^{-19} to 1.2 x 10^{-18} kJ cell^{-1} s^{-1}, respectively.

The hydrogen oxidation reaction (Reaction 13 in Table 5) yielded ΔG_r and FEF values ranging from -740 to -702 kJ mol^{-1} and -8.8 x 10^{-18} to -1.1 x 10^{-17} kJ cell^{-1} s^{-1}, respectively, while fermentation (Reaction 8 in Table 5) yielded values ranging from -237 to -203 kJ mol^{-1} and -2.2 x 10^{-14} to -1.3 x 10^{-14} kJ cell^{-1} s^{-1}, respectively.

Of the 22 biogeochemical reactions applicable to this study, 16 reactions were determined to be thermodynamically feasible in the shallow groundwater wells, using the minimum free energy yield of –20 kJ mol^{-1} (Table 6). The FEF values for the energetically favorable reactions range from –2.4×10^{-19} to –1.3×10^{-14} kJ cell^{-1} s^{-1} (Table 5).

Table 6. The free energy of reaction and free energy flux for energetically favorable biogeochemical reactions. [Free energy of the reaction (ΔG_r), kilojoules per mole (kJ mol^{-1}); Free energy flux (FEF), kilojoules per cell per second (kJ cell^{-1} s^{-1})]

Redox Reaction	RBI Well 11		RBI Well 12		Pristine Well 13	
	ΔG_r	FEF	ΔG_r	FEF	ΔG_r	FEF
2. Acetate + NO_3^- + H_2O → $2HCO_3^-$ + NH_3	-496	-2.6 x 10^{-14}	-498	-4.9 x 10^{-14}	-490	-4.9 x 10^{-14}
5. $4H_2$ + NO_3^- + H^+ → NH_3 + $3H_2O$	-482	-3.03 x 10^{-18}	-477	-7.53 x 10^{-18}		
6. Acetate + SO_4^{2-} → $2HCO_3^-$ + HS^-	-55	-2.9 x 10^{-15}	-56	-5.5 x 10^{-15}	-57	-5.7 x 10^{-15}
8. 4Acetate + $4H_2O$ → $4CH_4$ + $4HCO_3^-$	-237	-1.3 x 10^{-14}	-203	-2.0 x 10^{-14}	-226	-2.2 x 10^{-14}
11. Acetate + $8Fe(OH)_3$ + $15H^+$ → $8Fe_2^+$ + $20H_2O$ + $2HCO_3^-$	-409	-3.0 x 10^{-16}	-957	-6.9 x 10^{-16}	-413	-2.5 x 10^{-16}
12. HS^- + $8Fe(OH)_3$ + $15H^+$ → SO_4^{2-} + $8Fe^{2+}$ + $20H_2O$	-354	-2.6 x 10^{-16}	-363	-2.6 x 10^{-16}	-356	-2.2 x 10^{-16}
13. $4H_2$ + $2O_2$ → $4H_2O$	-740	-4.7 x 10^{-18}	-704	-1.1 x 10^{-17}	-702	-8.8 x 10^{-18}
14. Acetate + $2O_2$ → $2HCO_3^-$ + H^+	-781	-2.8 x 10^{-14}	-781	-2.3 x 10^{-14}	-782	-2.2 x 10^{-14}
15. CH_4 + $2O_2$ → HCO_3^- + H^+ + H_2O	-722	-3.2 x 10^{-17}	-730	-1.9 x 10^{-15}	-725	-2.0 x 10^{-16}
16. HS^- + $2O_2$ → SO_4^{2-} + H^+	-726	-6.1 x 10^{-15}	-725	-6.2 x 10^{-15}	-725	-6.7 x 10^{-15}
17. ($^4/_3$)NH_3 + $2O_2$ → ($^4/_3$)NO_2^- + ($^4/_3$)H^+ + ($^4/_3$)H_2O	-341	-2.5 x 10^{-19}	-370	-1.9 x 10^{-17}	-360	-9.5 x 10^{-18}
18. H_2S + $4NO_3^-$ → SO_4^{2-} + $4NO_2^-$ + $2H^+$	-471	-5.2 x 10^{-15}	-504	-5.5 x 10^{-15}	-496	-5.0 x 10^{-15}
19. $3H_2S$ + $4NO_2^-$ + $2H^+$ + $4H_2O$ → $3SO_4^{2-}$ + $4NH_4^+$	-1340	-9.9 x 10^{-16}	-1251	-9 x 10^{-16}	-1280	-7.8 x 10^{-16}
20. ($^4/_3$)NH_4^+ + $2O_2$ → ($^4/_3$)NO_2^- + ($^8/_3$)H^+ + ($^4/_3$)H_2O	-226	-1.0 x 10^{-16}	-251	-7.8 x 10^{-15}	-241	-3.2 x 10^{-15}
21. $4NO_2^-$ + $2O_2$ → $4NO_3^-$	-248	-5.6 x 10^{-15}	-213	-2.9 x 10^{-16}	-221	-4.0 x 10^{-15}
22. $8Fe^{2+}$ + $2O_2$ + $20H_2O$ → $8Fe(OH)_3$ + $16H^+$	-372	-2.7 x 10^{-15}	-362	-2.5 x 10^{-15}	-369	-2.6 x 10^{-15}

7.3 Shallow Groundwater Well Differentiation

The 16 favorable biogeochemical reactions were compared between the three

shallow groundwater wells to see if the influx of WWTP effluent is affecting the native

microbial community. Figure 12 shows the FEF distributions for all favorable

biogeochemical reactions in the three shallow groundwater wells. The favorable

biogeochemical reactions are listed on the horizontal axis in the order of most to least

favorable reaction for the pristine well. The vertical axis shows FEF values.
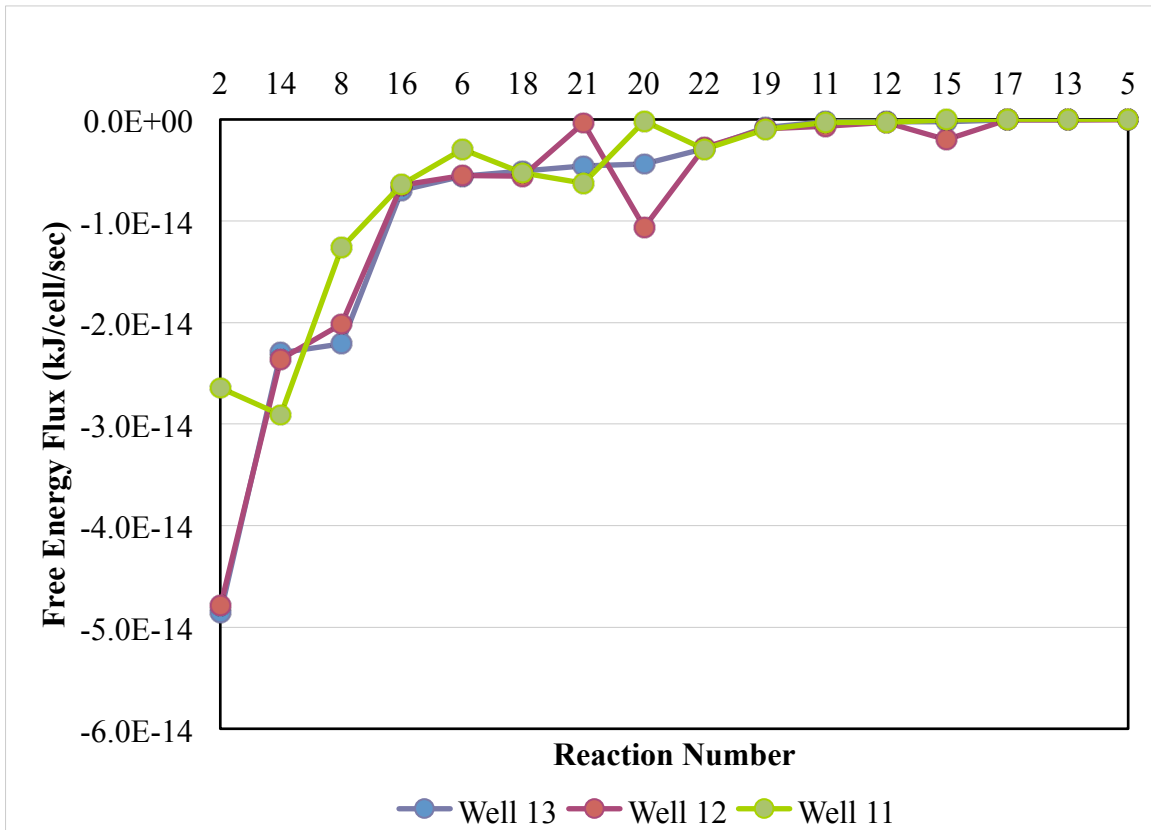
Figure 12. Free energy flux listed in order from most to least in the pristine well (Well 13).
[Free energy flux (FEF), kilojoules per cell per second (kJ cell^{-1} s^{-1})]

      All three wells have similar distributions for the various metabolic pathways.

Acetate oxidation using nitrate (reaction 2) is the most favorable metabolic pathway, with

acetate oxidation using oxygen and acetate fermentation (reactions 14 and 8) being the

next favorable, respectively. Five of the top six reactions are either heterotrophic

reactions using acetate or methane, or acetate fermentation. The remaining reactions

account for very little of the available FEF. Differences between the three wells are subtle

and generally follow the same pattern.

Figures 13-15 show the available FEF distributions for the highly favorable

heterotrophic and fermentation reactions in all three shallow groundwater wells.

Figure 13. Free energy flux distributions for heterotrophic and fermentation metabolic pathways in Well 11 calculated using the limiting reactant. Legend represents reaction numbers described in Table 4.
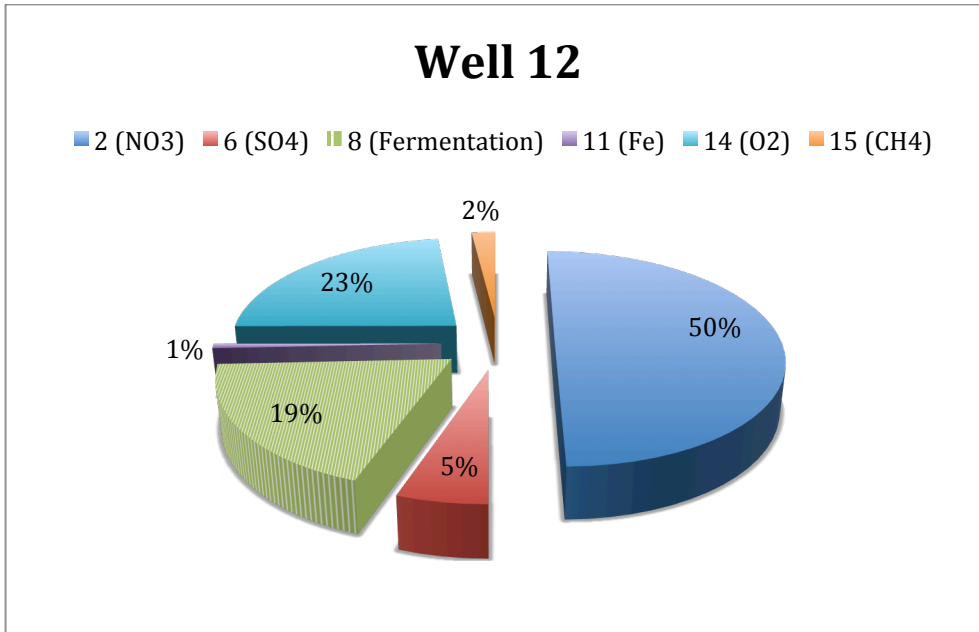
Figure 14. Free energy flux distributions for heterotrophic and fermentation metabolic pathways in Well 12 calculated using the limiting reactant. Legend represents reaction numbers described in Table 4.

Well 13

Legend: ■ 2 (NO3) ■ 6 (SO4) ▨ 8 (Fermentation) ■ 11 (Fe) ■ 14 (O2) ■ 15 (CH4)

0%

27%

0%   19%

7%

47%
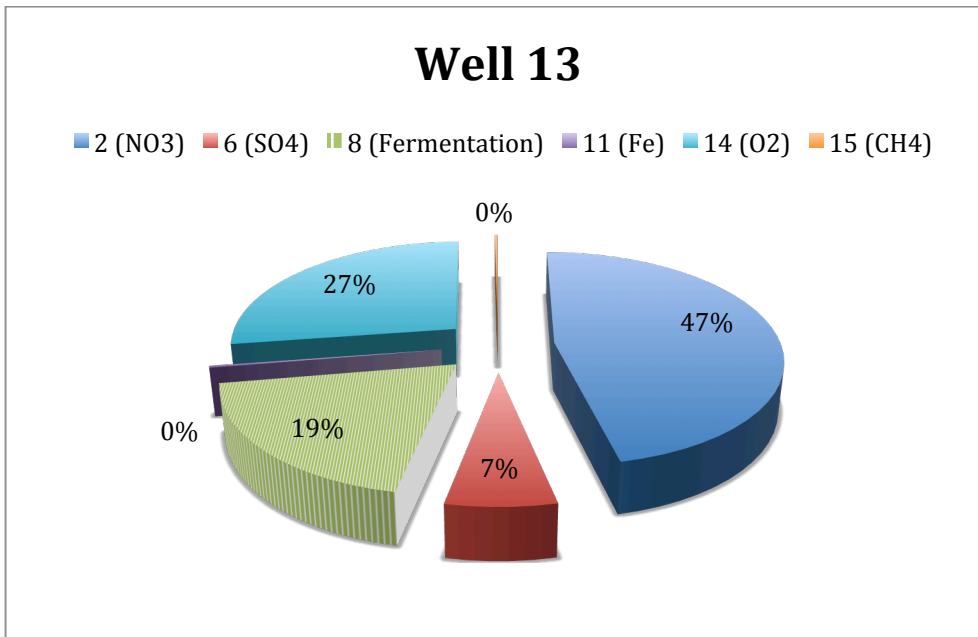
Figure 15. Free energy flux distributions for heterotrophic and fermentation metabolic pathways in Well 13 calculated using the limiting reactant. Legend represents reaction numbers described in Table 4.

FEF distributions were calculated using the limiting reactant of the equation, which determines the amount of free energy available for microorganisms to access. Among the heterotrophic reactions, nitrate is the primary available electron acceptor. Oxygen is the second most available electron acceptor after nitrate. RBI Well 12 and the pristine well, Well 13, appear to have similar distributions for FEF throughout all reactions. RBI Well 11 differs slightly with less available nitrate activity. Iron usage is more prevalent than expected, however, iron values are a maximum estimate since the limit of detection was used in thermodynamic calculations.

To ascertain the FEF actually being used in a given well as opposed to the total available FEF, the limiting constituent in Equation 6 was changed to include all constituents, not just the reactants. Figures 16-18 illustrate the relative amount of free energy actually being used for heterotrophic and fermentation reactions.

Comparisons between the available FEF (Figures 13-15) and the FEF actually being used (Figures 16-18) highlight several interesting features. Although there is an abundance of available fermentative FEF (reaction 8), very little is actually being used. Fermentation is used most in Well 12 (1%), compared to Well 11 or Well 13. Acetate oxidation by oxygen is dominant in all three wells, especially Well 11. The use of nitrate to oxidize acetate is the second most used in Well 12 and Well 13, at 32% and 19%, respectively; nitrate is more prevalent in Well 12. Ferrous iron is used to a greater extent (14-9%) than would be expected based on its contribution (1% or less) to the overall FEF. Acetate oxidation using sulfate is small and relatively constant in all three wells. The actual FEF used is approximately 10% of the total available.
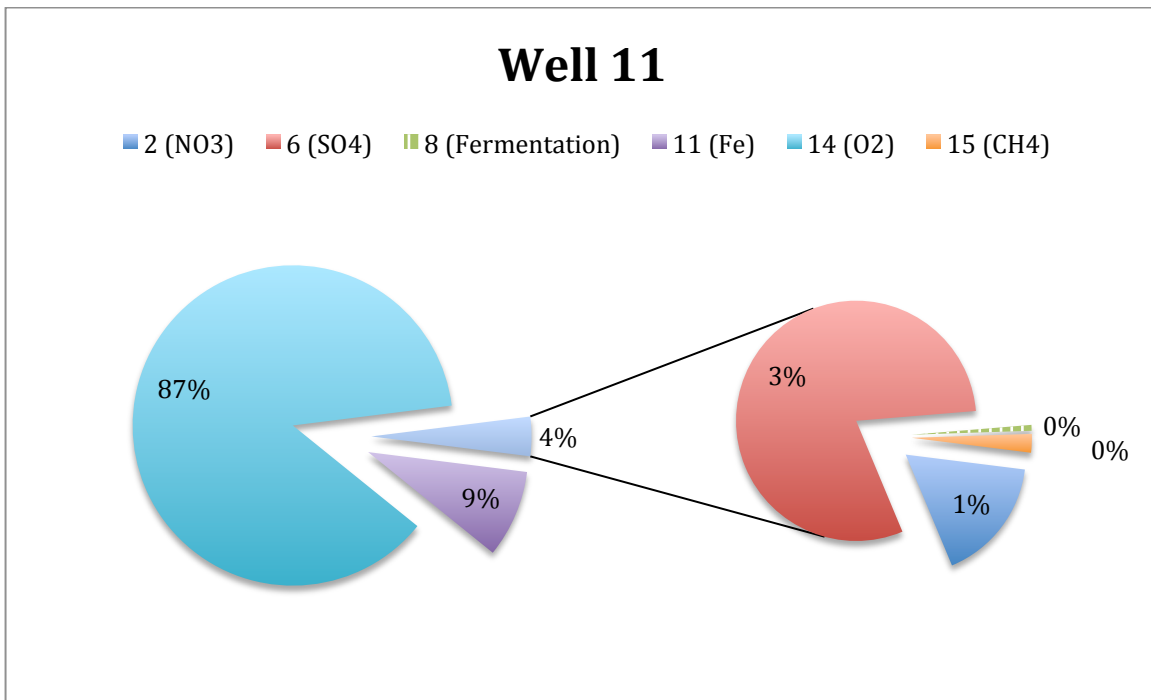
Figure 16. Free energy flux distributions for heterotrophic and fermentation metabolic pathways in Well 11 calculated using the overall limiting constituent. Legend represents reaction numbers described in Table 4.
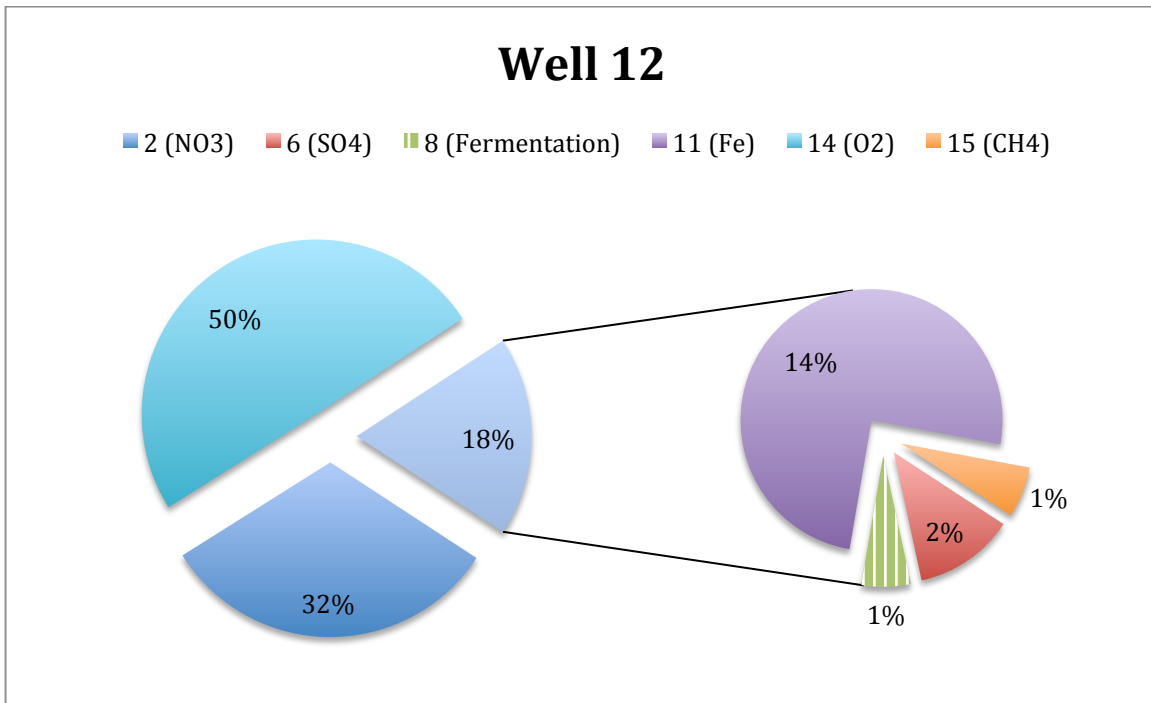
Figure 17. Free energy flux distributions for heterotrophic and fermentation metabolic pathways in Well 12 calculated using the overall limiting constituent. Legend represents reaction numbers described in Table 4.
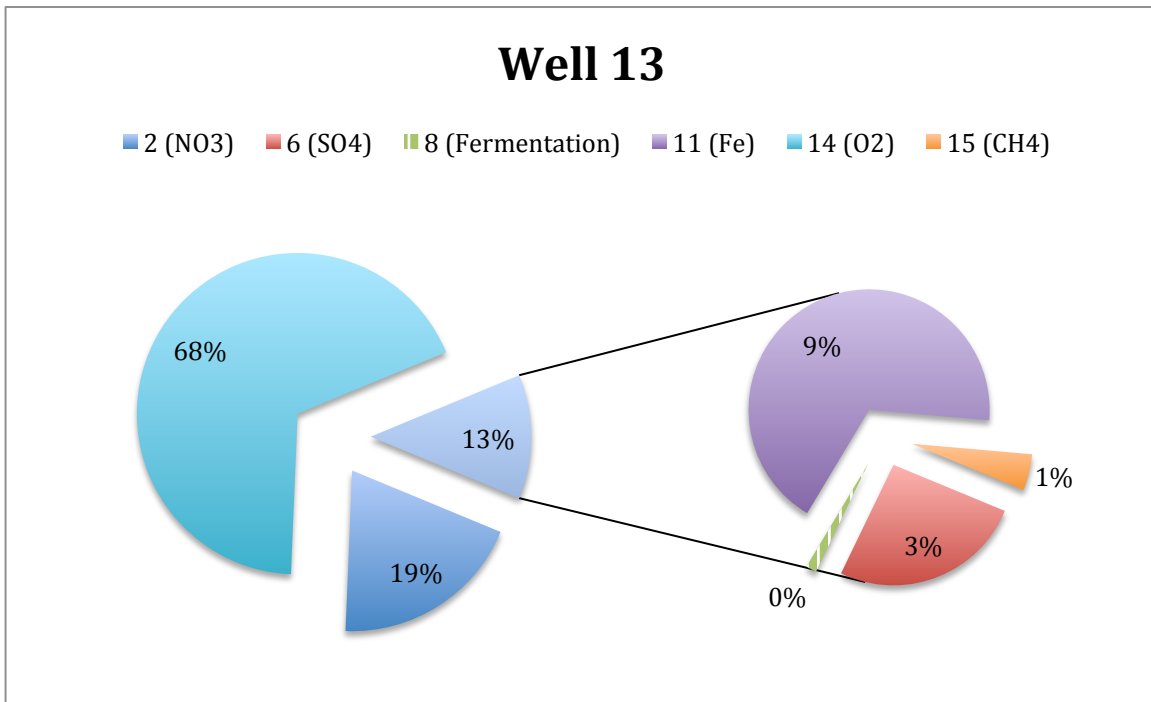
Figure 18. Free energy flux distributions for heterotrophic and fermentation metabolic pathways in Well 13 calculated using the overall limiting constituent. Legend represents reaction numbers described in Table 4.

Trends in FEF used indicate that Well 11 is closer to the pristine well (Well 13) than it is to Well 12. This is consistent with the fact that pumpage in Well 11 has been steadily declining and currently contributes less than 10% of the total pumpage out of the wellfield. As such, Well 11 pulls less water from the river than Well 12. This differential between the two RBI wells is also seen in the community data. It should be noted that the FEF analysis is limited to the high energy heter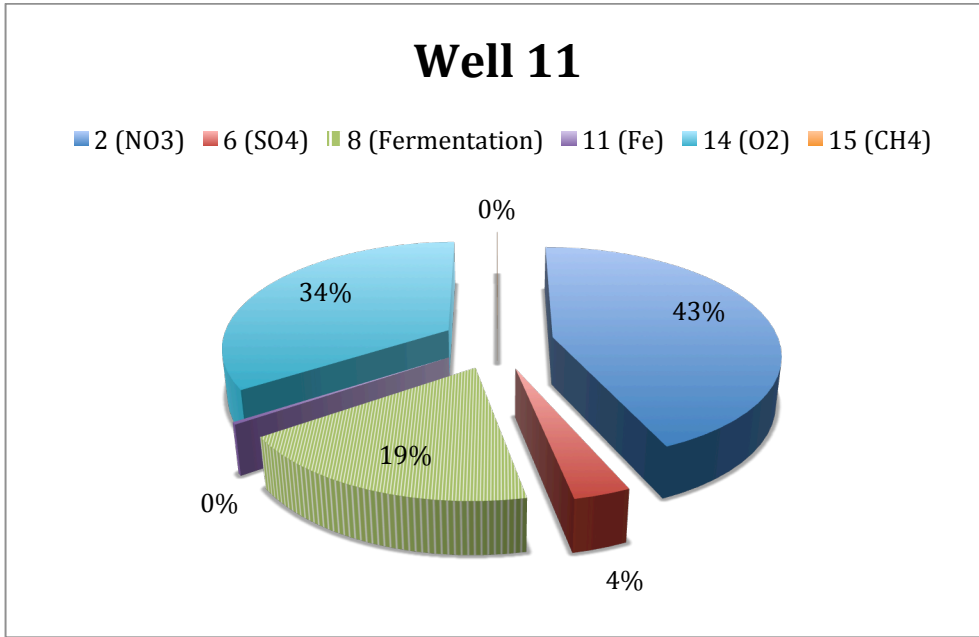otrophic and fermentation reactions. Many autotrophic reactions are likely occurring, especially in the impacted RBI well (Well 12). The genomic data indicate the presence of several taxa capable of autotrophic nitrogen cycle reactions. For example, the relative decrease in nitrate, increase in nitrite and ammonium observed in Well 12 are classic conditions indicative of anammox reactions (Lams and Kuypers, 2011). The bacteria mediating this process were discovered in 1999. This newly discovered reaction converts nitrite and ammonium directly to nitrogen and water. Well 12 also exhibits a high FEF for ammonium oxidation (reaction 20 in Figure 12). Taxa capable of performing both of these reactions are found in the genomic data.

7.4 Microbial Community Diversity Analyses

The energetically favorable biogeochemical reactions were compared with metagenomic possibilities to gain an understanding of the aquifer biome and its associated reactivity with an influx of effluent. Natalie Gayner from the School of Freshwater Sciences completed microbial analyses. Preliminary 16S rRNA gene sequencing indicated distinct microbial community differences between the WWTP, Fox River, and RBI well Well 12 (Figure 19). Microorganisms were not observed to be transferring through the soil matrix from the Fox River into the shallow groundwater, as

assumed in thermodynamic analyses. Only river water and its mobile chemical constituents were observed to be entering the RBI wells. Furthermore, preliminary community composition analysis of 16S rRNA gene sequencing indicated predominantly novel taxa and typical groundwater organisms in the wells like denitrifiers, iron oxidizers, and sulfide oxidizers.
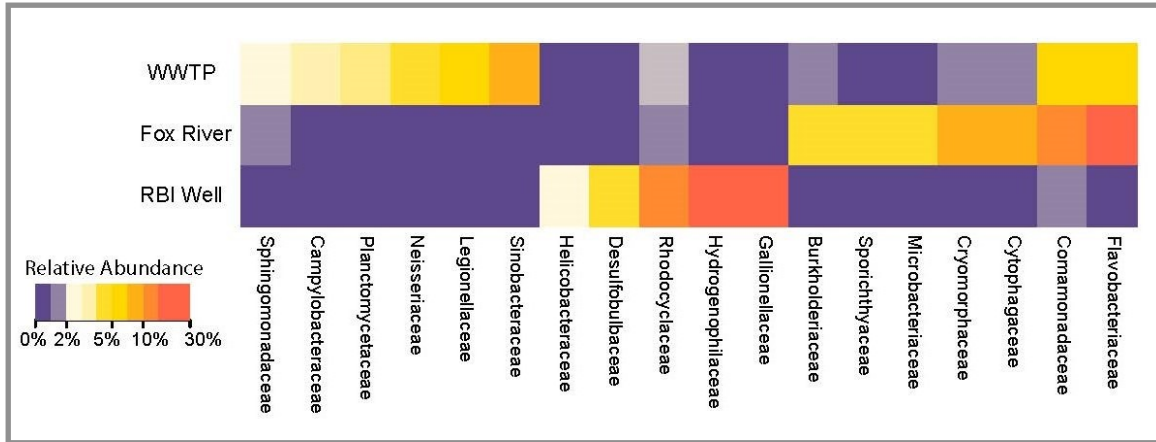
Figure 19. Heatmap showing the relative abundance of bacterial families (only families present at greater than 2% of the community composition in at least one sample depicted).

After preliminary analyses, extensive genomic samples were collected and data was statistically analyzed using the software R. After performing sequence data processing and rigorous quality control using DADA2 with an error rate of 0%, the sequence dataset (RNA and DNA, 0.1 µm and 0.2 µm fractions, from Well 11, Well 12, Well 13, and Fox River sites) included 51,331 unique amplicon sequence variants (ASVs), or taxa. Further processing in R removed sequences occurring at a relative abundance less than 0.01% in each sample. A threshold of 0.01% was chosen because it was strict enough to remove cross contamination of sequences among samples, however, rare community members were still included. Furthermore, the taxa that are in low abundances have little influence to overall community patterns. Using the threshold, the

dataset was cut down from 51,3331 to 21,910 unique amplicon sequence variants for analysis.

On Figure 20, the top 10 DNA and top 10 RNA amplicon sequence variants (ASVs), or unique 16S sequences that translate to unique organisms, were used to generate a heat map of relative abundance across all samples. A majority of the classifications resulted in the ASVs being unclassified/unknown due to groundwater being relatively unstudied. DNA is on the left and RNA is on the right, categorized by well and then by filter size. The most abundant organisms are not the same across samples. The color blue indicates 0% relative abundance and the warmer colors indicate higher relative abundances. There are observable differences between wells and filter sizes. Also, some ASVs were only identified in the RNA sequences. For example, the bottom unclassified ASV in Figure 20 is completely blue across all samples for DNA, indicating it is not present, however, the ASV was in the top ten most abundant organisms for the RNA sequences. Targeting strictly DNA may not be as all encompassing for the 16S rRNA gene practice.
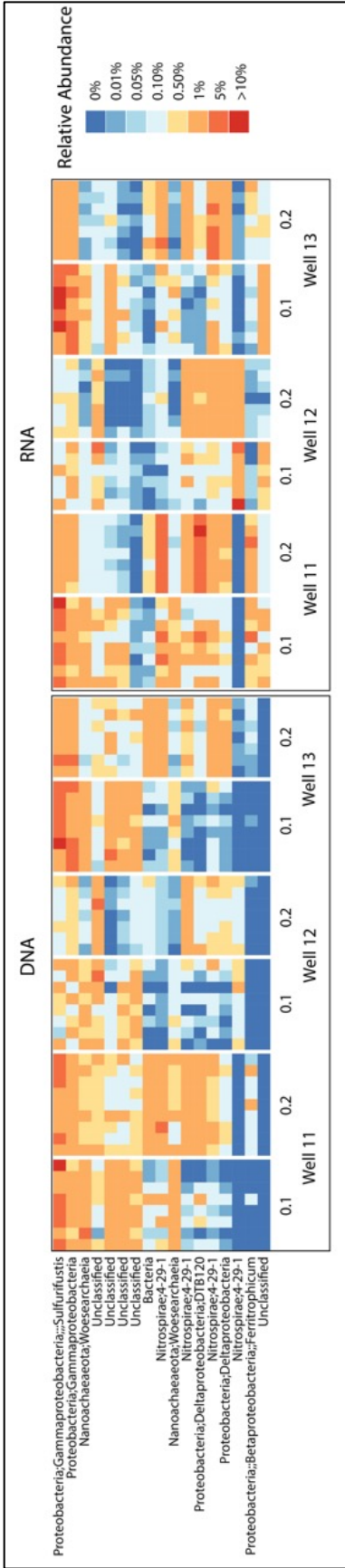
Figure 20. Heatmap of the top 10 most abundant DNA and RNA amplicon sequence variants (ASVs) categorized by filter size (0.1 μm and 0.2 μm) and well site.

Furthermore, organisms identifying with the recently discovered radiations called DPNN superphylum and CPR was discovered in the shallow groundwater wells. In this study, Nanoarchaea Woesearchaea (DPNN) and Nitrospirae (CPR) were discovered that identify with the newly discovered microorganisms. Novel and newly discovered organisms having been identified in this study, which answers "who" is in each shallow groundwater well, however, there is little characterization about their metabolic capabilities of these novel organisms.

The full dataset of 21,910 unique ASVs, which includes all groundwater and Fox River samples (Well 11, Well 12, and Well 13), was used to compare microbial communities. A community distance matrix was developed using Bray-Curtis dissimilarity in the vegan package in R (Oksanen et al., 2013). Non-metric Multidimensional Scaling was used to develop an ordination of all microbial communities. Complex data with many dimensions were condensed down into two-dimensional space for easier visualization and interpretation. The Fox River and groundwater samples clearly cluster independently from each other as shown in Figure 21, indicating microbial communities of the groundwater wells and the Fox River are distinct from one another. Well 12 also clusters independently of Well 11 and Well 13. Well 11 and Well 13 do not cluster independently, likely due to the decrease in pumping in Well 11 allowing it to revert back to its natural aquifer state.
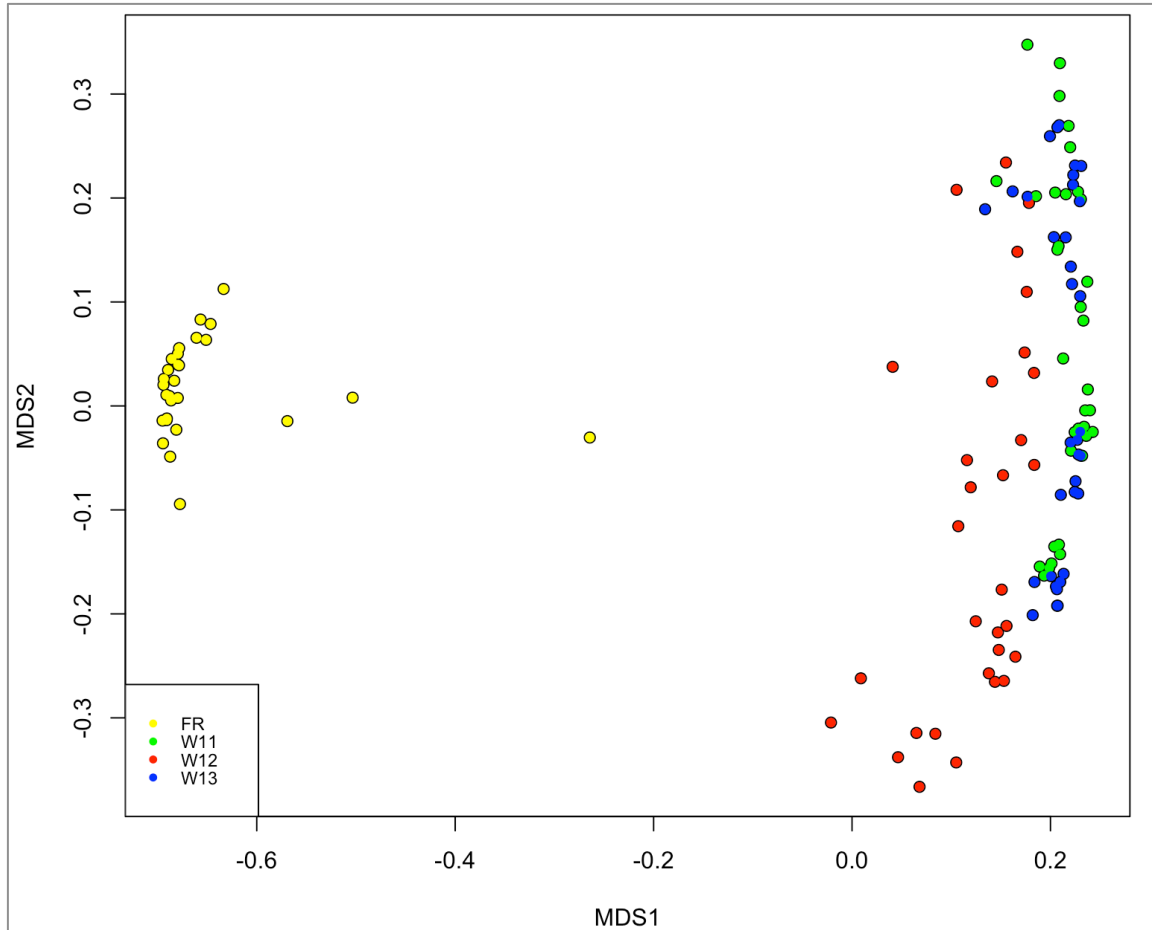
Figure 21. NMDS ordination of Fox River and groundwater microbial community samples.

The dataset consisting of just the groundwater samples (Well 11, Well 12, and Well 13) was used to compare groundwater microbial communities. In Figure 22, a dendrogram was generated in R for the entire groundwater dataset using hierarchical clustering of pairwise dissimilarity between samples using Bray-Curtis dissimilarity in the vegan package in R (Oksanen et al., 2013). A dendrogram is a tree diagram that depicts taxonomic relationships. The height at which the branches merge at each node is relative to their similarity showing relationships between the samples.

The first branch split (right to left) and therefore the largest factor contributing to the variation in the dataset is site location. Well 12 is different from Well 11 and Well 13.

49

The factor driving the second largest difference in the dataset is filter size. The 0.1 µm

and 0.2 µm communities differ within the dataset. The third factor driving a difference is,

again, site location between Well 11 and Well 13. The last factor significantly

contributing to a difference in the dataset is RNA and DNA.
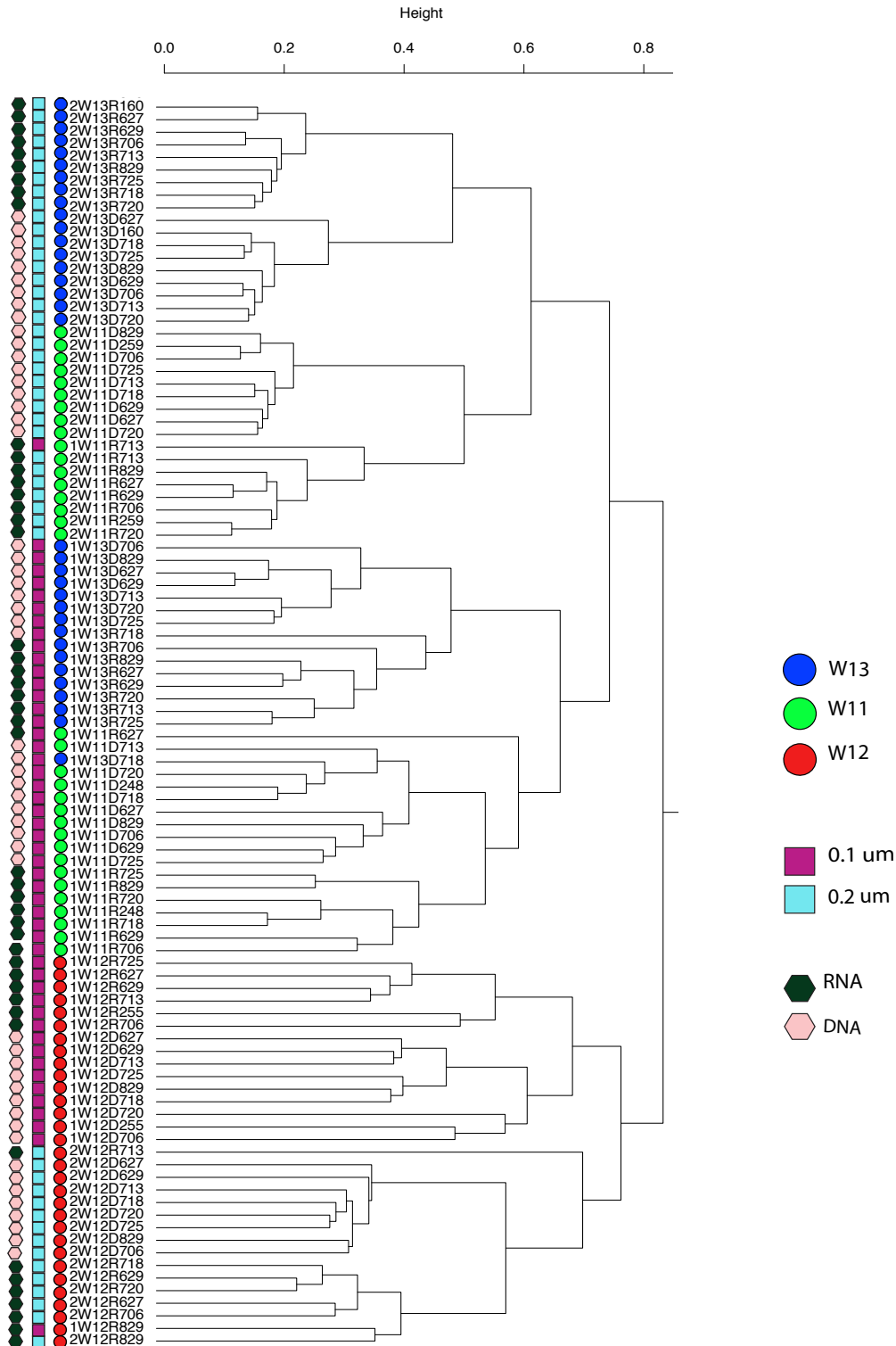
Figure 22. Groundwater microbial community dendrogram. NMDS and Bray-Curtis dissimilarity were used to generate a dendrogram demonstrating the differences across groundwater microbial community samples. The groundwater microbial communities cluster first by well location in that W12 is significantly different from the other two wells. Filter size fraction then cluster together, then Well 13 and Well 11 cluster separately, and then RNA and DNA cluster together.

Overall, the data indicates that the microbial community in Well 12 (RBI well actively drawing in river water) differs from Well 11 (former RBI well) and Well 13 (pristine well). This suggests that the former RBI well does not draw in river water and is returning to a state similar to the non-river infiltrated groundwater. The data also shows that bacterial size is a significant differentiator in microbial communities and explains community variation in Well 11 and Well 13. This means, the 0.1 μm communities in Well 11 are more similar to the 0.1 μm communities in Well 13 than to the 0.2 μm communities in Well 11, the same location, and vice versa.

Chapter 8: Conclusions

Microorganisms are also known to be key players in biogeochemical reactions that influence water quality and treatment processes. This study investigated if, and to what extent the microbial community present in the shallow groundwater of southeastern Wisconsin is affected by the influx of treated municipal wastewater effluent. This study combined two graduate students' research by merging geochemical analysis and microbial analyses to obtain a more complete picture of a valuable freshwater resource.

Thermodynamic analyses show 16 favorable biogeochemical reactions applicable to the shallow groundwater wells (Table 6). Trends in FEF used indicate that Well 11 is closer to the pristine well (Well 13) than it is to the impacted RBI well (Well 12). This is consistent with the fact that pumpage in Well 11 has been steadily declining and currently contributes less than 10% of the total pumpage out of the wellfield. Electrons are being transferred via several mechanisms. Many autotrophic reactions are likely occurring, especially in Well 12, however, FEF analysis was limited to the high energy heterotrophic and fermentation reactions. Nitrate and oxygen are dominant electron acceptors, while iron and sulfate account for very little. The actual FEF used is approximately 10% of the total available.

Microbial community analyses showed many unclassified and novel taxa have been discovered in the shallow groundwater wells. The novel taxa are found within the recently discovered ASVs that have expanded the tree of life. Genomic differences of this type have been observed before in deep aquifers, but never in such a shallow system. Because the microorganisms are newly discovered, not much is known about their functional capabilities. Well 12 communities differ most greatly from Well 11

(previously impacted) and Well 13 (pristine) communities (Figure 22), and there are observable differences between filter sizes.

Because so many taxa are undefined, trends between thermodynamic and microbial data are approximate, however, the genomic and the thermodynamic datasets are consistent. The taxa associated with the shallow groundwater microbial communities suggest the potential for fermentation, methanogenesis, nitrate reduction, sulfate reduction, nitrite oxidation, iron oxidation, and sulfur oxidation in the aquifer. RBI Well 12 contains specialists related to chemoautotrophs, methylotrophs, ferementers, sulfur-oxidizers (*Rhodocyclaceae),* sulfate reduction and nitrite oxidation (*Nitrospirae*), and iron or methane metabolisms (Woesarchaeota). The pristine well contains specialists potentially related to nitrite reduction, fermentation (Parcubacteria), iron oxidation (*Gallionellaceae*), and sulfur oxidation (*Sulfurifustis*). In thermodynamic analyses, FEF distributions show the related thermodynamic pathways for the taxa associated with the shallow groundwater are favorable.

Understanding groundwater systems will only become increasingly more valuable with increasing demands for freshwater and as natural and anthropogenic contamination threatens these vital water resources. The methods and results of this study are applicable to other groundwater systems and can be invaluable to the scientific community due to the relatively unstudied nature of microbial systems in groundwater, which can lead to discovering new life.

References

Amend, J. and Shock, E., 2001, Energetics of overall metabolic reactions of themophilic and hyperthermophilic Archaea and Bacteria: FEMS Micobiolgy Reviews, v. 25, p. 175-243.

Ball, J., and D. Nordstrom.1991. User's ,annual for WATEQ4F, with revised thermodynamic data base and text cases for calculating speciation of major, trace, and redox elements in natural waters. Open-File Report 91-183.

Cape, M. and T. Grundl. 2006. Geochemical Factors Controlling Radium Activity in a Sandstone Aquifer. Ground Water 44(4):518-527.

Castelle, C. J., Wrighton, K. C., Thomas, B. C., Hug, L. A., Brown, C. T., Wilkins, M. J., … Banfield, J. F. (2015b). Genomic expansion of domain archaea highlights roles for organisms from new phyla in anaerobic carbon cycling. *Current Biology*, *25*(6), 690–701. https://doi.org/10.1016/j.cub.2015.01.014

Davidson, M., Silver, B., Onstott, T., Moser, D., Gihring, T., Pratt, L., Boice, E., Lollar, B., Lippmann-Pipke, J., Pfiffner, S., Kieft, T., Seymore, W., and Ralston, C., 2011, Capture of planktonic microbial diversity in fractures by long-term monitoring of flowing boreholes, Evander Basin, South Africa: Geomicrobiology Journal, v. 28, p. 275–300.

Delmont, T. O., Simonet, P., & Vogel, T. M. (2012). Describing microbial communities and performing global comparisons in the 'omic era. *The ISME Journal*, *6*(9), 1625–1628. http://doi.org/10.1038/ismej.2012.55

Eme, L., Ford Doolittle, W. (2015). Microbial diversity: A bonanza of phyla. *Current Biology*, *25*(6), R227–R230. https://doi.org/10.1016/j.cub.2014.12.044

Feinstein, D., Cherkauer, D., and Grundl, T. 2010. Examining the viability of riverbank inducement (RBI) as another source of water in Wisconsin. USGS & UWM: Community Presentation.

Fields-Sommers, Laura Rachel, "Assessing the Effects of Riverbank Inducement on a Shallow Aquifer in Southeastern Wisconsin" (2015). *Theses and Dissertations*. 1049. https://dc.uwm.edu/etd/1049

Fox River Study Group, Inc. 2018.

Gaumnitz, Lisa, et al. "A Growing Thirst for Groundwater." *Wisconsin Natural Resources*, June 2004.

Hug, L. A., Baker, B. J., Anantharaman, K., Brown, C. T., Probst, A. J., Castelle, C. J., … Banfield, J. F. (2016). A new view of the tree of life. *Nature Microbiology*, *1*(5). https://doi.org/10.1038/nmicrobiol.2016.48

Klump, S., Grundl, T., Purtschert, R., Kipfer. R. 2008. Groundwater and climate dynamics derived from noble gas, ^{14}C, and stable isotope data. *Geology*; 36 (5): 395–398. doi: https://doi.org/10.1130/G24604A.1

Lam, Phyllis, and Marcel M.m. Kuypers. "Microbial Nitrogen Cycling Processes in Oxygen Minimum Zones." *Annual Review of Marine Science*, vol. 3, no. 1, 2011, pp. 317–345., doi:10.1146/annurev-marine-120709-142814.

Lin, X., McKinley, J., Resch, C. T., Kaluzny, R., Lauber, C. L., Fredrickson, J. Knight, R., and Konopka, A. 2012. Spatial and temporal dynamics of the microbial community in the Hanford unconfined aquifer. *ISME J.* 6:1665-1676.

Liu, X., Li, M., Castelle, C. J., Probst, A. J., Zhou, Z., Pan, J., … Gu, J.-D. (2018). Insights into the ecology, evolution, and metabolism of the widespread Woesearchaeotal lineages. *Microbiome*, *6*(1), 102. https://doi.org/10.1186/s40168-018-0488-2

Lisle, J.T. 2014. Survival of Bacterial Indicators and the Functional Diversity of Native Microbial Communities in the Floridan Aquifer System, South Florida: U.S. Geological Survey Open–File Report 2014-1011, 70 p., http://dx.doi.org/10.3133/ofr20141011

Luef, B., Frischkorn, K. R., Wrighton, K. C., Holman, H.-Y. N., Birarda, G., Thomas, B. C., Singh, A., Williams, K. H., Siegerist, C. E., Tringe, S. G., Downing, K. H., Comolli, L. R. and Banfield, J. F. 2015. Diverse uncultivated ultra-small bacteria cells in groundwater. *Nat. Commun.* 6:6372.

McCoy, Mary Kate. "As Wells Go Deeper, Radium Levels Rise in State Tap Water." *WisconsinWatch.org*, 31 Mar. 2016, wisconsinwatch.org/2016/03/as-wells-go-deeper-radium-levels-rise-in-state-tap-water/

National Oceanic and Atmospheric Association. https://www.ncdc.noaa.gov/cdo-web/datasets/ANNUAL/stations/COOP:478937/detail

Oksanen, J., Blanchet, F. G., Kindt, R., Legendre, P., Minchin, P. R., O'Hara, R. B., … Wagner, H. (2013). Package 'vegan.' *R Package Ver. 2.0–8*, 254. https://doi.org/10.4135/9781412971874.n145

Onstott, T., 2005, Impact of CO2 injections on deep subsurface microbial ecosystems and potential ramifications for the surface biosphere, in Benson, S., Oldenburg, C., Hoversten, M., Imbus, S., eds., Carbon Dioxide Capture for Storage in Deep

Geologic Formations—Results from the CO2 Capture Project: Elsevier, p. 1207–1239.

Parada, A. E., Needham, D. M., & Fuhrman, J. A. (2016). Every base matters: Assessing small subunit rRNA primers for marine microbiomes with mock communities, time series and global field samples. *Environmental Microbiology*, *18*(5), 1403–1414. https://doi.org/10.1111/1462-2920.13023

Parkhurst, D., and Appelo, C. 2005. User's Guide to PHREEQC (Version 2)- A computer program for speciation, batch-reaction, one-dimensional transport, and inverse geochemical calculations. United States Geological Survey (USGS).

Rinke, C., Schwientek, P., Sczyrba, A., Ivanova, N. N., Anderson, I. J., Cheng, J. F., … Woyke, T. (2013). Insights into the phylogeny and coding potential of microbial dark matter. *Nature*, *499*(7459), 431–437. https://doi.org/10.1038/nature12352

Shink B. 1997. Energetics of syntrophic cooperation in methanogenic degradation. Microbiol Mol Biol Rev 61:262–280.

Smith, R. J., Jeffries, T. C., Roudnew, B., Fitch, A. J., Seymour, J. R., Delpin, M. W., Newton, K., Brown, M. H., and Mitchell, J. G. 2012. Metagenomic comparison of microbial communities inhabiting confined and unconfined aquifer ecosystems. *Environ. Microbiol.* 14:240-253.

Thauer, R., Jungermann, K., and Decker, K., 1977, Energy conservation in chemotrophic anaerobic bacteria: Bacteriological Reviews, v. 41, p. 100–180.

Thorp, Anna Maria, "Applying Geochemistry to Investigate the Occurrence of Riverbank Inducement into a Shallow Aquifer in Southeastern Wisconsin" (2013). *Theses and Dissertations*. 240. https://dc.uwm.edu/etd/240

Vengosh, A., Starinsky, A., Kolodny, Y., and Chivas, A.R., 1991. Boron isotope geochemistry as a tracer for the evolution of brines and associated hot springs from the Dead Sea, Israel. Geochemica et Cosmochimica Acta, 55: 1689-1695.

Walters, W., Hyde, E. R., Berg-Lyons, D., Ackermann, G., Humphrey, G., Parada, A., … Knight, R. (2016). Improved Bacterial 16S rRNA Gene (V4 and V4-5) and Fungal Internal Transcribed Spacer Marker Gene Primers for Microbial Community Surveys. *MSystems*, *1*(1), e00009-15. https://doi.org/10.1128/mSystems.00009-15

Waukesha County. https://www.waukeshacounty.gov/globalassets/parks--land-use/planning-zoning/chapter-3-final-ag-cultur-natur-print-ready.pdf.

Waukesha Water Utility. 2014. Public Radium Notice. Public Notice.

Waukesha Water Utility, Waukesha Water Utility, 18 Sept. 2017.

APPENDICES

APPENDIX A:

Sample Collection Information

Coordinates of Sampling Sites in Decimal Degrees

Sampling Site	Latitude	Longitude
EM275	43.099327	-88.103161
IZ385	43.063351	-88.183740
IZ386	43.051841	-88.176827
SV631	42.901237	-88.059776
Well 11	42.959938	-88.279256
Well 12	42.961012	-88.279063
Well 13	42.961236	-88.289167
Hygeia Spring	42.879817	-88.205125
Fox 0	43.120068	-88.164715
Fox 1	43.011395	-88.234244
Fox 2	42.977690	-88.264797
Fox 3	42.876283	-88.210559
Root River	42.858027	-87.997586
Sussex Creek	43.102008	-88.210367
Underwood Creek	43.042935	-88.056498
Brookfield WWTP	43.052745	-88.177110
Sussex WWTP	43.126171	-88.216985
Waukesha WWTP	42.998190	-88.249151

Contacts for Sampling Sites

Municipality	Contact Person	Contact Information	Location
Brookfield Water Utility	Mike Terry	Telephone: (262) 796-6717 Email: terrym@ci.brookfield.wi.us	19700 Riverview Drive, Brookfield, WI
St. Martin of Tours	Tom Breedom	Telephone: (414) 333-47000	7963 South 116 St, Franklin, WI
Waukesha Water Utility	Randy Dehn	Email: rdehn@waukesha-water.com	3815 Creekside Drive, Waukesha, WI
Brookfield WWTP	Bob Berenson	Email: berenson@ci.brookfield.wi.us	21225 Enterprise Ave, Brookfield, WI
Sussex WWTP	Jon Baumann	Telephone: (262) 246-5184	23525 Clover Drive, Sussex, WI
Waukesha WWTP	Greg Markle	Telephone: (262) 524-3631 Email: gmarkle@waukesha-wi.gov	600 Sentry Drive, Waukesha, WI

Microseeps Gas Stripping Instructions

Pace Analytical®

Microseeps Gas Stripping Cell Instructions

INSTALLATION AND OPERATION

To place the gas stripping cell into service:

1. Remove one of the cell assemblies from the packing carton. Refer to Figure 1 to become familiar with the parts of the cell.
2. Connect the inlet tube of the cell to the outlet of your pump. The inlet tube is designed to connect to ¼ inch O.D. hard tubing. Secure the connection (nylon wire ties are recommended).
3. Insert the drain tube of the cell into a waste container, keeping the end of the tube at the bottom of the container. Any waste container of suitable size may be used. A 2-liter soda pop bottle may be placed in the waste container to determine pumping flow rate.
4. Secure the cell assembly so that the housing cover is above the glass housing (*i.e.* upright). A ring stand and clamp are recommended for this purpose.
5. Turn the pump on and check for leaks. If any leaks are found seal them before proceeding. Measure, in ml per minute, the flow rate of the pump. If a 2-liter soda pop bottle was used, the flow rate can be determined by measuring how many minutes it takes to fill the bottle, then substituting the measured time into the following equation.

Flow = 2000 ml/time to fill in minutes

Consult Table 1 to determine the equilibrium time needed to gas strip at this flow rate.
NOTE: Use a flow rate between 100 ml/min and 500 ml/min. Do not turn off the pump.

6. Unclamp the cell assembly, invert it and re-secure the assembly in the inverted position. Make sure the drain tube is still in the waste container and the end of the drain tube is near the bottom of the bottle.
7. Connect the (supplied) stopcock to the syringe and the (supplied) needle to the stopcock. Place the stopcock in the open position (*i.e.* so that the stopcock handle is in-line with the syringe). Draw the plunger back on the syringe to the 20.0-mL mark. Keeping the cell in the inverted position, insert the needle into the needle guide. Pierce the septum and inject the air into the cell. Then remove the needle and syringe from the assembly and carefully cover the needle. Do not discard the syringe apparatus.

8. Start timing and let the ground water pump through the cell for the time specified in Table 1 for your particular pumping speed. Meanwhile, be sure that the sample vial is properly labeled and that the flow rate and any other relevant field data are recorded in the field log.
NOTE: Be sure to keep the end of the drain tube at the bottom of the waste container. This will insure that outside air is not drawn into the cell. Failure to do this will invalidate the sample.
9. When the equilibration time is up, **turn off the pump,** unclamp the cell and reclamp it in its upright position. Verify that the plunger of the syringe is pushed all the way in and that the stopcock is in the open position, then insert the needle into the needle guide and pierce the septum. Withdraw 1-mL of gas by pulling back on the syringe plunger while holding the syringe body in place, remove the syringe from the cell and expel the sample. Immediately re-insert the needle into the needle guide and pierce the septum. Withdraw a 15-mL sample of gas and, with the needle still through the septum, close the stopcock. Rapidly withdraw the needle from the septum and place it through septum on the sample vial (see Figure 2). Open the stopcock and completely depress the syringe barrel. Discard the syringe apparatus according to Local, State and Federal regulations.

Decontamination/Cleaning

Pump at least 1 liter of potable water through the cell. The cell assembly is now ready for re-use.

The only expendable part of the cell is the sampling septum (part 7). Normally, each septum may be used for the collection of up to 5 samples. If bubbles are seen rising up from the septum when the cell is inverted the septum MUST be replaced. Instructions for replacing the septum are provided on the reverse.

SAMPLING QUESTIONS?
CALL PAES AT **1-412-826-5245**
MON.- FRI.9 TO 5 PM EST

Figures and Tables on Reverse

Figure 1. Cross section of Microseeps Gas
Stripping Cell
1. Housing Cover
2. Jet Spray Nozzle
3. Nylon Tie
4. Inlet Tube
5. Needle Guide Port
6. Drain Tube
7. Replaceable Septum
8. Glass Housing
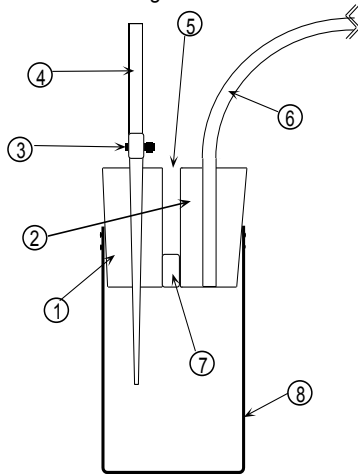
Figure 2. Cross section of septum bottle
1. Septum
2. Metal Closure
3. Glass vial
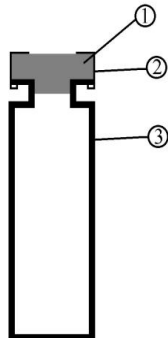
Table 1.

Flow rate (ml/min)	Sampling time (min)
100-120	30
130-150	25
160-200	20
210-300	15
>300	10

Replacing the Sampling Port Septum
All part numbers refer to Figure 1.
1. Remove the housing cover (part 1) from the glass housing (part 8).
2. Use a handy, blunt tipped object to push the replaceable septum (part 7) out of the housing cover. The cover to a needle works well for this purpose, but be sure that the needle is **NOT** in the cover. Discard the old septum.
4. Take a new septum and wet both the new septum and the housing cover with potable water.
5. Carefully using the same blunt instrument used in step three above, slide the new septum into the hole from which the old septum was removed. The bottom of the new septum must be flush with the narrow end of the housing cover.
6. If the housing cover is not still wet, wet it again with potable water. Place the bottom end of the housing cover into the glass housing and push it in until less than 3/8" are above the rim of the glass housing. This may require some force.
7. Follow the cleaning procedures described above to prepare the cell for a return to service.

APPENDIX B:

Field and Analytical Results

Field Analysis

Field Analysis Parameters

Name	Date	pH	Specific Conductivity (mmhos/cm)	Temperature (°C)	Dissolved Oxygen by Meter (mg/L)	Calculated HCO_3^-
EM275	11/2/16	7.03	0.77	9.90	0.26	NA
EM275	8/25/17	7.02	NA	10.20	0.55	324.52
IZ385	11/2/16	NA	0.04	6.79	1.05	NA
IZ385	8/25/17	6.89	NA	11.50	0.49	407.48
IZ386	11/2/16	6.81	1.30	11.20	0.06	NA
SV631	11/7/16	7.11	0.81	14.90	0.09	472.15
SV631	9/15/17	7.51	NA	17.50	0.29	361.12
Well 11	11/3/16	6.85	1.23	6.95	0.16	522.33
Well 11	2/28/17	6.68	1.28	10.00	0.13	616.98
Well 11	7/27/17	7.00	NA	10.50	0	NA
Well 11	8/1/17	7.05	NA	10.50	0	541.68
Well 11	11/8/17	7.19	1.20	10.30	NA	395.28
Well 11	11/29/17	6.90	NA	NA	NA	390.40
Well 11	12/1/17	6.84	NA	NA	NA	397.72
Well 11	1/26/18	7.06	0.96	10.20	NA	431.88
Well 12	11/3/16	7.05	1.17	10.40	0.04	469.84
Well 12	2/28/17	6.97	0.18	NA	0.01	600.39
Well 12	7/27/17	6.50	NA	10.40	0.25	NA
Well 12	8/1/17	6.90	NA	10.50	0.39	636.84
Well 12	11/8/17	7.18	NA	10.60	0.02	370.88
Well 12	11/29/17	7.15	0.65	10.80	0.11	356.24
Well 12	12/1/17	7.08	NA	NA	NA	353.80
Well 12	1/26/18	6.97	NA	NA	NA	424.56
Well 13	11/17/16	6.96	0.93	10.50	0.00	453.01
Well 13	2/28/17	5.14	0.95	10.50	0.00	563.86
Well 13	7/27/17	7.50	NA	10.50	0.30	NA

Field Analysis Parameters (Continued)						
Well 13	8/1/17	7.21	NA	10.50	0.00	468.48
Well 13	11/8/17	7.21	NA	10.50	0.46	324.52
Well 13	11/29/17	7.10	NA	NA	NA	363.56
Well 13	12/1/17	7.12	NA	NA	NA	351.36
Well 13	1/26/18	7.15	0.79	10.50	NA	390.40
Hygeia Spring	11/7/16	6.87	0.87	12.70	6.43	392.03
Hygeia Spring	8/20/17	6.90	NA	NA	6.59	315.98
Fox 0	11/7/16	7.49	0.90	10.50	Fox 0	448.00
Fox 0	8/5/17	7.10	0.81	19.80	Fox 0	341.60
Fox 1	11/7/16	6.90	1.06	10.80	10.00	420.60
Fox 1	8/19/17	8.09	NA	23.50	6.95 - 7.21	317.20
Fox 2	11/7/16	7.59	1.20	12.80	9.96	390.00
Fox 2	8/20/17	7.92	NA	23.50	4.14	353.80
Fox 3	11/7/16	6.86	0.92	10.70	7.00	386.55
Fox 3	8/20/17	7.58	NA	NA	1.6 - 1.89	422.12
Root River	11/7/16	6.81	1.06	9.40	8.70	413.36
Root River	8/31/17	8.32	NA	19.80	6.40	283.04
Sussex Creek	11/7/16	8.09	1.34	13.10	12.37	451.76
Sussex Creek	8/5/17	8.36	NA	19.00	5.43	351.36
Underwood Creek	11/7/16	8.44	14.22	13.80	19.00	346.23
Underwood Creek	8/20/17	8.36	NA	24.10	13.40	270.84

Atomic Absorption Spectroscopy with Calibration Curves for Major Ions

Calcium Standards AA Spectrometer Fall 2016				
Standard	Concentration (mg/L)	Absorption Start	Absorption Final	Absorption Average
Blank	0	0.0037	0.0035	0.0035
1	0.5	0.01849	0.0182	0.0185
2	1	0.0340	0.0339	0.0338
3	3	0.0906	0.0903	0.0906
4	5	0.1444	0.1456	0.1449
5	10	0.2465	0.2467	0.2469
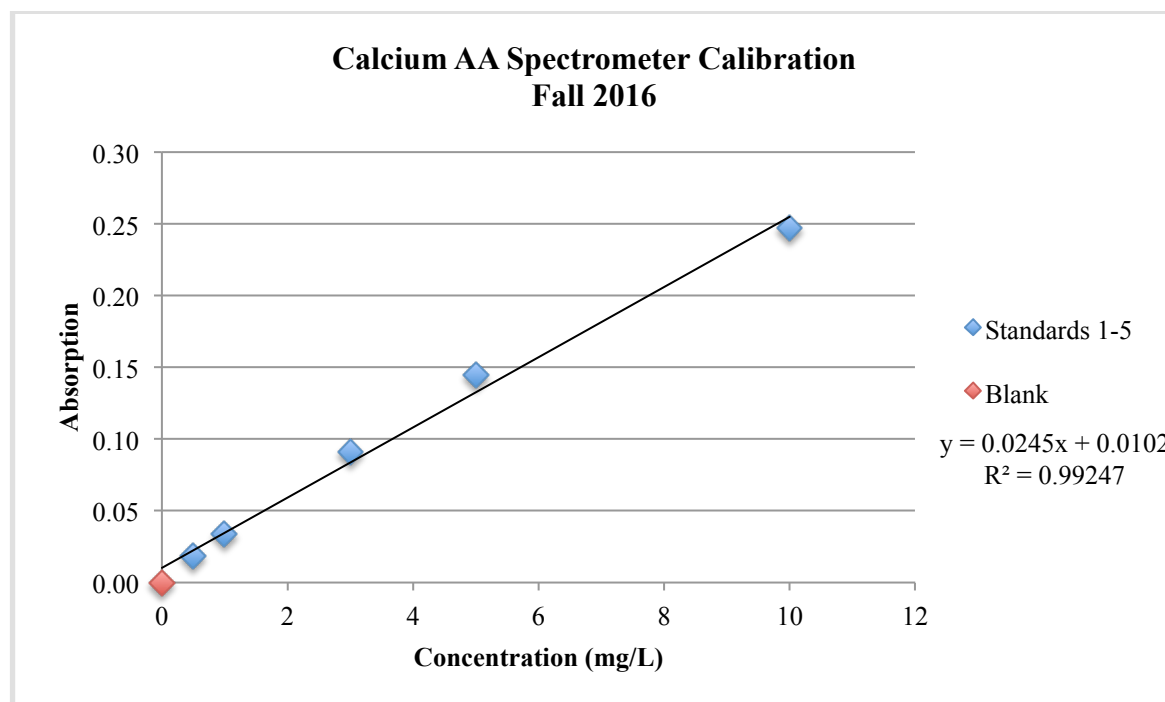
Calcium AA Spectrometer Calibration Fall 2016

Standards 1-5

Blank

$y = 0.0245x + 0.0102$
$R^2 = 0.99247$

Calcium AA Spectrometer Results Fall 2016

Sample ID	Sample Date	Absorption	Calculated Concentration (mg/L)	Dilution Factor	Corrected Concentration (mg/L)
EM275	11/2/16	0.0338	0.9973	100	96.36
IZ385	11/2/16	0.0412	1.2470	100	126.79
IZ386	11/2/16	0.0403	1.2159	100	123.07
SV631	11/7/16	0.0264	0.7603	100	66.14
Well 11	11/3/16	0.0369	1.0990	100	109.01
Well 11	2/28/17	0.0367	1.0934	100	108.33
Well 12	11/3/16	0.0371	1.1071	100	109.99
Well 12	2/28/17	0.0359	1.0680	100	105.26
Well 13	11/17/16	0.0324	0.9543	100	90.84
Well 13	2/28/17	0.0326	0.9592	100	91.48
Hygeia Spring	11/7/16	0.0261	0.7524	100	65.15
Fox 0	11/7/16	0.0288	0.8375	100	75.96
Fox 1	11/7/16	0.0262	0.7567	100	65.69
Fox 2	11/7/16	0.0279	0.8105	100	72.54
Fox 3	11/7/16	0.0262	0.7567	100	65.69
Root River	11/7/16	0.0277	0.8043	100	71.75
Sussex Creek	11/7/16	0.0316	0.9272	100	87.40
Underwood Creek	11/7/16	0.0307	0.8993	100	83.83
Brookfield WWTP	11/2/16	0.0340	1.0033	100	97.25
Sussex WWTP	11/3/16	0.0301	0.8814	100	81.56
Waukesha WWTP	11/3/16	0.0334	0.9846	100	94.73

Magnesium Standards AA Spectrometer Fall 2016

Standard	Concentration (mg/L)	Absorption Start	Absorption Final	Absorption Average
Blank	0	0.0025	0.0027	0.0026
1	0.1	0.1371	0.1397	0.1383
2	0.25	0.3202	0.3201	0.3208
3	0.5	0.6117	0.6143	0.6100
4	1	1.0472	1.0564	1.0520
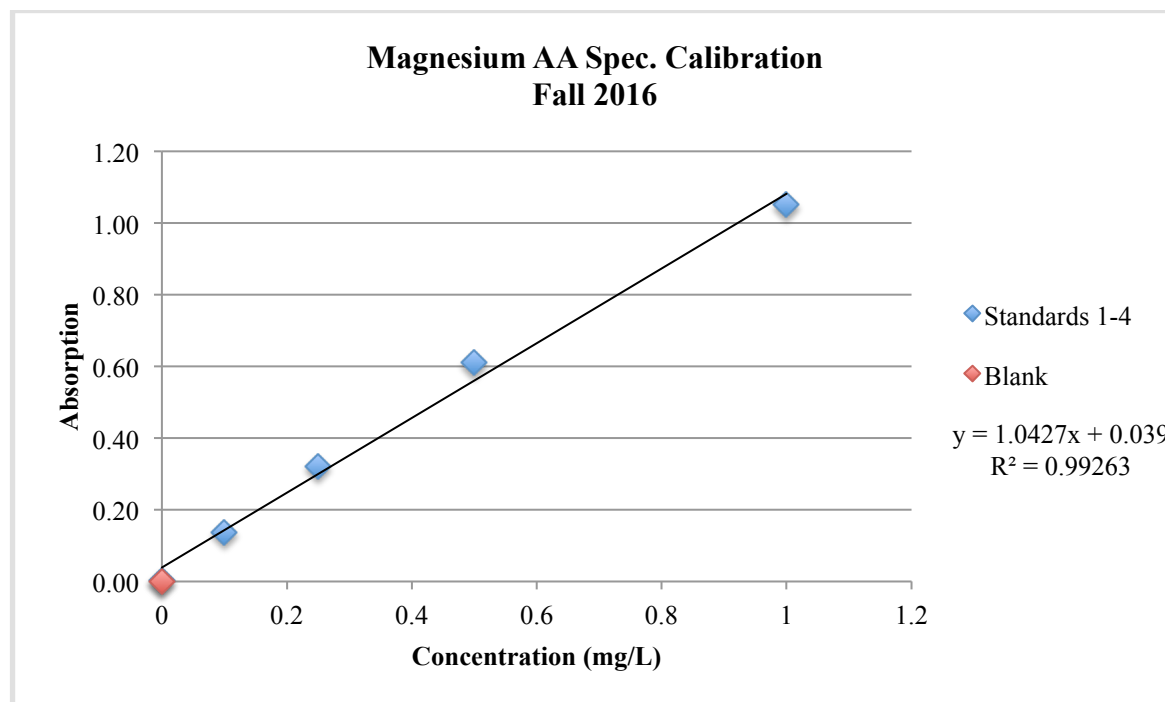
Magnesium AA Spec. Calibration Fall 2016

Standards 1-4

Blank

$y = 1.0427x + 0.039$
$R^2 = 0.99263$

Absorption

Concentration (mg/L)

Magnesium AA Spectrometer Results Fall 2016

Sample ID	Sample Date	Absorption	Calculated Concentration (mg/L)	Dilution Factor	Corrected Concentration (mg/L)
EM275	11/2/16	0.5062	0.4054	100	44.81
IZ385	11/2/16	0.6462	0.5312	100	58.24
IZ386	11/2/16	0.6721	0.5564	100	60.72
SV631	11/7/16	0.6822	0.5663	100	61.69
Well 11	11/3/16	0.6242	0.5105	100	56.13
Well 11	2/28/17	0.6171	0.5043	100	55.44
Well 12	11/3/16	0.6252	0.5115	100	56.22
Well 12	2/28/17	0.6163	0.5037	100	55.37
Well 13	11/17/17	0.6329	0.5185	100	56.96
Well 13	2/28/17	0.6385	0.5239	100	57.50
Hygeia Spring	11/7/16	0.4574	0.3621	100	40.13
Fox 0	11/7/16	0.5002	0.4000	100	44.25
Fox 1	11/7/16	0.4722	0.3748	100	41.55
Fox 2	11/7/16	0.4839	0.3854	100	42.68
Fox 3	11/7/16	0.4624	0.3663	100	40.61
Root River	11/7/16	0.4913	0.3920	100	43.38
Sussex Creek	11/7/16	0.5335	0.4300	100	47.43
Underwood Creek	11/7/16	0.5774	0.4697	100	51.64
Brookfield WWTP	11/2/16	0.5421	0.4377	100	48.25
Sussex WWTP	11/3/16	0.4874	0.3885	100	43.01
Waukesha WWTP	11/3/16	0.4987	0.3987	100	44.10

Sodium Standards AA Spectrometer Fall 2016				
Standard	Concentration (mg/L)	Absorption Start	Absorption Final	Absorption Average
Blank	0	0.0196	0.0234	0.0218
1	0.1	0.0840	0.0848	0.0838
2	0.25	0.1664	0.1676	0.1668
3	0.5	0.3066	0.3080	0.3085
4	1	0.5498	0.5450	0.5473
5	2	0.9133	0.9133	0.9062
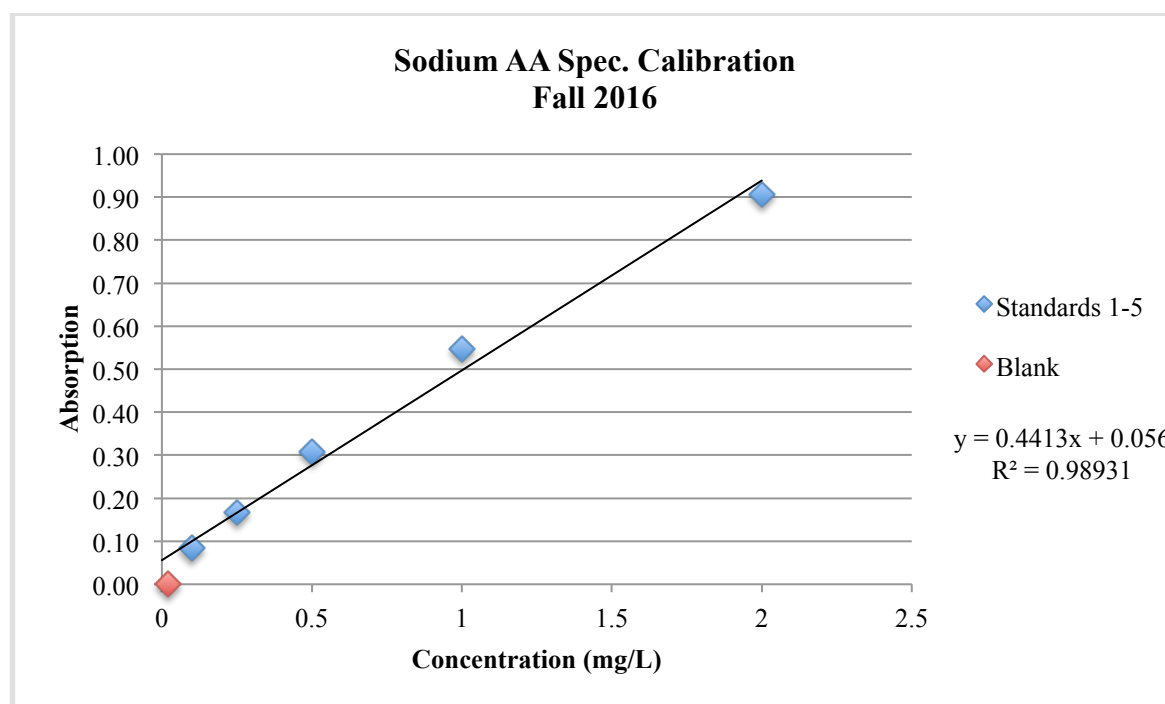
Sodium AA Spec. Calibration Fall 2016

$y = 0.4413x + 0.056$
$R^2 = 0.98931$

Sodium AA Spectrometer Results Fall 2016					
Sample ID	Sample Date	Absorption	Calculated Concentration (mg/L)	Dilution Factor	Corrected Concentration (mg/L)
EM275	11/2/16	0.1101	0.1446	100	12.27
IZ385	11/2/16	0.6198	1.1614	100	127.78
IZ386	11/2/16	0.4581	0.7960	100	91.13
SV631	11/7/16	0.1352	0.1895	100	17.96
Well 11	11/3/16	0.5487	1.0000	100	111.65
Well 11	2/28/17	0.5346	0.9686	100	108.45
Well 12	11/3/16	0.4506	0.7792	100	89.43
Well 12	2/28/17	0.4284	0.7296	100	84.39
Well 13	11/17/17	0.2425	0.3817	100	42.47
Well 13	2/28/17	0.2335	0.3659	100	40.24
Hygeia Spring	11/7/16	0.3404	0.5583	100	64.45
Fox 0	11/7/16	0.3428	0.5629	100	65.00
Fox 1	11/7/16	0.5262	0.9494	100	106.56
Fox 2	11/7/16	0.6118	1.1420	100	125.95
Fox 3	11/7/16	0.3969	0.6679	100	77.25
Root River	11/7/16	0.5185	0.9317	100	104.81
Sussex Creek	11/7/16	0.7376	1.4555	100	154.46
Underwood Creek	11/7/16	0.8348	1.7606	100	176.48
Brookfield WWTP	11/2/16	0.1503	0.2180	100	213.69
Sussex WWTP	11/3/16	0.1316	0.1827	100	171.33
Waukesha WWTP	11/3/16	0.1394	0.1975	100	189.16

Potassium Standards AA Spectrometer Fall 2016				
Standard	Concentration (mg/L)	Absorption Start	Absorption Final	Absorption Average
Blank	0	0.0121	0.0134	0.0123
1	0.25	0.1579	0.1587	0.1573
2	0.5	0.2800	0.2824	0.2806
3	1	0.4922	0.4913	0.4893
4	2	0.8536	0.8440	0.8558
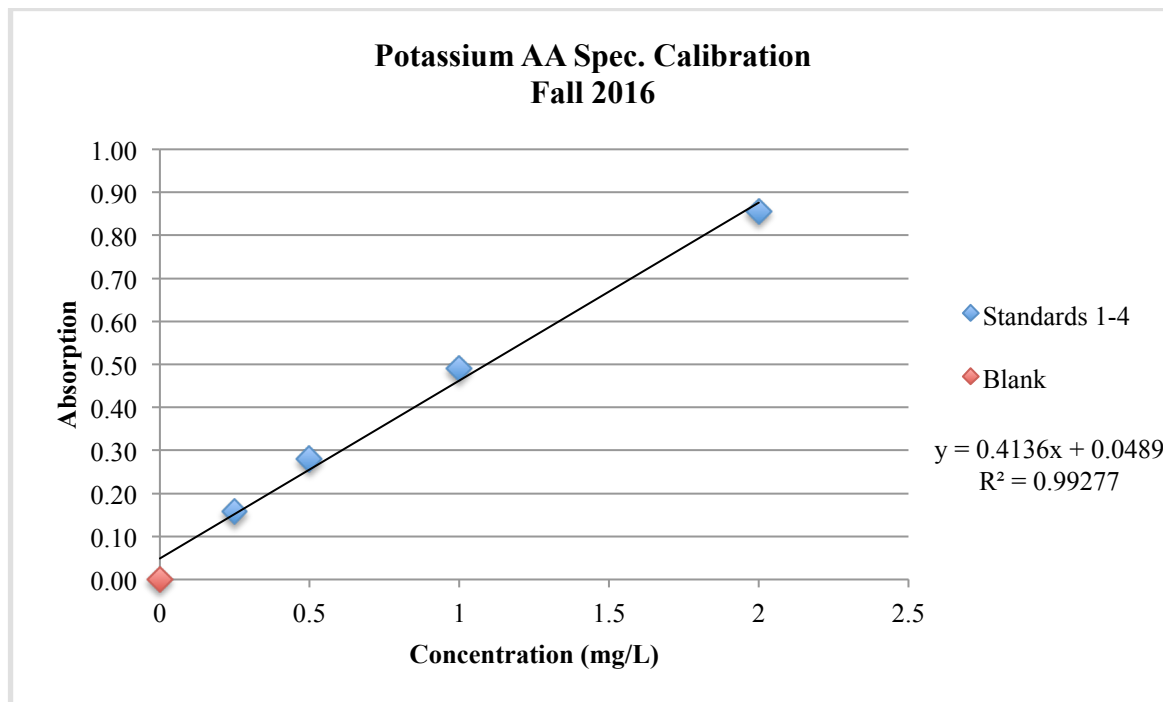
Potassium AA Spec. Calibration Fall 2016

$y = 0.4136x + 0.0489$
$R^2 = 0.99277$

Potassium AA Spectrometer Results Fall 2016					
Sample ID	Sample Date	Absorption	Calculated Concentration (mg/L)	Dilution Factor	Corrected Concentration (mg/L)
EM275	11/2/16	0.1279	0.1992	10	1.91
IZ385	11/2/16	0.1662	0.2654	10	2.84
IZ386	11/2/16	0.1519	0.2406	10	2.49
SV631	11/7/16	0.0822	0.1205	10	0.81
Well 11	11/3/16	0.1568	0.2491	10	2.61
Well 11	2/28/17	0.1184	0.1829	10	1.68
Well 12	11/3/16	0.1494	0.2363	10	2.43
Well 12	2/28/17	0.1416	0.2228	10	2.24
Well 13	11/17/17	0.1181	0.1394	10	1.67
Well 13	2/28/17	0.0932	0.1823	10	1.07
Hygeia Spring	11/7/16	0.1125	0.1726	10	1.54
Fox 0	11/7/16	0.1519	0.2405	10	2.49
Fox 1	11/7/16	0.1581	0.2409	10	2.64
Fox 2	11/7/16	0.1901	0.3106	10	3.42
Fox 3	11/7/16	0.1504	0.2380	10	2.45
Root River	11/7/16	0.1429	0.2251	10	2.27
Sussex Creek	11/7/16	0.2998	0.5378	10	6.07
Underwood Creek	11/7/16	0.6385	1.3604	10	14.26
Brookfield WWTP	11/2/16	0.4177	0.8080	10	8.92
Sussex WWTP	11/3/16	0.4182	0.8092	10	8.93
Waukesha WWTP	11/3/16	0.5244	1.0785	10	11.50

Calcium Standards AA Spectrometer Fall 2017				
Standard	Concentration (mg/L)	Absorption Start	Absorption Final	Absorption Average
Blank	0	0.0045	0.0044	0.0045
1	0.5	0.0257	0.0258	0.0258
2	1	0.0473	0.0474	0.0476
3	3	0.1292	0.1291	0.1290
4	5	0.2016	0.2040	0.2030
5	10	0.3683	0.3674	0.3689

Calcium AA Spec. Calibration Fall 2017

Standards 1-5

Blank

$y = 0.0365x + 0.0114$
$R^2 = 0.99721$

Absorption (y-axis)

Concentration (mg/L) (x-axis)

Calcium AA Spectrometer Results Fall 2017

Sample ID	Sample Date	Absorption	Calculated Concentration (mg/L)	Dilution Factor	Corrected Concentration (mg/L)
EM275	8/25/17	0.0461	0.9665	100	95.31
IZ385	8/25/17	0.0531	1.1282	100	114.48
SV631	9/15/17	0.0038	0.8011	100	75.34
Well 11	6/29/17	0.0543	1.1566	100	117.75
Well 11	7/27/17	0.0254	0.4872	100	38.50
Well 12	6/29/17	0.0509	1.0760	100	108.44
Well 12	7/27/17	0.0291	0.5765	100	48.69
Well 13	6/29/17	0.0476	0.9996	100	99.34
Well 13	7/27/17	0.0339	0.6899	100	61.86
Hygeia Spring	8/20/17	0.0392	0.8086	100	76.24
Fox 0	8/5/17	0.0345	0.7021	100	63.52
Fox 1	8/19/17	0.0385	0.7925	100	74.30
Fox 2	8/20/17	0.0417	0.8663	100	83.20
Fox 3	8/20/17	0.0363	0.7437	100	68.44
Root River	8/31/17	0.0387	0.7967	100	74.81
Sussex Creek	8/5/17	0.0418	0.8686	100	83.48
Underwood Creek	8/20/17	0.0453	0.9482	100	93.09
Brookfield WWTP	8/24/17	0.0518	1.0973	100	110.91
Sussex WWTP	8/31/17	0.0456	0.9547	100	93.88
Waukesha WWTP	8/31/17	0.0474	0.9955	100	98.82

Magnesium Standards AA Spectrometer Fall 2017				
Standard	Concentration (mg/L)	Absorption Start	Absorption Final	Absorption Average
Blank	0	0.0038	0.0042	0.0040
1	0.1	0.1131	0.1150	0.1146
2	0.25	0.2826	0.2816	0.2831
3	0.5	0.5215	0.5240	0.5236
4	1	0.9124	0.9233	0.9193

Magnesium AA Spec. Calibration Fall 2017

$y = 0.9104x + 0.0321$
$R^2 = 0.99386$

Magnesium AA Spectrometer Results Fall 2017					
Sample ID	Sample Date	Absorption	Calculated Concentration (mg/L)	Dilution Factor	Corrected Concentration (mg/L)
EM275	8/25/17	0.4556	0.4235	100	46.13
IZ385	8/25/17	0.5578	0.5346	100	57.74
SV631	9/15/17	0.5795	0.5586	100	60.12
Well 11	6/29/17	0.5522	0.5284	100	57.13
Well 11	7/27/17	0.5052	0.4918	100	51.96
Well 12	6/29/17	0.5384	0.5136	100	51.67
Well 12	7/27/17	0.4771	0.4618	100	48.88
Well 13	6/29/17	0.5592	0.5361	100	57.90
Well 13	7/27/17	0.4992	0.4854	100	51.30
Hygeia Spring	8/20/17	0.4111	0.3748	100	41.62
Fox 0	8/5/17	0.4073	0.3707	100	41.21
Fox 1	8/19/17	0.4710	0.4405	100	48.20
Fox 2	8/20/17	0.4819	0.4525	100	49.40
Fox 3	8/20/17	0.4422	0.4088	100	45.04
Root River	8/31/17	0.4670	0.4362	100	47.77
Sussex Creek	8/5/17	0.4691	0.4384	100	48.00
Underwood Creek	8/20/17	0.5375	0.5125	100	55.51
Brookfield WWTP	8/24/17	0.5202	0.4955	100	53.61
Sussex WWTP	8/31/17	0.4699	0.4393	100	48.09
Waukesha WWTP	8/31/17	0.4412	0.4077	100	44.93

Sodium Standards AA Spectrometer Fall 2017				
Standard	Concentration (mg/L)	Absorption Start	Absorption Final	Absorption Average
Blank	0	0.0049	0.0047	0.0047
1	0.1	0.0604	0.0610	0.0616
2	0.25	0.1416	0.1359	0.1395
3	0.5	0.2609	0.2612	0.2595
4	1	0.5019	0.4979	0.4997
5	2	0.8635	0.8536	0.8564
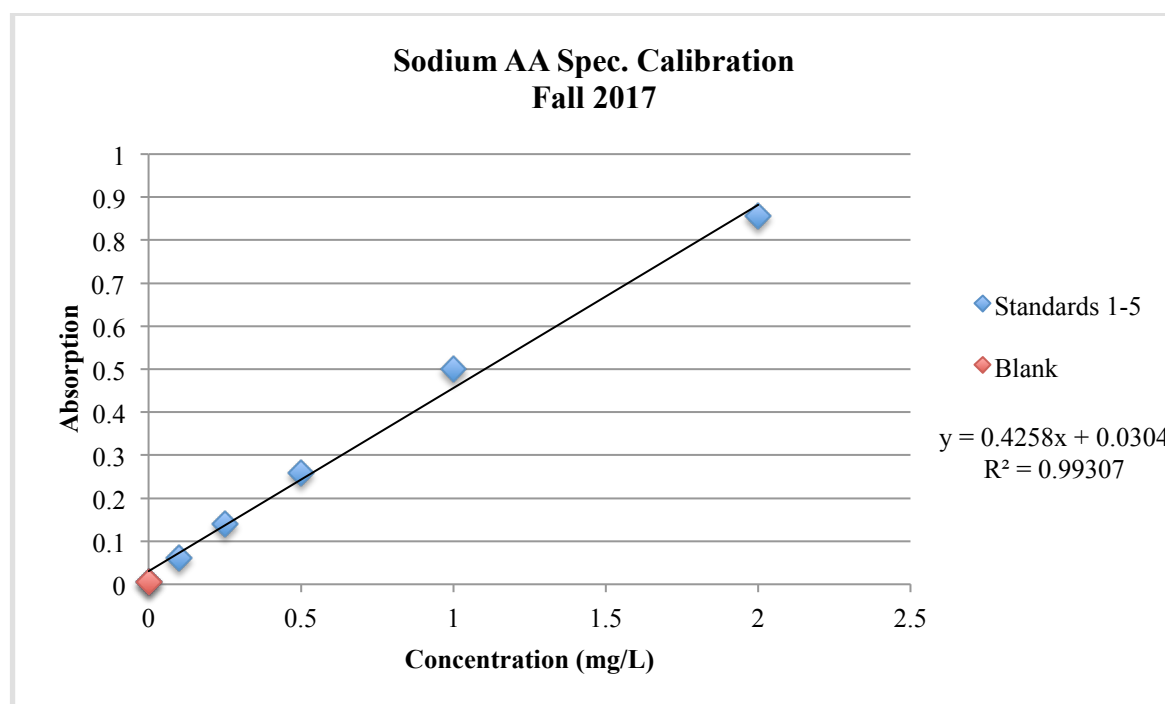
Sodium AA Spec. Calibration Fall 2017

Standards 1-5

Blank

$y = 0.4258x + 0.0304$
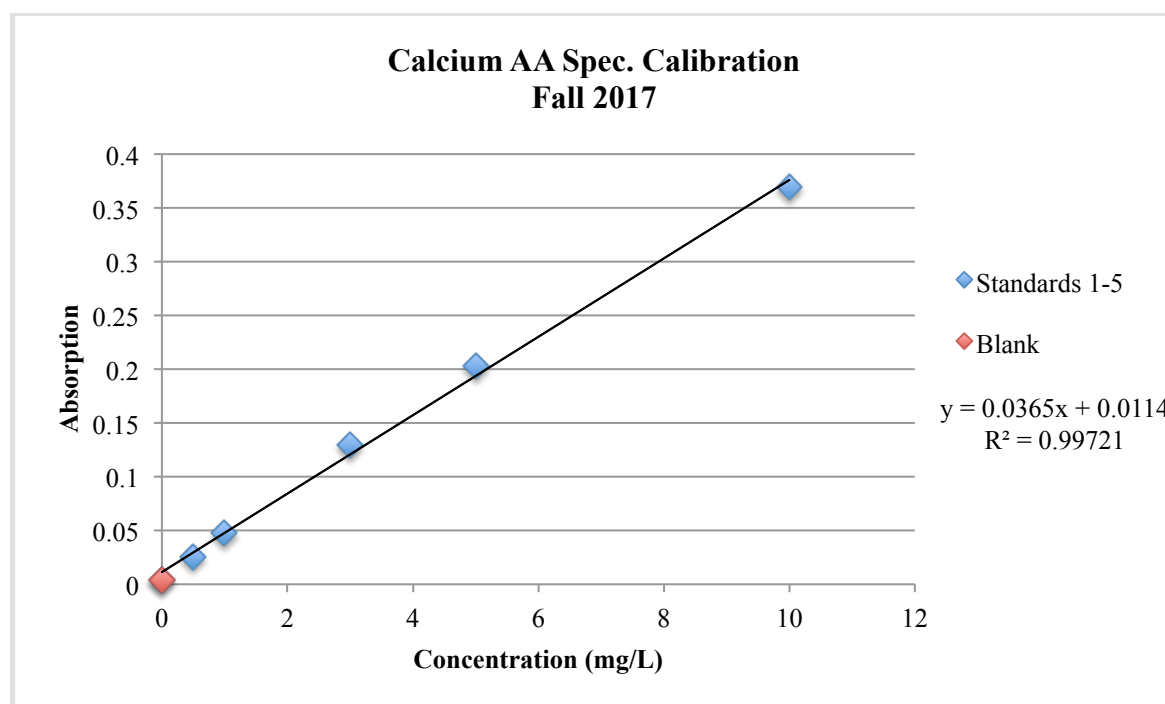$R^2 = 0.99307$

Absorption

Concentration (mg/L)

Sodium AA Spectrometer Results Fall 2017

Sample ID	Sample Date	Absorption	Calculated Concentration (mg/L)	Dilution Factor	Corrected Concentration (mg/L)
EM275	8/25/17	0.1080	0.1865	100	18.24
IZ385	8/25/17	0.4981	0.9963	100	109.86
SV631	9/15/17	0.1423	0.2548	100	26.29
Well 11	6/29/17	0.4879	0.9740	100	107.46
Well 11	7/27/17	0.4429	0.9450	100	98.37
Well 12	6/29/17	0.4013	0.7888	100	87.11
Well 12	7/27/17	0.3719	0.7714	100	80.21
Well 13	6/29/17	0.2056	0.3808	100	41.15
Well 13	7/27/17	0.1887	0.3708	100	37.18
Hygeia Spring	8/20/17	0.3283	0.6383	100	69.97
Fox 0	8/5/17	0.2916	0.5637	100	61.34
Fox 1	8/19/17	0.6969	1.4885	100	156.52
Fox 2	8/20/17	0.6846	1.4505	100	153.65
Fox 3	8/20/17	0.4221	0.8330	100	91.98
Root River	8/31/17	0.6233	1.2933	100	139.25
Sussex Creek	8/5/17	0.5271	1.0576	100	116.64
Underwood Creek	8/20/17	0.7825	1.7558	100	176.63
Brookfield WWTP	8/24/17	0.1852	0.3309	100	36.35
Sussex WWTP	8/31/17	0.1656	0.3003	100	31.76
Waukesha WWTP	8/31/17	0.1705	0.3099	100	32.90

Potassium Standards AA Spectrometer Fall 2017				
Standard	Concentration (mg/L)	Absorption Start	Absorption Final	Absorption Average
Blank	0	0.0075	0.0068	0.0057
1	0.25	0.1020	0.1068	0.1044
2	0.5	0.2395	0.2397	0.2381
3	1	0.4143	0.4221	0.4207
4	2	0.7555	0.7653	0.7611
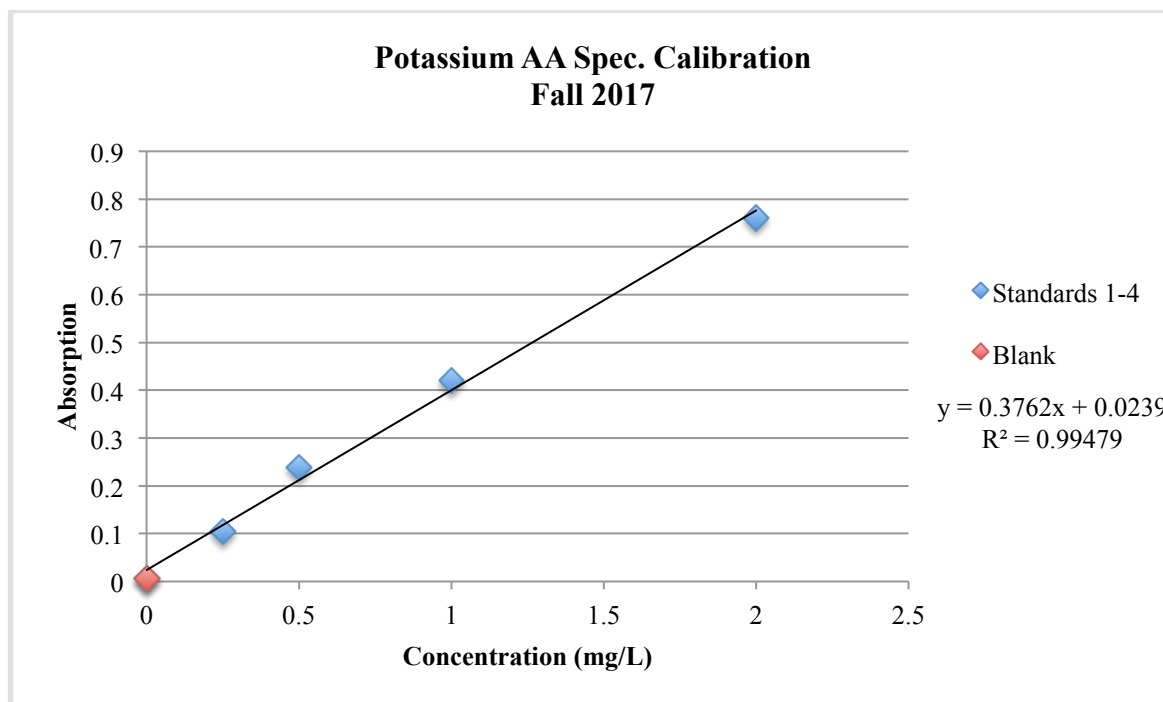
Potassium AA Spec. Calibration Fall 2017
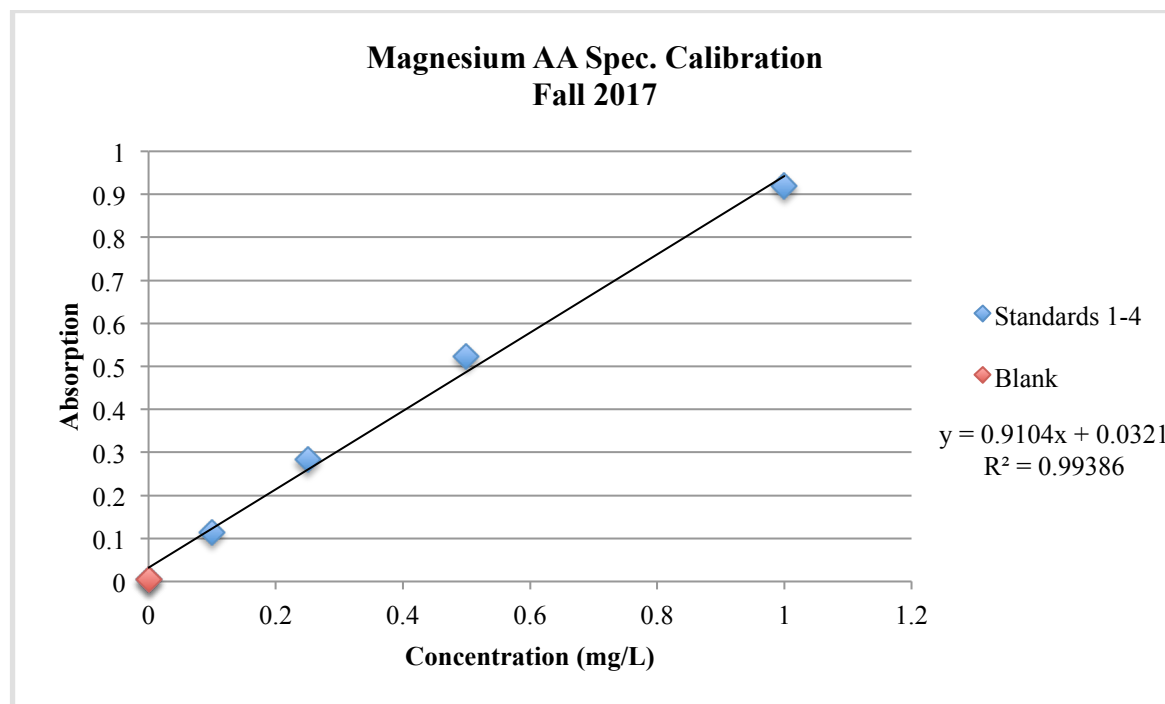
$y = 0.3762x + 0.0239$
$R^2 = 0.99479$

Potassium AA Spectrometer Results Fall 2017

Sample ID	Sample Date	Absorption	Calculated Concentration (mg/L)	Dilution Factor	Corrected Concentration (mg/L)
EM275	8/25/17	0.1063	0.2164	10	2.19
IZ385	8/25/17	0.1488	0.3077	10	3.32
SV631	9/15/17	0.0813	0.1626	10	1.52
Well 11	6/29/17	0.1414	0.2919	10	3.12
Well 11	7/27/17	0.5145	0.3447	10	3.37
Well 12	6/29/17	0.1327	0.2731	10	2.89
Well 12	7/27/17	0.1508	0.3319	10	3.12
Well 13	6/29/17	0.1097	0.0237	10	2.82
Well 13	7/27/17	0.1176	0.2732	10	2.49
Hygeia Spring	8/20/17	0.1202	0.2462	10	2.56
Fox 0	8/5/17	0.1225	0.2510	10	2.62
Fox 1	8/19/17	0.2130	0.4458	10	5.03
Fox 2	8/20/17	0.2212	0.4633	10	5.24
Fox 3	8/20/17	0.1368	0.2818	10	3.00
Root River	8/31/17	0.1871	0.3900	10	4.34
Sussex Creek	8/5/17	0.2223	0.4658	10	5.27
Underwood Creek	8/20/17	0.2796	0.5982	10	6.80
Brookfield WWTP	8/24/17	0.4605	1.1016	10	11.60
Sussex WWTP	8/31/17	0.4843	1.1659	10	12.24
Waukesha WWTP	8/31/17	0.1202	1.2484	10	2.56

Calcium Standards AA Spectrometer Winter 2017				
Standard	Concentration (mg/L)	Absorption Start	Absorption Final	Absorption Average
Blank	0	0.0032	0.0028	0.0031
1	0.5	0.0261	0.026	0.0503
2	1	0.0503	0.0501	0.0503
3	3	0.1393	0.1388	0.1392
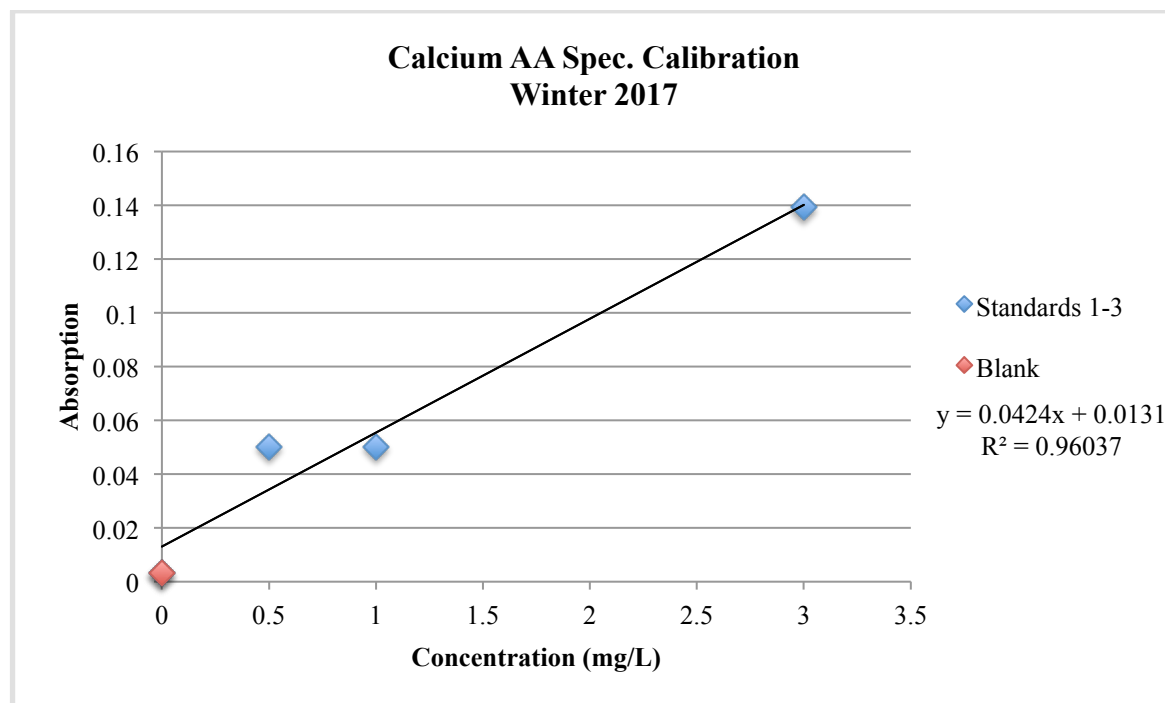
Calcium AA Spec. Calibration Winter 2017

Standards 1-3

Blank

$y = 0.0424x + 0.0131$
$R^2 = 0.96037$

Absorption

Concentration (mg/L)

Calcium AA Spectrometer Results Winter 2017					
Sample ID	Sample Date	Absorption	Calculated Concentration (mg/L)	Dilution Factor	Corrected Concentration (mg/L)
Well 11	11/8/17	0.0566	1.1347	100	102.59
Well 11	11/29/17	0.0534	1.0645	100	95.05
Well 11	12/1/17	0.0531	1.0594	100	94.34
Well 11	1/26/18	0.0535	1.0682	100	95.28
Well 12	11/8/17	0.0532	1.0603	100	94.58
Well 12	11/29/17	0.0519	1.0342	100	91.51
Well 12	12/1/17	0.0523	1.0416	100	92.45
Well 12	1/26/18	0.0523	1.0421	100	92.45
Well 13	11/8/17	0.0531	1.058	100	94.34
Well 13	11/29/17	0.0467	0.9299	100	79.25
Well 13	12/1/17	0.0474	0.9433	100	80.90
Well 13	1/26/18	0.0465	0.9251	100	78.77

Magnesium Standards AA Spectrometer Winter 2017				
Standard	Concentration (mg/L)	Absorption Start	Absorption Final	Absorption Average
Blank	0	0.0032	0.0028	0.0029
1	0.1	0.1189	0.1183	0.1184
2	0.25	0.2849	0.2833	0.2826
3	0.5	0.5482	0.5422	0.5460
4	1	0.9532	0.9382	0.9414
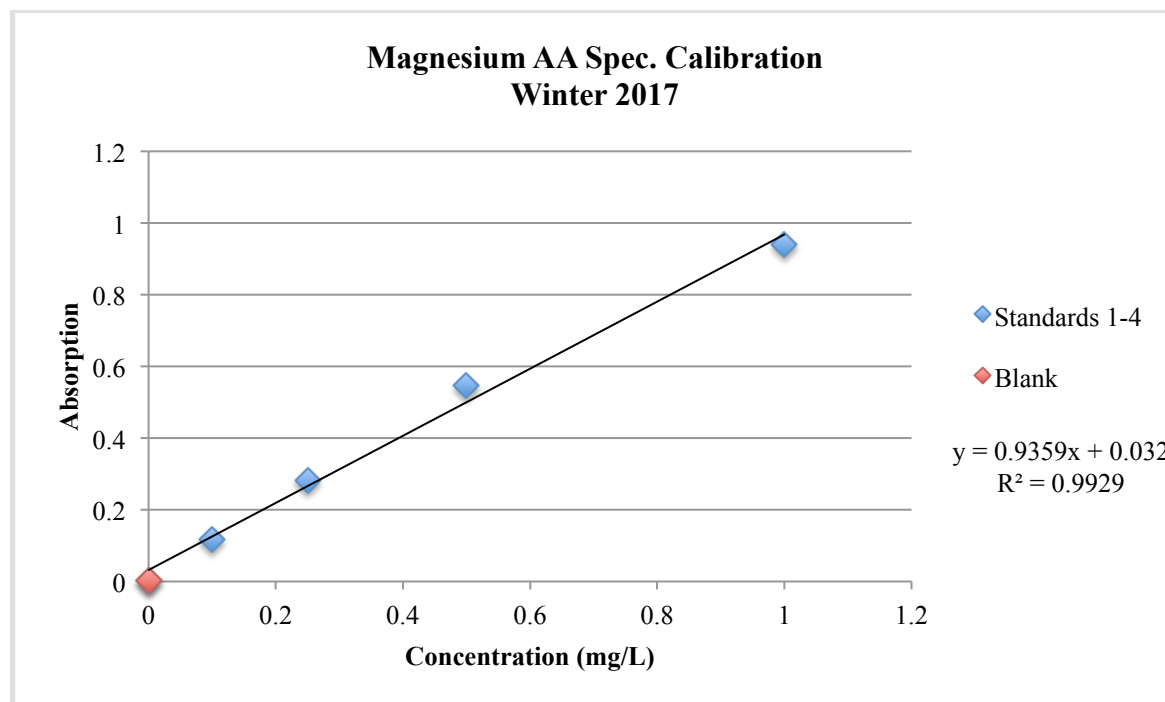
Magnesium AA Spec. Calibration Winter 2017

Standards 1-4

Blank

$y = 0.9359x + 0.032$
$R^2 = 0.9929$

Absorption (y-axis)

Concentration (mg/L) (x-axis)

91

Magnesium AA Spectrometer Results Winter 2017					
Sample ID	Sample Date	Absorption	Calculated Concentration (mg/L)	Dilution Factor	Corrected Concentration (mg/L)
Well 11	11/8/17	0.5612	0.5131	100	56.54
Well 11	11/29/17	0.5431	0.4969	100	54.61
Well 11	12/1/17	0.54	0.4937	100	54.28
Well 11	1/26/18	0.5427	0.4965	100	54.57
Well 12	11/8/17	0.5284	0.4823	100	53.04
Well 12	11/29/17	0.5299	0.4838	100	53.20
Well 12	12/1/17	0.5312	0.485	100	53.34
Well 12	1/26/18	0.5353	0.4891	100	53.78
Well 13	11/8/17	0.6336	0.5918	100	64.28
Well 13	11/29/17	0.5454	0.4992	100	54.86
Well 13	12/1/17	0.5521	0.5041	100	55.57
Well 13	1/26/18	0.5517	0.5038	100	55.53

Sodium Standards AA Spectrometer Winter 2017				
Standard	Concentration (mg/L)	Absorption Start	Absorption Final	Absorption Average
Blank	0	0	0.0001	0.0000
1	0.1	0.0591	0.0584	0.0586
2	0.25	0.136	0.1407	0.1390
3	0.5	0.2695	0.2667	0.2683
4	1	0.5331	0.5194	0.5241
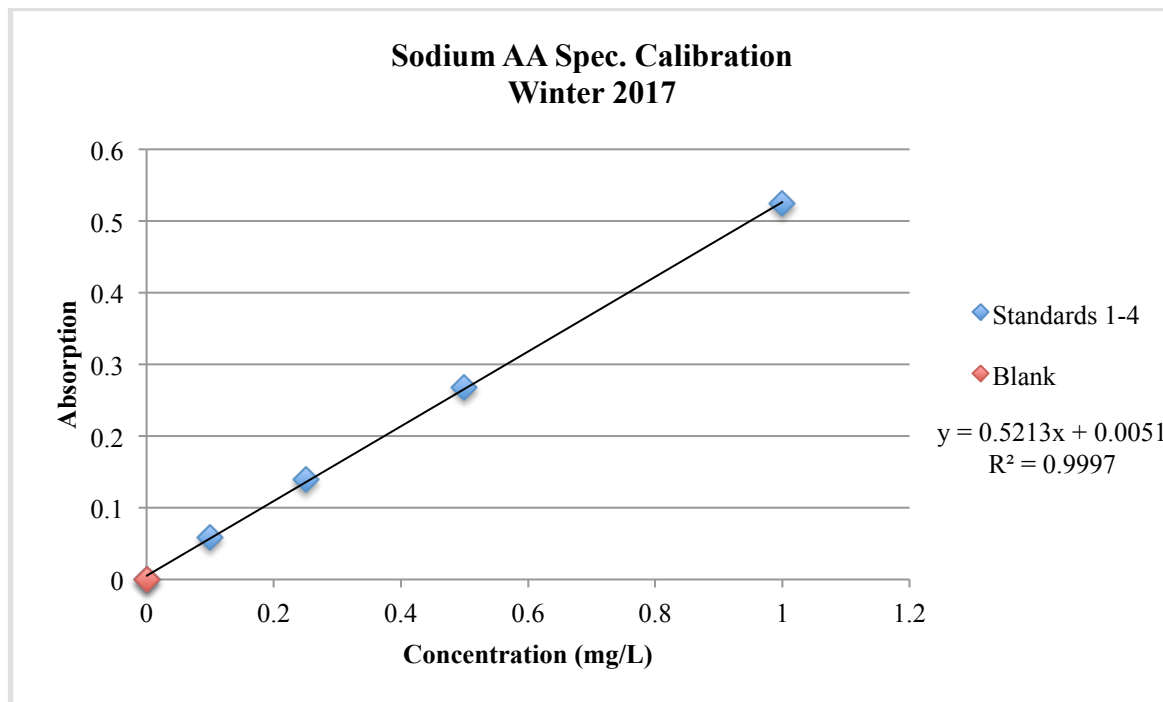
Sodium AA Spec. Calibration Winter 2017

Standards 1-4

Blank

$y = 0.5213x + 0.0051$
$R^2 = 0.9997$

Absorption (y-axis)

Concentration (mg/L) (x-axis)

Sodium AA Spectrometer Results Winter 2017					
Sample ID	Sample Date	Absorption	Calculated Concentration (mg/L)	Dilution Factor	Corrected Concentration (mg/L)
Well 11	11/8/17	0.5176	0.9865	100	98.31
Well 11	11/29/17	0.5041	0.9592	100	95.72
Well 11	12/1/17	0.531	1.01	100	100.88
Well 11	1/26/18	0.5307	1.0095	100	100.82
Well 12	11/8/17	0.4155	0.7823	100	78.73
Well 12	11/29/17	0.4126	0.7765	100	78.17
Well 12	12/1/17	0.417	0.7853	100	79.01
Well 12	1/26/18	0.4226	0.7964	100	80.09
Well 13	11/8/17	0.2222	0.4072	100	41.65
Well 13	11/29/17	0.2108	0.3845	100	39.46
Well 13	12/1/17	0.2112	0.3818	100	39.54
Well 13	1/26/18	0.21	0.3828	100	39.31

Potassium Standards AA Spectrometer Winter 2017				
Standard	Concentration (mg/L)	Absorption Start	Absorption Final	Absorption Average
Blank	0	-0.0056	-0.002	-0.0006
1	0.25	0.1052	0.1049	0.1087
2	0.5	0.2395	0.2473	0.2401
3	1	0.4412	0.4413	0.4417
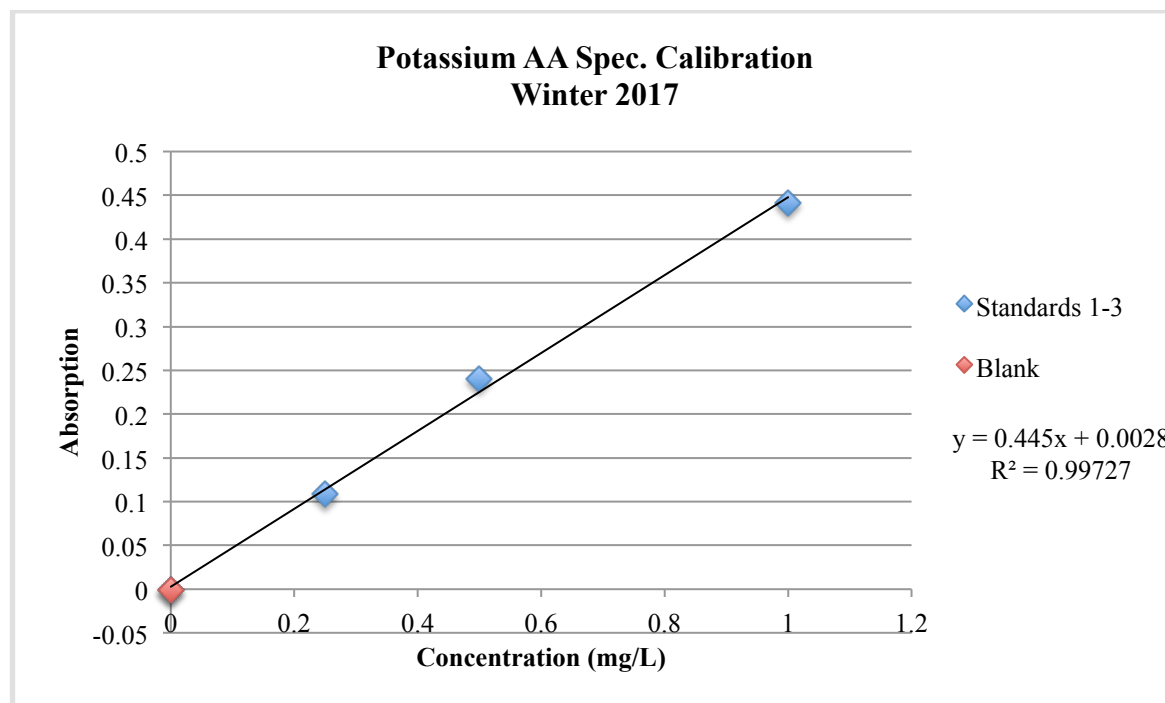
Potassium AA Spec. Calibration Winter 2017

Standards 1-3

Blank

$y = 0.445x + 0.0028$
$R^2 = 0.99727$

		Potassium AA Spectrometer Results Winter 2017			
Sample ID	Sample Date	Absorption	Calculated Concentration (mg/L)	Dilution Factor	Corrected Concentration (mg/L)
Well 11	11/8/17	0.1662	0.3709	10	3.67
Well 11	11/29/17	0.1766	0.3915	10	3.91
Well 11	12/1/17	0.1682	0.3749	10	3.72
Well 11	1/26/18	0.1637	0.3656	10	3.62
Well 12	11/8/17	0.1576	0.3532	10	3.48
Well 12	11/29/17	0.1521	0.3418	10	3.36
Well 12	12/1/17	0.1538	0.3453	10	3.39
Well 12	1/26/18	0.1588	0.3556	10	3.51
Well 13	11/8/17	0.1411	0.3191	10	3.11
Well 13	11/29/17	0.1298	0.2958	10	2.85
Well 13	12/1/17	0.1309	0.298	10	2.88
Well 13	1/26/18	0.1205	0.2763	10	2.64

Ion Chromatography with Calibration Curves for Major Ions

Chloride Standards IC Fall 2016		
Standard	Concentration (mg/L)	Area (µS*min)
1	50	10.0989
2	100	27.3091
3	200	49.6441
4	300	90.0969
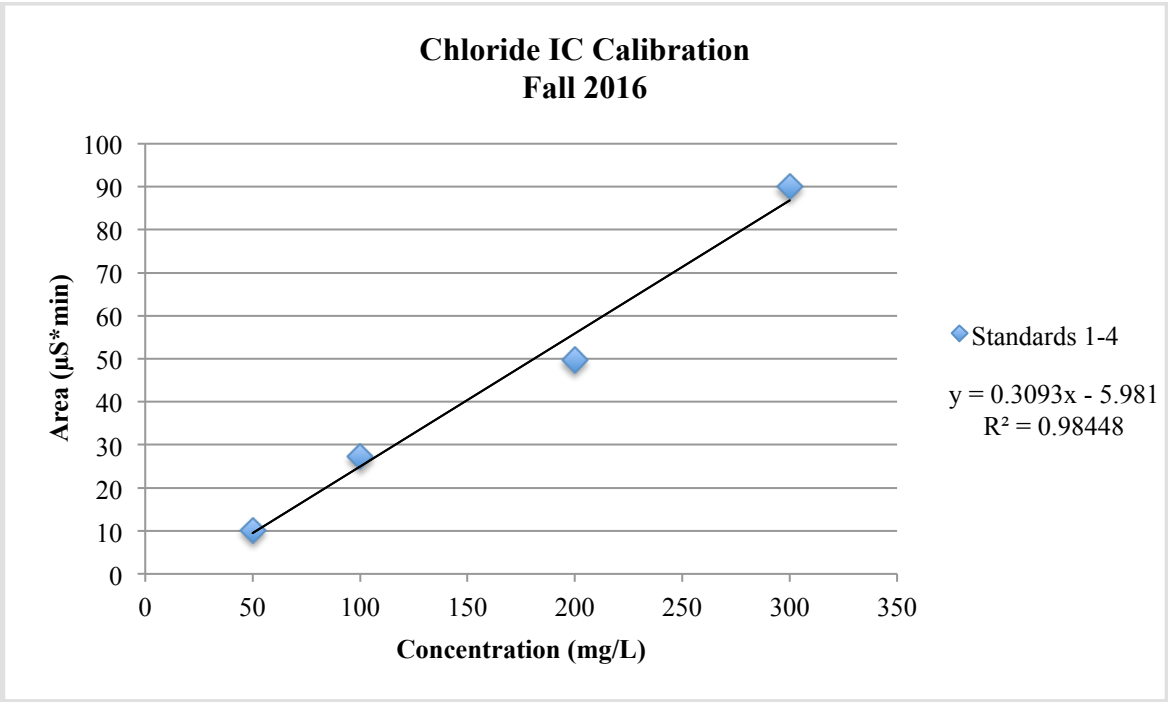
Chloride IC Calibration
Fall 2016

Area (µS*min) vs Concentration (mg/L)

Standards 1-4

$y = 0.3093x - 5.981$
$R^2 = 0.98448$

Chloride IC Results Fall 2016

Sample ID	Sample Date	Area (µS*min)	Dilution	Corrected Concentration (mg/L)
EM275	11/2/16	4.0022	1	32.27
IZ385	11/2/16	58.5499	1	208.63
IZ386	11/2/16	48.1804	1	175.10
SV631	11/7/16	11.5855	1	56.79
Well 11	11/3/16	46.2608	1	168.90
Well 11	2/28/17	52.0216	1	175.28
Well 12	11/3/16	39.231	1	146.17
Well 12	2/28/17	42.764	1	144.66
Well 13	11/3/16	18.3607	1	78.69
Well 13	2/28/17	20.8693	1	72.26
Hygeia Spring	11/7/16	24.9133	1	99.88
Fox 0	11/7/16	22.453	1	91.93
Fox 1	11/7/16	43.5043	1	159.99
Fox 2	11/7/16	49.2394	1	178.53
Fox 3	11/7/16	29.6878	1	115.32
Root River	11/7/16	36.9636	1	138.84
Sussex Creek	11/7/16	58.7363	1	209.24
Underwood Creek	11/7/16	74.157	1	259.09
Brookfield WWTP	11/2/16	107.0934	1	365.58
Sussex WWTP	11/3/16	92.2269	1	317.52
Waukesha WWTP	11/3/16	122.1651	1	414.31

Nitrate Standards IC Fall 2016		
Standard	Concentration (mg/L)	Area (µS*min)
1	1	0.0638
2	5	0.3862
3	10	0.9519
4	50	4.1398
5	100	10.5294
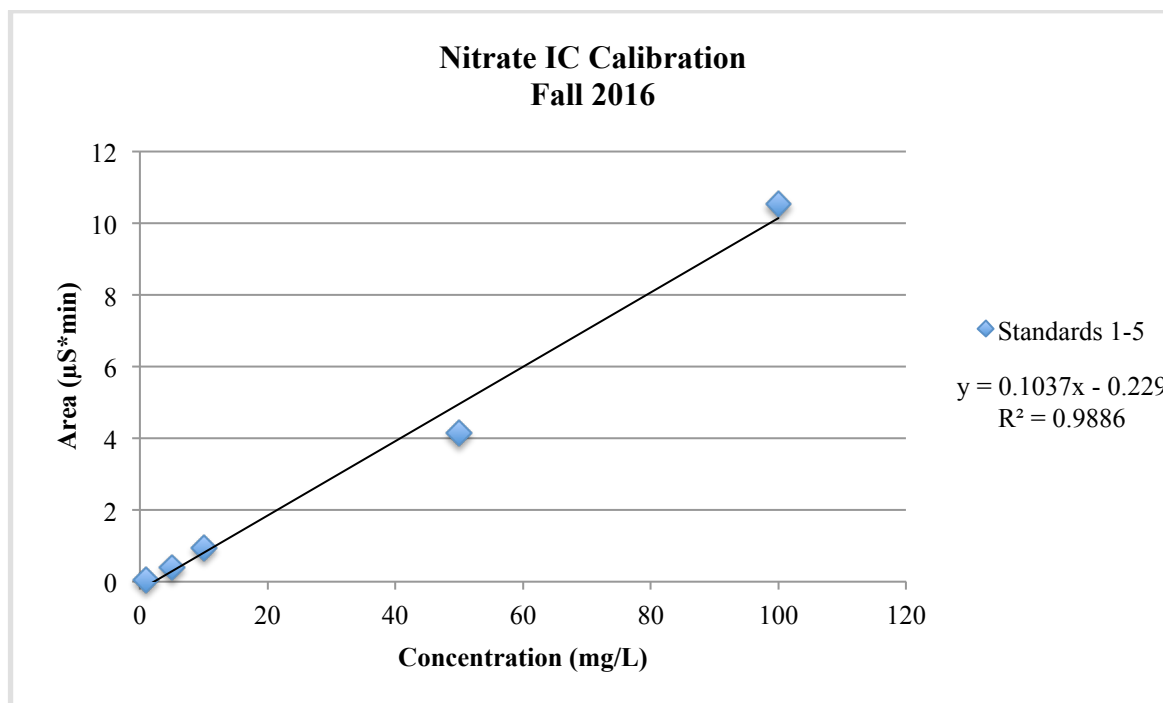
Nitrate IC Calibration
Fall 2016

Standards 1-5

$y = 0.1037x - 0.229$
$R^2 = 0.9886$

X-axis: Concentration (mg/L)
Y-axis: Area (µS*min)

Nitrate IC Results Fall 2016

Sample ID	Sample Date	Area (μS*min)	Dilution	Corrected Concentration (mg/L)
EM275	11/2/16	ND	1	ND
IZ385	11/2/16	0.3585	1	5.66
IZ386	11/2/16	0.1118	1	3.28
SV631	11/7/16	0.1032	1	3.20
Well 11	11/3/16	4.1247	1	41.98
Well 11	2/28/17	ND	1	ND
Well 12	11/3/16	0.1074	1	3.25
Well 12	2/28/17	ND	1	ND
Well 13	11/3/16	0.0924	1	3.09
Well 13	2/28/17	0.0524	1	2.99
Hygeia Spring	11/7/16	0.6899	1	8.86
Fox 0	11/7/16	0.1636	1	3.79
Fox 1	11/7/16	0.416	1	6.22
Fox 2	11/7/16	0.8414	1	10.32
Fox 3	11/7/16	0.3763	1	5.84
Root River	11/7/16	0.1837	1	3.98
Sussex Creek	11/7/16	0.772	1	9.65
Underwood Creek	11/7/16	0.1287	1	3.45
Brookfield WWTP	11/2/16	3.5628	1	36.57
Sussex WWTP	11/3/16	1.1434	1	13.23
Waukesha WWTP	11/3/16	8.7041	1	86.14

Phosphate Standards IC Fall 2016		
Standard	Concentration (mg/L)	Area (µS*min)
1	1	0.1092
2	5	0.3054
3	10	0.5971

Phosphate IC Calibration
Fall 2016

Standards 1-3

$y = 0.0544x + 0.0472$
$R^2 = 0.99765$

Phosphate IC Results Fall 2016				
Sample ID	**Sample Date**	**Area (μS*min)**	**Dilution**	**Corrected Concentration (mg/L)**
EM275	11/2/16	ND	1	ND
IZ385	11/2/16	ND	1	ND
IZ386	11/2/16	ND	1	ND
SV631	11/7/16	ND	1	ND
Well 11	11/3/16	ND	1	ND
Well 11	2/28/17	ND	1	ND
Well 12	11/3/16	ND	1	ND
Well 12	2/28/17	ND	1	ND
Well 13	11/3/16	ND	1	ND
Well 13	2/28/17	ND	1	ND
Hygeia Spring	11/7/16	ND	1	ND
Fox 0	11/7/16	ND	1	ND
Fox 1	11/7/16	ND	1	ND
Fox 2	11/7/16	ND	1	ND
Fox 3	11/7/16	ND	1	ND
Root River	11/7/16	ND	1	ND
Sussex Creek	11/7/16	0.0178	1	0.0019
Underwood Creek	11/7/16	ND	1	ND
Brookfield WWTP	11/2/16	0.111	1	0.06
Sussex WWTP	11/3/16	0.0237	1	0.0027
Waukesha WWTP	11/3/16	ND	1	ND

Sulfate Standards IC Fall 2016		
Standard	**Concentration (mg/L)**	**Area (µS*min)**
1	50	4.6667
2	100	12.3116
3	200	29.0221
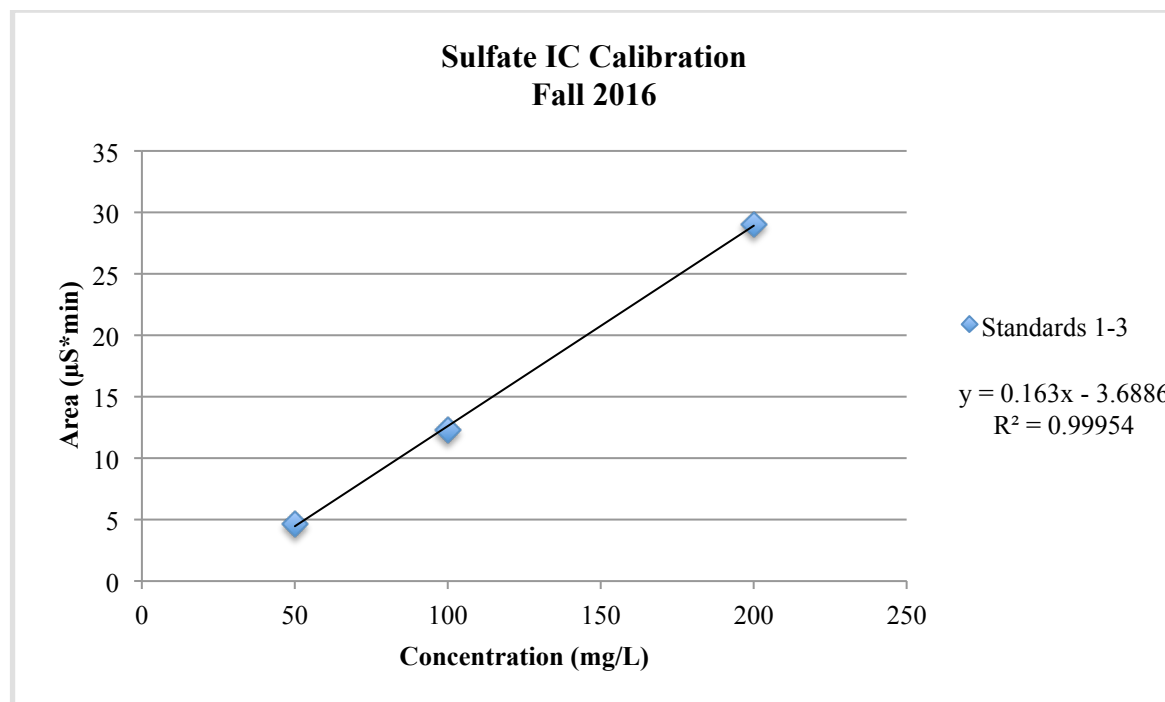
Sulfate IC Calibration Fall 2016

y = 0.163x - 3.6886
R² = 0.99954

Standards 1-3

Sulfate IC Results Fall 2016

Sample ID	Sample Date	Area (μS*min)	Dilution	Corrected Concentration (mg/L)
EM275	11/2/16	22.4255	1	160.20
IZ385	11/2/16	8.4671	1	74.57
IZ386	11/2/16	10.752	1	88.59
SV631	11/7/16	8.2001	1	72.93
Well 11	11/3/16	7.9747	1	71.55
Well 11	2/28/17	9.7141	1	69.96
Well 12	11/3/16	9.6638	1	81.91
Well 12	2/28/17	11.0009	1	77.76
Well 13	11/3/16	12.8349	1	101.37
Well 13	2/28/17	15.9286	1	111.44
Hygeia Spring	11/7/16	3.6049	1	44.75
Fox 0	11/7/16	4.3006	1	49.01
Fox 1	11/7/16	4.4014	1	49.63
Fox 2	11/7/16	4.9983	1	53.29
Fox 3	11/7/16	3.8671	1	46.35
Root River	11/7/16	8.1171	1	72.43
Sussex Creek	11/7/16	6.1127	1	60.13
Underwood Creek	11/7/16	16.9717	1	126.75
Brookfield WWTP	11/2/16	12.0731	1	96.70
Sussex WWTP	11/3/16	7.9351	1	71.31
Waukesha WWTP	11/3/16	9.4018	1	80.31

Chloride Standards IC Fall 2017

Standard	Concentration (mg/L)	Area (µS*min)
1	1	0.1588
2	5	0.8667
3	10	1.8691
4	25	5.5210
5	50	13.0045
6	100	35.5377
7	200	76.4078

Chloride IC Calibration Fall 2017

Standards 1-7

$y = 0.3883x - 2.638$
$R^2 = 0.9942$

Chloride IC Results Fall 2017

Sample ID	Sample Date	Area (µS*min)	Dilution	Corrected Concentration (mg/L)
EM275	8/25/17	4.1439	1	17.47
IZ385	8/25/17	53.0246	1	143.35
SV631	9/15/17	12.2988	1	38.47
Well 11	6/29/17	54.3669	1	146.81
Well 11	7/27/17	85.5905	1	227.22
Well 12	6/29/17	45.8174	1	124.79
Well 12	7/27/17	54.7766	1	147.86
Well 13	6/29/17	21.2926	1	61.63
Well 13	7/27/17	17.9344	1	52.98
Hygeia Spring	8/20/17	25.0345	1	71.27
Fox 0	8/5/17	18.8974	1	55.46
Fox 1	8/19/17	61.3881	1	164.89
Fox 2	8/20/17	62.0397	1	166.57
Fox 3	8/20/17	33.7927	1	93.82
Root River	8/31/17	54.9556	1	148.32
Sussex Creek	8/5/17	42.0709	1	115.14
Underwood Creek	8/20/17	80.8923	1	215.12
Brookfield WWTP	8/24/17	135.9637	1	356.94
Sussex WWTP	8/31/17	111.7741	1	294.65
Waukesha WWTP	8/31/17	122.4699	1	322.19

Nitrate Standards IC Fall 2017		
Standard	Concentration (mg/L)	Area (µS*min)
1	1	0.0571
2	5	0.3901
3	10	0.8197
4	25	2.2688
5	50	5.1365

Nitrate IC Calibration
Fall 2017

Standards 1-5

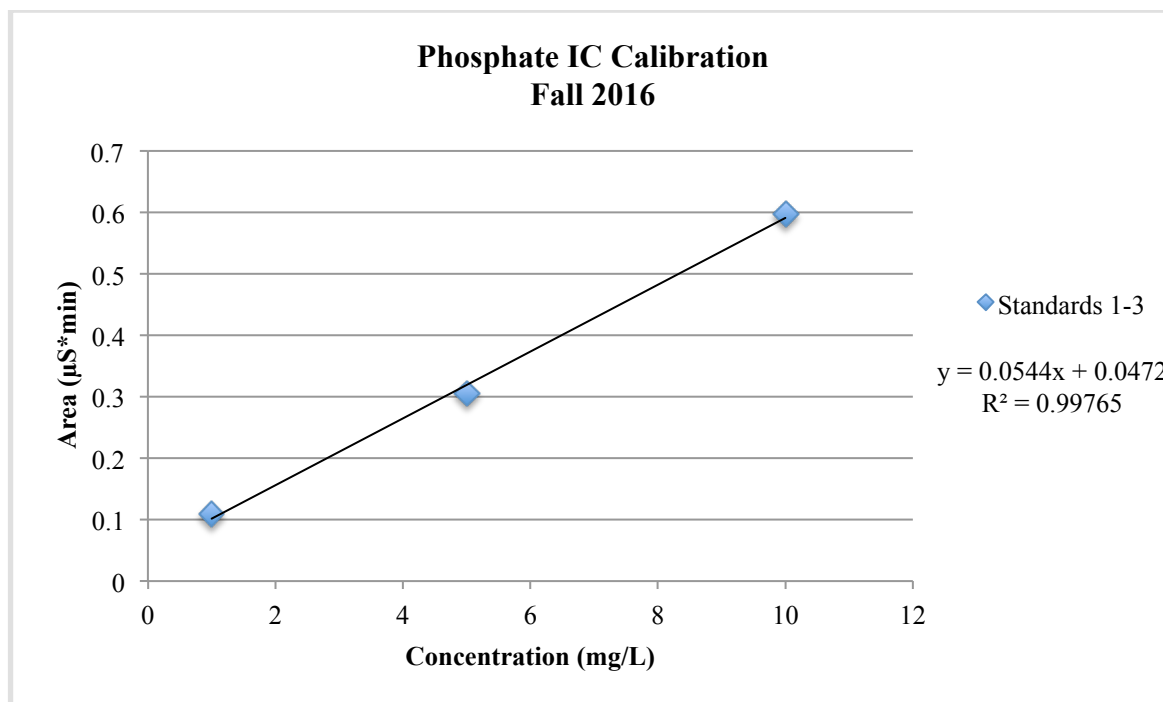$y = 0.104x - 0.159$
$R^2 = 0.99677$

Area (µS*min) vs Concentration (mg/L)

Nitrate IC Results Fall 2017

Sample ID	Sample Date	Area (μS*min)	Dilution	Corrected Concentration (mg/L)
EM275	8/25/17	0.0165	1	1.69
IZ385	8/25/17	0.2304	1	3.74
SV631	9/15/17	ND	1	ND
Well 11	6/29/17	0.0232	1	1.75
Well 11	7/27/17	0.1411	1	2.89
Well 12	6/29/17	ND	1	ND
Well 12	7/27/17	ND	1	ND
Well 13	6/29/17	0.0702	1	2.20
Well 13	7/27/17	0.0807	1	2.30
Hygeia Spring	8/20/17	0.8932	1	10.12
Fox 0	8/5/17	0.1353	1	2.83
Fox 1	8/19/17	0.5033	1	6.37
Fox 2	8/20/17	1.0025	1	11.17
Fox 3	8/20/17	0.2064	1	3.51
Root River	8/31/17	0.0481	1	1.99
Sussex Creek	8/5/17	0.6957	1	8.22
Underwood Creek	8/20/17	ND	1	ND
Brookfield WWTP	8/24/17	3.7249	1	37.35
Sussex WWTP	8/31/17	2.152	1	22.22
Waukesha WWTP	8/31/17	6.7554	1	64.80

Phosphate Standards IC Fall 2017		
Standard	Concentration (mg/L)	Area (µS*min)
1	1	0.0767
2	5	0.2476
3	10	0.4581
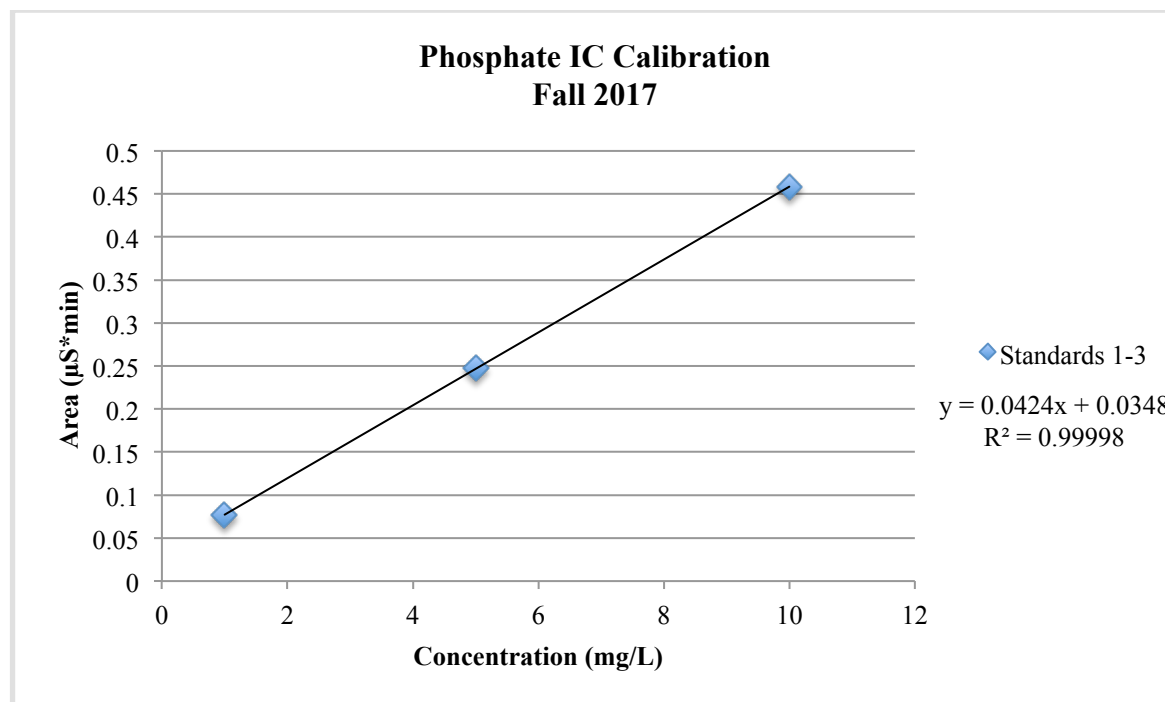
Phosphate IC Calibration
Fall 2017

Standards 1-3

y = 0.0424x + 0.0348
R² = 0.99998

X-axis: Concentration (mg/L)
Y-axis: Area (µS*min)

Phosphate IC Results Fall 2017				
Sample ID	Sample Date	Area (µS*min)	Dilution	Corrected Concentration (mg/L)
EM275	8/25/17	ND	1	ND
IZ385	8/25/17	ND	1	ND
SV631	9/15/17	ND	1	ND
Well 11	6/29/17	ND	1	ND
Well 11	7/27/17	ND	1	ND
Well 12	6/29/17	ND	1	ND
Well 12	7/27/17	ND	1	ND
Well 13	6/29/17	ND	1	ND
Well 13	7/27/17	ND	1	ND
Hygeia Spring	8/20/17	ND	1	ND
Fox 0	8/5/17	ND	1	ND
Fox 1	8/19/17	0.0236	1	0.0018
Fox 2	8/20/17	0.0202	1	0.0015
Fox 3	8/20/17	ND	1	ND
Root River	8/31/17	0.0218	1	0.0016
Sussex Creek	8/5/17	0.0264	1	0.0020
Underwood Creek	8/20/17	ND	1	ND
Brookfield WWTP	8/24/17	0.0373	1	0.0028
Sussex WWTP	8/31/17	0.0856	1	0.0065
Waukesha WWTP	8/31/17	0.0257	1	0.0019

Sulfate Standards IC Fall 2017

Standard	Concentration (mg/L)	Area (µS*min)
1	1	0.1056
2	5	0.4478
3	10	0.8955
4	25	2.4633
5	50	5.8342
6	100	12.5346
7	200	28.7261
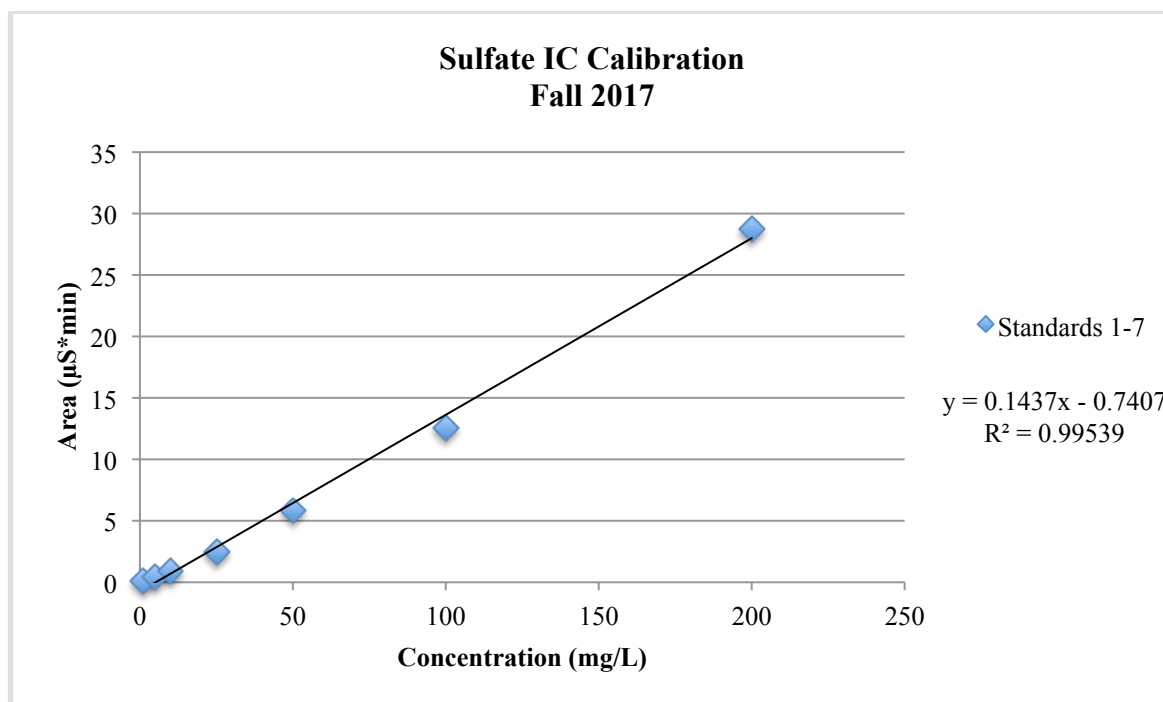
Sulfate IC Calibration Fall 2017

◆ Standards 1-7

$y = 0.1437x - 0.7407$
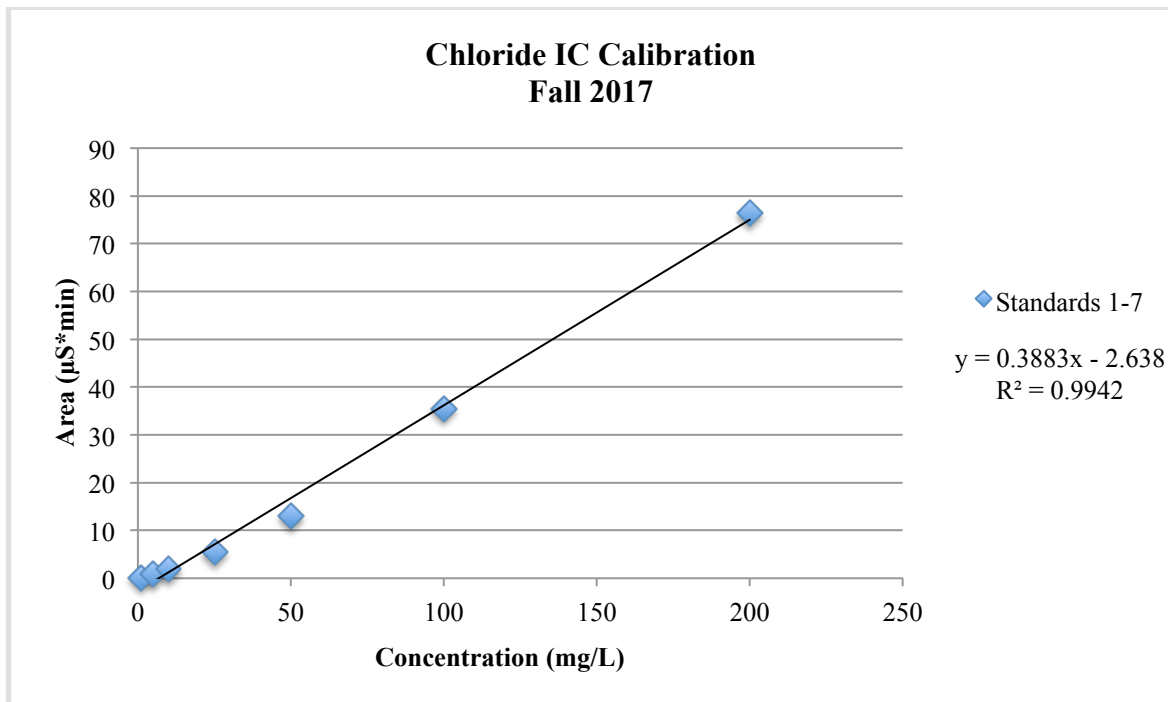$R^2 = 0.99539$

x-axis: Concentration (mg/L)
y-axis: Area (µS*min)

Sulfate IC Results Fall 2017

Sample ID	Sample Date	Area (µS*min)	Dilution	Corrected Concentration (mg/L)
EM275	8/25/17	20.3758	1	146.94
IZ385	8/25/17	7.9666	1	60.59
SV631	9/15/17	8.3029	1	62.93
Well 11	6/29/17	9.0886	1	68.49
Well 11	7/27/17	14.2338	1	104.20
Well 12	6/29/17	10.6804	1	79.47
Well 12	7/27/17	12.4047	1	91.47
Well 13	6/29/17	15.2694	1	111.41
Well 13	7/27/17	13.7305	1	100.70
Hygeia Spring	8/20/17	3.4659	1	29.27
Fox 0	8/5/17	4.2497	1	34.73
Fox 1	8/19/17	4.8882	1	39.17
Fox 2	8/20/17	4.7785	1	38.41
Fox 3	8/20/17	2.8173	1	24.76
Root River	8/31/17	8.3242	1	63.08
Sussex Creek	8/5/17	5.272	1	41.84
Underwood Creek	8/20/17	17.4386	1	126.51
Brookfield WWTP	8/24/17	10.5057	1	78.26
Sussex WWTP	8/31/17	9.0061	1	67.83
Waukesha WWTP	8/31/17	10.3772	1	77.37

Chloride Standards IC Winter 2017		
Standard	Concentration (mg/L)	Area (μS*min)
1	100	11.8654
2	200	29.3045
3	300	46.8190

**Chloride IC Calibration
Winter 2017**

y = 0.1748x - 5.624
R² = 1

Chloride IC Results Winter 2017

Sample ID	Sample Date	Area (µS*min)	Dilution	Corrected Concentration (mg/L)
Well 11	11/8/17	46.4727	1	298.03
Well 11	11/29/17	41.0466	1	266.99
Well 11	12/1/17	38.1643	1	250.50
Well 11	1/26/18	40.6966	1	264.99
Well 12	11/8/17	39.9688	1	260.82
Well 12	11/29/17	34.7154	1	230.77
Well 12	12/1/17	37.0727	1	244.26
Well 12	1/26/18	39.0832	1	255.76
Well 13	11/8/17	15.435	1	120.47
Well 13	11/29/17	17.0975	1	129.98
Well 13	12/1/17	15.8553	1	122.87
Well 13	1/26/18	15.441	1	120.50

Nitrate Standards IC Winter 2017		
Standard	**Concentration (mg/L)**	**Area (μS*min)**
1	5	0.3530
2	10	0.8537
3	25	1.6857
4	50	3.9544
5	100	9.6821
6	200	21.1019
7	300	33.8444

Nitrate IC Calibration Winter 2017

◆ Standards 1-7

$y = 0.1136x - 0.9868$
$R^2 = 0.99681$

Y-axis: Area (μS*min)
X-axis: Concentration (mg/L)

Nitrate IC Results Winter 2017				
Sample ID	Sample Date	Area (µS*min)	Dilution	Corrected Concentration (mg/L)
Well 11	11/8/17	0.0523	1	0.0184
Well 11	11/29/17	0.0502	1	0.4860
Well 11	12/1/17	0.0521	1	0.0027
Well 11	1/26/18	0.0417	1	0.0020
Well 12	11/8/17	ND	1	ND
Well 12	11/29/17	ND	1	ND
Well 12	12/1/17	ND	1	ND
Well 12	1/26/18	ND	1	ND
Well 13	11/8/17	0.0415	1	0.0699
Well 13	11/29/17	0.0421	1	1.42
Well 13	12/1/17	0.0398	1	0.0016
Well 13	1/26/18	0.0333	1	0.0014

Phosphate Standards IC Winter 2017

Standard	Concentration (mg/L)	Area (µS*min)
1	5	0.2203
2	10	0.4000
3	25	0.9369
4	50	1.8839
5	100	4.2517
6	200	10.0808
7	300	16.7702
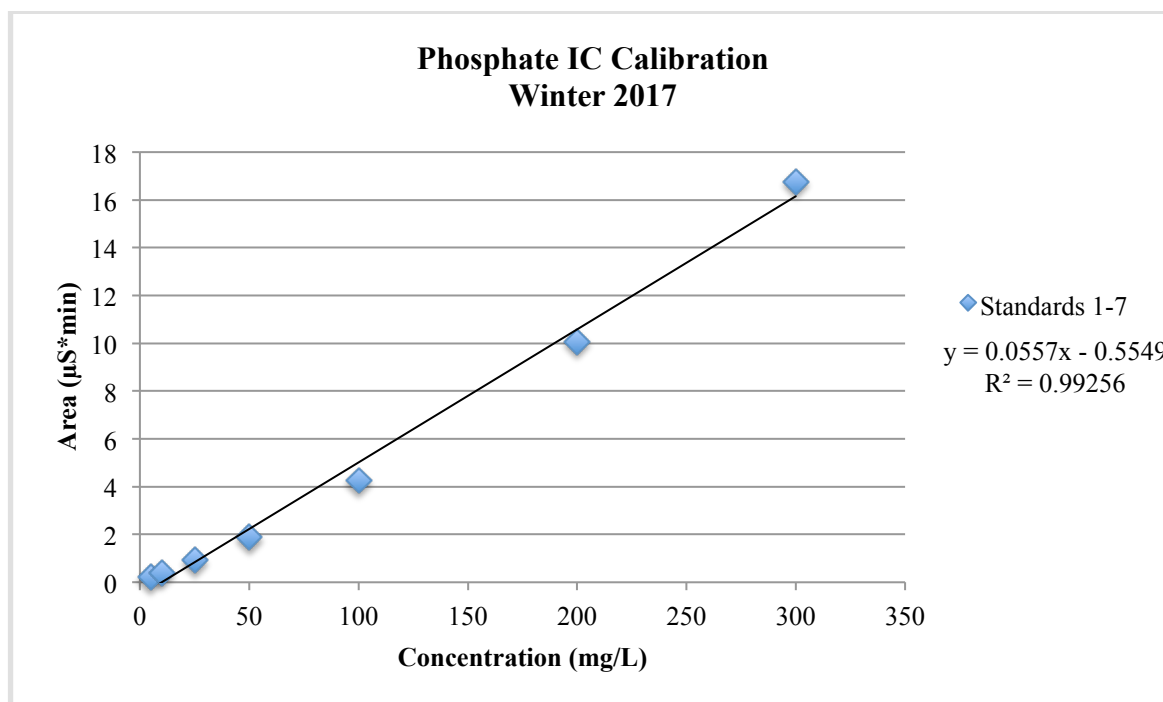
Phosphate IC Calibration
Winter 2017

◆ Standards 1-7

$y = 0.0557x - 0.5549$
$R^2 = 0.99256$

Phosphate IC Results Winter 2017				
Sample ID	Sample Date	Area (µS*min)	Dilution	Corrected Concentration (mg/L)
Well 11	11/8/17	ND	1	ND
Well 11	11/29/17	ND	1	ND
Well 11	12/1/17	ND	1	ND
Well 11	1/26/18	ND	1	ND
Well 12	11/8/17	ND	1	ND
Well 12	11/29/17	ND	1	ND
Well 12	12/1/17	ND	1	ND
Well 12	1/26/18	ND	1	ND
Well 13	11/8/17	ND	1	ND
Well 13	11/29/17	ND	1	ND
Well 13	12/1/17	ND	1	ND
Well 13	1/26/18	ND	1	ND

Sulfate Standards IC Winter 2017		
Standard	Concentration (mg/L)	Area (µS*min)
1	10	1.0738
2	25	2.7580
3	50	4.6449
4	100	12.3233
5	200	28.2426
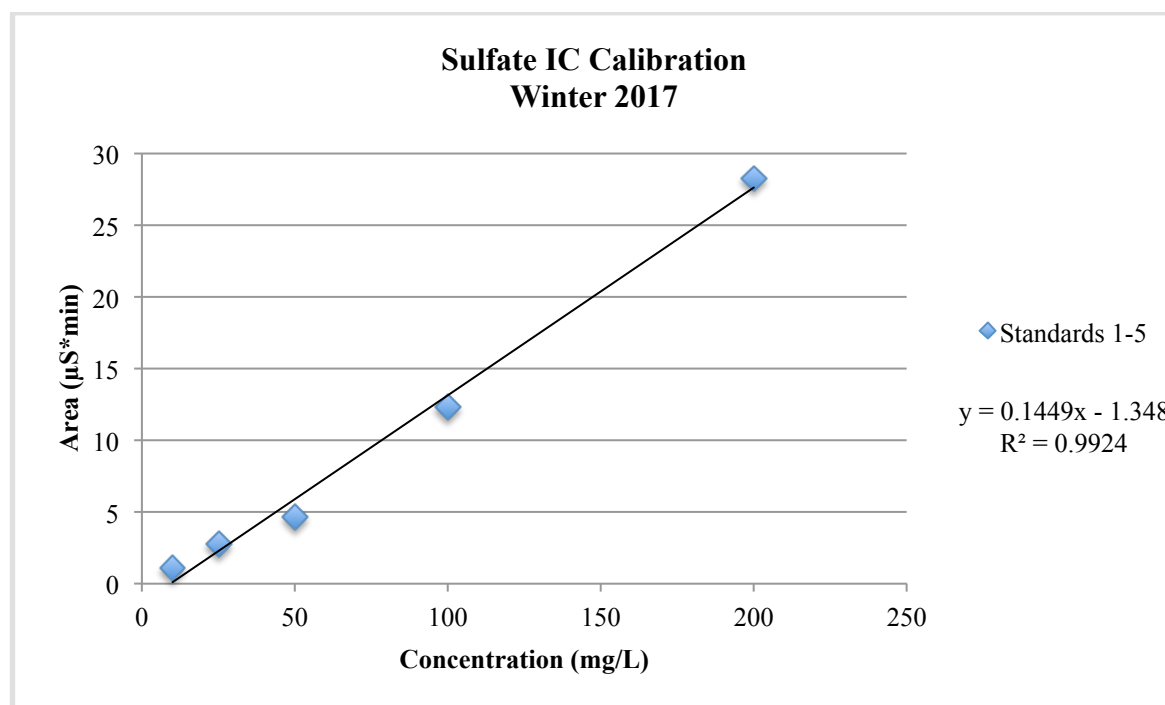
Sulfate IC Calibration
Winter 2017

y = 0.1449x - 1.348
R² = 0.9924

Phosphate IC Results Winter 2017				
Sample ID	Sample Date	Area (µS*min)	Dilution	Corrected Concentration (mg/L)
Well 11	11/8/17	6.8345	1	56.46
Well 11	11/29/17	6.2591	1	52.49
Well 11	12/1/17	5.683	1	48.52
Well 11	1/26/18	5.8526	1	49.69
Well 12	11/8/17	6.6284	1	55.04
Well 12	11/29/17	6.7624	1	55.97
Well 12	12/1/17	6.865	1	56.68
Well 12	1/26/18	7.4614	1	60.79
Well 13	11/8/17	11.4399	1	88.25
Well 13	11/29/17	12.1385	1	93.07
Well 13	12/1/17	11.2587	1	87.00
Well 13	1/26/18	11.1772	1	86.44

Ion Chromatography with Calibration Curves for Nutrient Species

Nitrate Standards IC Fall 2017		
Standard	Concentration (mg/L)	Area (µS*min)
1	1	0.0571
2	5	0.3901
3	10	0.8197
4	25	2.2688
5	50	5.1365

Nitrate IC Calibration
Fall 2017

Standards 1-5

$y = 0.104x - 0.159$
$R^2 = 0.99677$

Nitrate IC Results Fall 2017				
Sample ID	Sample Date	Area (µS*min)	Dilution	Corrected Concentration (mg/L)
Well 11	6/29/17	0.0232	1	1.75
Well 11	7/13/17	0.0467	1	1.98
Well 11	7/18/17	0.0283	1	1.80
Well 11	7/20/17	0.0335	1	1.85
Well 11	7/25/17	0.1115	1	2.60
Well 11	7/27/17	0.1411	1	2.89
Well 12	6/29/17	ND	1	ND
Well 12	7/13/17	ND	1	ND
Well 12	7/18/17	ND	1	ND
Well 12	7/20/17	ND	1	ND
Well 12	7/25/17	ND	1	ND
Well 12	7/27/17	ND	1	ND
Well 13	6/29/17	0.0702	1	2.20
Well 13	7/13/17	0.1306	1	2.78
Well 13	7/18/17	0.0730	1	2.23
Well 13	7/20/17	0.0790	1	2.29
Well 13	7/25/17	0.2075	1	3.52
Well 13	7/27/17	0.0807	1	2.30
Fox River	7/25/17	0.4230	1	5.60

Nitrate Standards IC Winter 2017		
Standard	**Concentration (mg/L)**	**Area (µS*min)**
1	5	0.3530
2	10	0.8537
3	25	1.6857
4	50	3.9544
5	100	9.6821
6	200	21.1019
7	300	33.8444

Nitrate IC Calibration Winter 2017
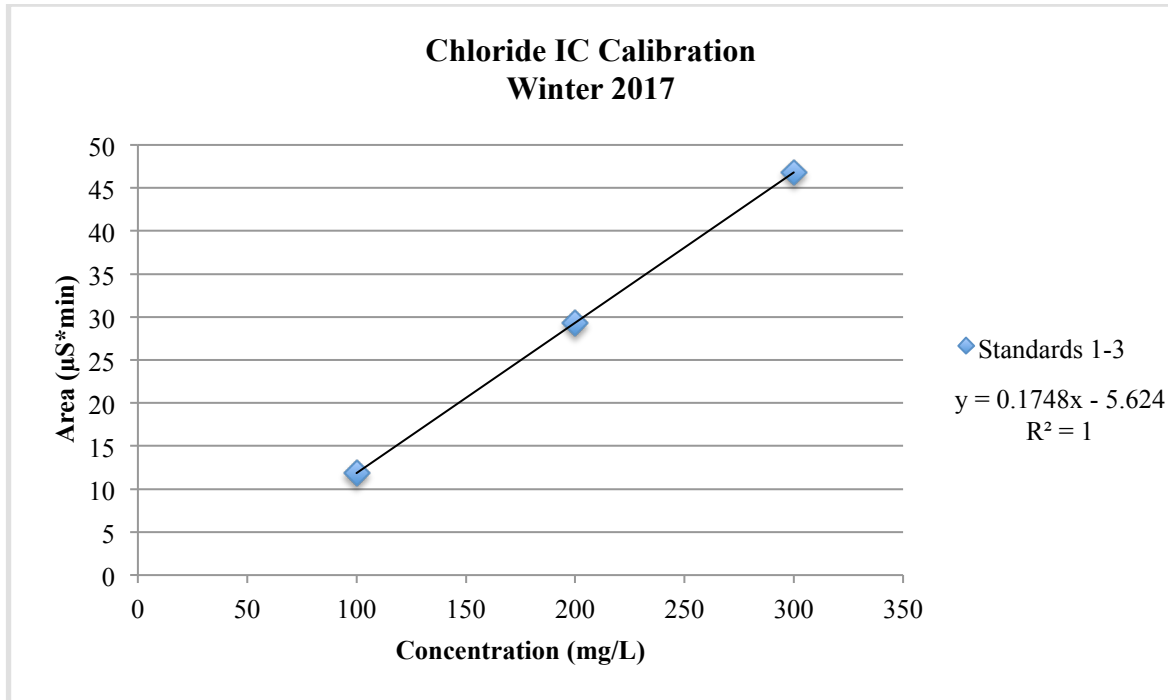
$y = 0.1136x - 0.9868$
$R^2 = 0.99681$

◆ Standards 1-7

Nitrate IC Results Winter 2017

Sample ID	Sample Date	Area (μS*min)	Dilution	Corrected Concentration (mg/L)
Well 11	11/8/17	0.0523	1	0.0184
Well 11	11/29/17	0.0502	1	0.4860
Well 11	12/1/17	0.0521	1	0.0027
Well 11	1/26/18	0.0417	1	0.0020
Well 12	11/8/17	ND	1	ND
Well 12	11/29/17	ND	1	ND
Well 12	12/1/17	ND	1	ND
Well 12	1/26/18	ND	1	ND
Well 13	11/8/17	0.0415	1	0.0699
Well 13	11/29/17	0.0421	1	1.42
Well 13	12/1/17	0.0398	1	0.0016
Well 13	1/26/18	0.0333	1	0.0014

Auto Analyzer with Calibration Curves for Nutrient Species

SEAL Analytical
Application Lab

Name of run :170405A.run   Name of analysis :Nitrite-Ammonia.ANL
Comment   :Low Range NH3   Date of report :4/5/2017

Peak [%]

Conc. [mg/L]
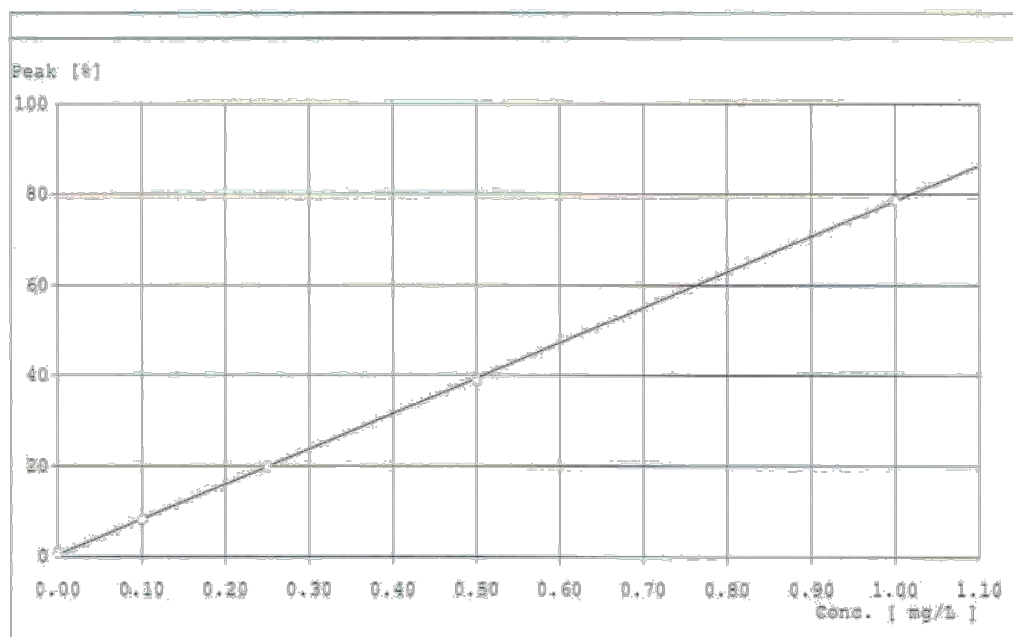
Channel   :2   Date of Run :4/5/2017
Method   :Ammonia
Curve fit   :Linear
Corr.coeff.(r)   :0.9999

Equation   :y = bx + a

                  y = conc. in
                  x = peak height in digital units
                  a = -6.7540E-002
                  b = 1.9545E-005

Corrections
Baseline Corr.   done
Drift Correction   no
Carryover Corr.   done   0.34 %

Calibrant Values

Type	Calculated	Target	Diff.[mg/L]	Diff. (%)
1C	1.003	1.000	0.003	0.30
2C	0.495	0.500	-0.005	-1.01
3C	0.249	0.250	-0.001	-0.55
4C	0.098	0.100	-0.002	-1.56
5C	0.005	0.000	0.005	---

Page 1 of 1

SEAL Analytical
Application Lab

Name of run :170405A.run   Name of analysis :Nitrite-Ammonia.ANL
Comment   :Low Range NH3   Date of report :4/5/2017
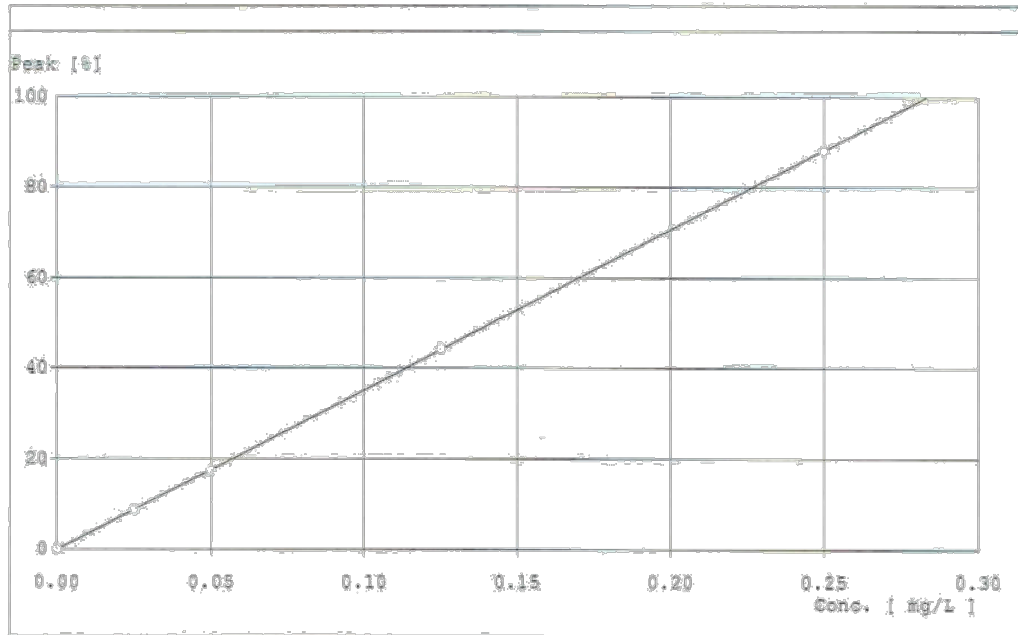
Peak [%]

Channel	:1
Method	:Nitrite
Curve fit	:Linear
Corr.coeff.(r)	:1.0000

Date of run :4/5/2017

Equation   :y = bx + a

    y = conc. in
    x = peak height in digital units
    a = -1.2068E-002
    b = 4.3166E-006

Corrections
Baseline Corr.   done
Drift Correction   no
Carryover Corr.   done   0.34 %

Calibrant Values

Type	Calculated	Target	Diff.[mg/L]	Diff. (%)
1C	0.250	0.250	0.000	-0.08
2C	0.126	0.125	0.001	0.53
3C	0.049	0.050	-0.001	-1.12
4C	0.025	0.025	0.000	-0.51
5C	0.000	0.000	0.000	---

Page 1 of 1

129

SEAL Analytical

Application Lab

Name of Run   : 170405A   Name of Analysis : Nitrite-Ammonia.ANL
Date of Report   : 4/5/2017   System   : 1 / AA3 HR
Run Start   : 4/5/2017 4:09:51 PM Run Stop   : 4:37:48 PM
Operator   :
Comment   : Low Range NH3

Channel	:	1	2
Method	:	Nitrite	Ammonia
Unit	:	mg/L	mg/L
Calibr. Fit	:	Linear	Linear
Corr. Coeff.(r)	:	1.0000	0.9999
Base	:	-9646	-4882
Gain	:	181	13
Sensitivity	:	0.0487	0.6034
Sample Limit 1	:		
Sample Limit 2	:		

Pk	Cup		Sample ID	Value	Value
0	0	B	Baseline	0.000	-0.005
1	901	P	Primer	0.250	0.999
2	901	D	Drift	0.250	1.008
3	901	C	1 ppm NH4 0.250NO2	0.250	1.003
4	902	C	0.5ppm NH4 0.125NO2	0.126	0.495
5	903	C	0.25ppm NH4 0.05NO2	0.049	0.249
6	904	C	0.1ppm NH4 0.025NO2	0.025	0.098
7	905	C	Standard 0 ppb	0.000	0.005
8	901	H1	High	0.250	0.996
9	904	L1	Low	0.025	0.098
10	904	L1	Low	0.025	0.098
11	1	S	Well 11 H	0.088	0.007
12	2	S	Well 11 T	0.086	0.001
13	3	S	Well 12 H	0.004	0.068
14	4	S	Well 12 T	0.004	0.072
15	5	S	Well 13 H	0.043	0.029
16	7	S	Well 13 T	4.214*	1.232*
17	901	D	Drift	0.236	0.969
18	0	B	Final Base	0.000	-0.005

CORRECTIONS			
Channel	:	1	2
Baseline	:	Yes	Yes
Drift	:	No	No
Carryover	:	Yes	Yes
%	:	0.3	0.3

```
* ... Sample offscale
+ ... Result higher than sample limit
- ... Result lower than sample limit
P ... Standard passed
F ... Standard failed
N ... Value not calculated or not used
R ... Resample after offscale
M ... Peak marker moved manually
D ... Diluted sample
H ... Dual calibration used

** <END OF REPORT> **
```

SEAL Analytical
Application Lab

Name of run :171103.run   Name of analysis :Nitrite-Ammonia.ANL
Comment   :Low Range NH3   Date of report :2/26/2018

Peak [%]

Conc. [mg/L]
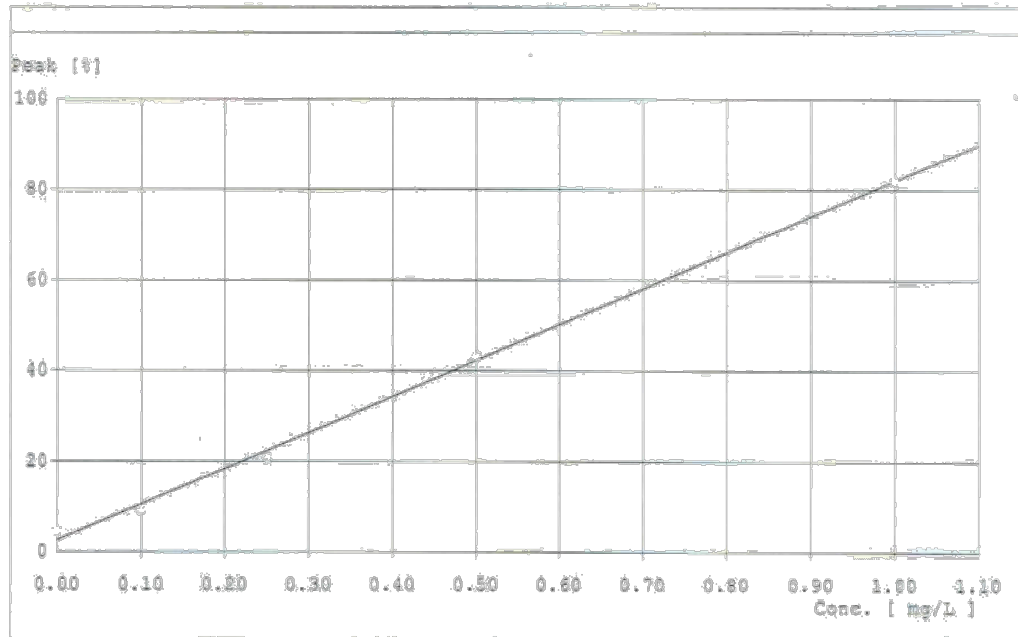
Channel   :2   Date of run :11/3/2017
Method   :Ammonia
Curve fit   :Linear
Corr.coeff.(r)   :0.9990

Equation   :y = bx + a

                   y = conc. in
                   x = peak height in digital units
                   a = -9.4212E-002
                   b = 1.9204E-005

Corrections
Baseline Corr.   done
Drift Correction   done
Carryover Corr.   done   0.43 %

Calibrant Values

Type	Calculated	Target	Diff.[mg/L]	Diff. (%)
1C	0.999	1.000	-0.001	-0.12
2C	0.512	0.500	0.012	2.43
3C	0.232	0.250	-0.018	-7.28
4C	0.084	0.100	-0.016	-16.18
5C	0.023	0.000	0.023	---

Page 1 of 1

131

SEAL Analytical
Application Lab

Name of run :171103.run   Name of analysis :Nitrite-Ammonia.ANL
Comment   :Low Range NH3   Date of report :2/9/2018

Peak [%]

Conc. [mg/L]

Channel   :1   Date of run :11/3/2017
Method   :Nitrite
Curve Fit   :Linear
Corr.coeff.(r)   :1.0000

Equation   :y = bx + a

                  y = conc. in
                  x = peak height in digital units
                  a = +1.5387E-002
                  b = 4.5628E-006

Corrections
Baseline Corr.   done
Drift Correction   done
Carryover Corr.   done   0.13 %

Calibrant Values

Type	Calculated	Target	Diff.[mg/L]	Diff. (%)
1C	0.250	0.250	0.000	-0.11
2C	0.126	0.125	0.001	0.64
3C	0.049	0.050	-0.001	-1.03
4C	0.025	0.025	0.000	-0.68
5C	0.000	0.000	0.000	---

Page 1 of 1

132

SEAL Analytical
Application Lab

Name of Run   : 171103   Name of Analysis : Nitrite-Ammonia.ANL
Date of Report : 2/9/2018   System   : 1 / AA3 HR
Run Start   : 11/3/2017 2:20:34 PM   Run Stop   : 3:05:55 PM
Operator   :
Comment   : Low Range NH3

Channel :	1	2
Method :	Nitrite	Ammonia
Unit :	mg/L	mg/L
Calibr. Fit :	Linear	Linear
Corr. Coeff.(r) :	1.0000	0.9990
Base :	-9324	-4883
Gain :	81	19
Sensitivity :	0.1028	0.4194
Sample Limit 1 :		
Sample Limit 2 :		

| Pk	Cup		Sample ID	Value	Value
0	0	B	Baseline	0.000	-0.032
1	901	P	Primer	0.249	0.971
2	901	D	Drift	0.249	0.977
3	901	C	1 ppm NH4 0.250NO2	0.250	0.999
4	902	C	0.5ppm NH4 0.125NO2	0.126	0.512
5	903	C	0.25ppm NH4 0.05NO2	0.049	0.232
6	904	C	0.10ppmNH4 0.025NO2	0.025	0.084
7	905	C	Standard 0 ppb	0.000	0.023
8	901	H1	High	0.249	0.964
9	904	L1	Low	0.025	0.088
10	904	L1	Low	0.025	0.088
11	1	S	Well 11 6-29	0.036	-0.010
12	2	S	12 6-29	0.001	0.081
13	3	S	13 6-29	0.043	0.025
14	4	S	14 6-29	0.000	-0.017
15	5	S	11 7-13	0.031	0.002
16	6	S	12 7-13	0.001	0.063
17	7	S	13 7-13	0.048	0.040
18	8	S	11 7-18	0.023	-0.019
19	9	S	12 7-18	0.001	0.059
20	10	S	13 7-18	0.023	0.006
21	11	S	14 7-18	0.000	-0.025
22	12	S	11 7-20	0.027	-0.012
23	13	S	12 7-20	0.001	0.083
24	14	S	13 7-20	0.037	0.022
25	15	S	14 7-20	0.000	-0.025
26	16	S	11 7-25	0.040	-0.013
27	17	S	12 7-25	0.001	0.057
28	18	S	13 7-25	0.025	0.014
29	19	S	14 7-25	0.000	-0.012
30	20	S	riv 7-25	0.046	0.026
31	21	S	11 7-27	0.024	-0.023
32	22	S	12 7-27	0.001	0.075
33	23	S	13 7-27	0.036	0.023
34	24	S	14 7-27	0.000	-0.026
35	901	D	Drift	0.249	0.977
36	0	B	Final Base	0.000	-0.032

CORRECTIONS		1	2
Channel :		1	2
Baseline :		Yes	Yes
Drift :		Yes	Yes
Carryover :		Yes	Yes

133

%:   0.1   0.4

* ... Sample offscale
+ ... Result higher than sample limit
- ... Result lower than sample limit
P ... Standard passed
F ... Standard failed
N ... Value not calculated or not used
R ... Resample after offscale
M ... Peak marker moved manually
D ... Diluted sample
H ... Dual calibration used

** <END OF REPORT> **

SEAL Analytical
Application Lab

Name of run :180202A.run   Name of analysis :Nitrite-Ammonia.ANL
Comment   :Low Range NH3   Date of report :2/26/2018

Peak [%]

(Conc. [mg/L])

Channel   :2   Date of run :2/2/2018
Method   :Ammonia
Curve fit   :Linear
Corr.coeff.(r)   :0.9996

Equation   :y = bx + a

                   y = conc. in
                   x = peak height in digital units
                   a = -9.5807E-002
                   b = 1.9348E-005

Corrections
Baseline Corr.   done
Drift Correction   done
Carryover Corr.   done   0.61 %

Calibrant Values

Type	Calculated	Target	Diff.[mg/L]	Diff. (%)
1C	0.991	1.000	-0.009	-0.91
2C	0.526	0.500	0.026	5.28
3C	0.221	0.250	-0.029	-11.48
4C	0.113	0.100	0.013	13.1%
5C	-0.002	0.000	-0.002	---

Page 1 of 1

135

SEAL Analytical
Application Lab

Name of run :180202A.run   Name of analysis :Nitrite-Ammonia.AML
Comment   :Low Range NH3   Date of report :2/9/2018
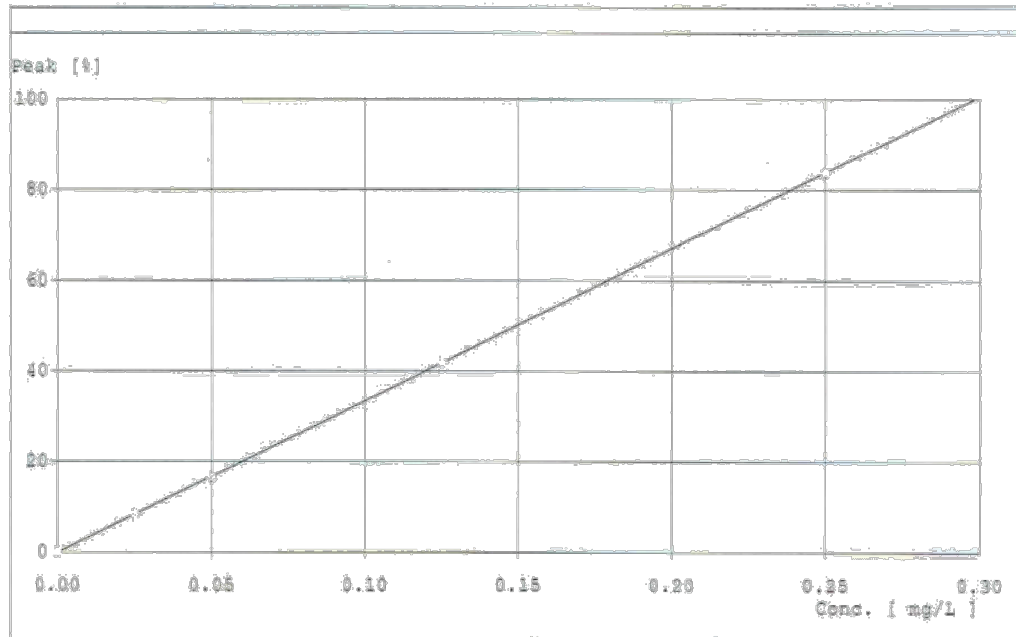
Peak [%]

Conc. [mg/L]

Channel   :1   Date of run :2/2/2018
Method   :Nitrite
Curve fit   :Linear
Corr.coeff.(r) :1.0000

Equation   :y = bx + a

                y = conc. in
                x = peak height in digital units
                a = -1.4817E-002
                b = 4.5436E-006

Corrections
Baseline Corr.   done
Drift Correction done
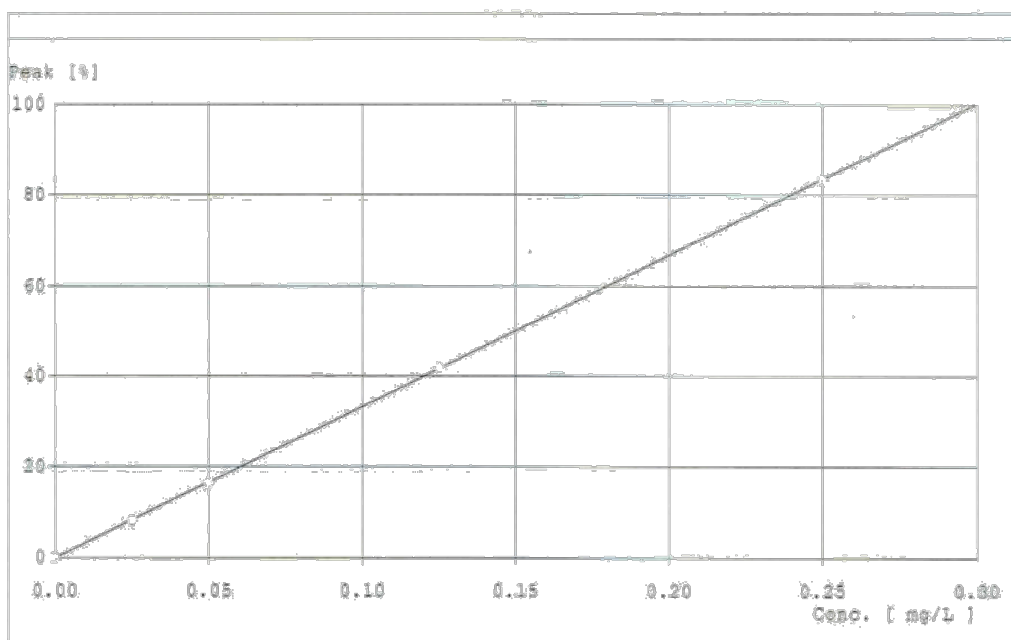Carryover Corr.   done   0.23 %

Calibrant Values

Type	Calculated	Target	Diff.[mg/L]	Diff. (%)
1C	0.250	0.250	0.000	-0.05
2C	0.125	0.125	0.000	0.36
3C	0.050	0.050	0.000	-0.88
4C	0.025	0.025	0.000	-0.72
5C	0.000	0.000	0.000	---

Page 1 of 1

136

SEAL Analytical
Application Lab

Name of Run	: 180202A	Name of Analysis	: Nitrite-Ammonia.ANL
Date of Report	: 2/9/2018	System	: 1 / AA3 HR
Run Start	: 2/2/2018 2:42:26 PM	Run Stop	: 3:19:58 PM
Operator	: Maddy		
Comment	: Low Range NH3		
	Wells		

	1	2
Channel :		
Method :	Nitrite	Ammonia
Unit :	mg/L	mg/L
Calibr. Fit :	Linear	Linear
Corr. Coeff.(r) :	1.0000	0.9986
Base :	-9393	-4727
Gain :	71	17
Sensitivity :	0.1178	0.4728
Sample Limit 1 :		
Sample Limit 2 :		

Pk	Cup		Sample ID	Value	Value
0	0	B	Baseline	0.000	-0.033
1	901	P	Primer	0.249	0.987
2	901	D	Drift	0.249	0.983
3	901	C	1 ppm NH4 0.250NO2	0.250	0.991
4	902	C	0.5ppm NH4 0.125NO2	0.125	0.526
5	903	C	0.25ppm NH4 0.05NO2	0.050	0.221
6	904	C	0.10ppmNH4 0.025NO2	0.025	0.113
7	905	C	Standard 0 ppb	0.000	-0.002
8	901	H1	High	0.250	0.990
9	904	L1	Low	0.025	0.115
10	904	L1	Low	0.025	0.116
11	1	S	Well 11 11-8	0.054	-0.011
12	2	S	12 11-8	0.005	0.072
13	3	S	13 11-8	0.045	0.031
14	4	S	14 11-8	0.001	0.004
15	5	S	11 11-29	0.051	-0.011
16	6	S	12 11-29	0.004	0.070
17	7	S	13 11-29	0.045	0.031
18	8	S	14 11-29	0.002	-0.002
19	9	S	11 12-1	0.047	-0.017
20	10	S	12 12-1	0.004	0.076
21	11	S	13 12-1	0.045	0.022
22	12	S	14 12-1	0.001	-0.020
23	13	S	11 1-26	0.047	0.004
24	14	S	12 1-26	0.004	0.098
25	15	S	13 1-26	0.042	0.046
26	16	S	14 1-26	0.001	0.012
27	901	D	Drift	0.249	0.983
28	0	B	Final Base	0.000	-0.033

CORRECTIONS

Channel :	1	2
Baseline :	Yes	Yes
Drift :	Yes	Yes
Carryover :	Yes	Yes
%:	0.2	0.6

* ... Sample offscale
+ ... Result higher than sample limit
~ ... Result lower than sample limit
P ... Standard passed

F ... Standard failed
N ... Value not calculated or not used
R ... Resample after offscale
M ... Peak marker moved manually
D ... Diluted sample
H ... Dual calibration used

** <END OF REPORT> **

Spectrophotometer with Calibration Curves for Total Dissolved Phosphorous

TDP Standards SRP Fall 2017				
Standard	Concentration (µg/L)	Absorbance	Corrected Absorbance	F Factor
Blank	0	-0.0001	-	-
1	1	0.0054	0.0055	181.8181
2	2.5	0.0139	0.0140	178.5714
3	5	0.0280	0.0281	177.9359
4	10	0.0570	0.0571	175.1313
5	20	0.1137	0.1138	175.7469
6	50	0.2829	0.2830	176.6784
7	100	0.5766	0.5767	173.4003

SRP Calibration Curve Fall 2017

$y = 173.55x + 0.2217$
$R^2 = 0.99992$
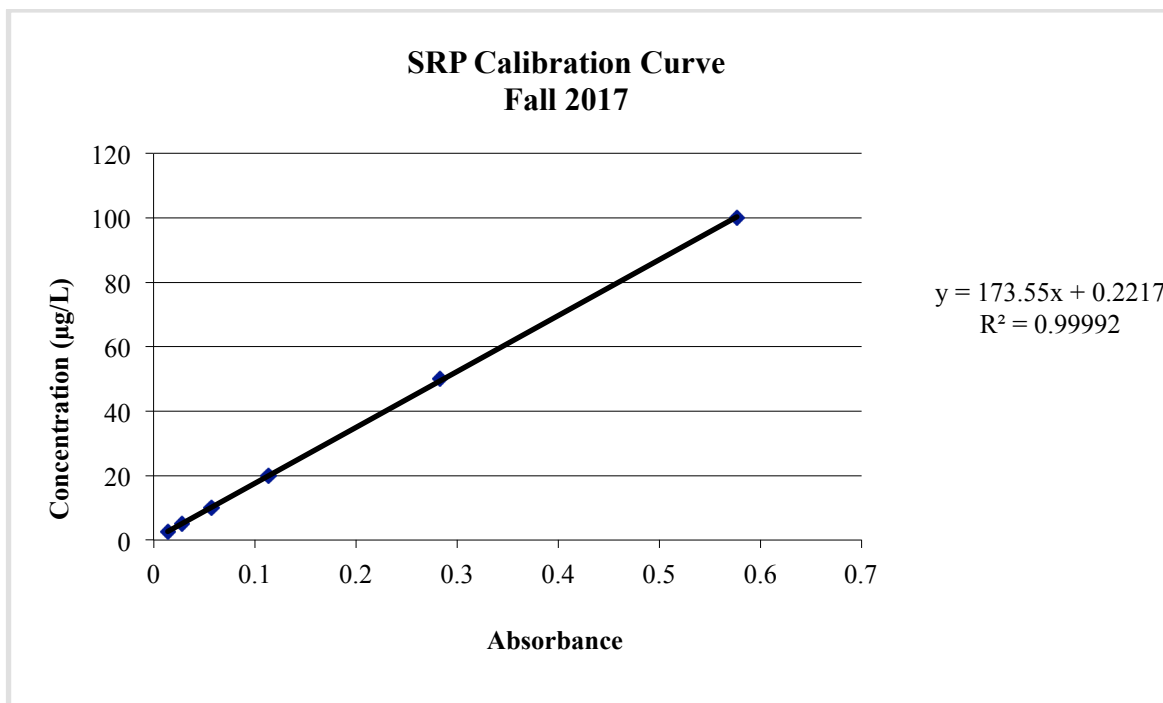
TDP IC Results Fall 2017			
Sample ID	Sample Date	Absorbance	Corrected Concentration (µg/L)
Well 11	6/29/27	0.0172	1.63
Well 11	7/13/17	0.0366	4.71
Well 11	7/18/17	0.0249	2.75
Well 11	7/20/17	0.0264	3.16
Well 11	7/25/17	0.0125	0.8386
Well 11	7/27/17	0.0140	1.07
Well 12	6/29/17	0.0271	3.38
Well 12	7/13/17	0.0358	4.91
Well 12	7/18/17	0.0502	6.99
Well 12	7/20/17	0.0515	7.37
Well 12	7/25/17	0.0228	2.56
Well 12	7/27/17	0.0287	3.66
Well 13	6/29/17	0.0124	0.7930
Well 13	7/13/17	0.0368	4.74
Well 13	7/18/17	0.0385	5.03
Well 13	7/20/17	0.0232	2.63
Well 13	7/25/17	0.0207	2.21
Well 13	7/27/17	0.0251	2.95
Fox River	7/25/17	0.3586	58.88

TDP Standards SRP Winter 2017

Standard	Concentration (µg/L)	Absorbance	Corrected Absorbance	F Factor
Blank	0	-0.0022	-	-
1	1	0.0032	0.0054	185.1851852
2	2.5	0.0101	0.0123	203.2520325
3	5	0.0242	0.0264	189.3939394
4	10	0.0499	0.0521	191.9385797
5	20	0.1038	0.106	188.6792453
6	50	0.2661	0.2683	186.3585539
7	100	0.5391	0.5413	184.7404397

SRP Calibration Curve
Winter 2017

$y = 184.37x + 0.3251$
$R^2 = 0.99998$
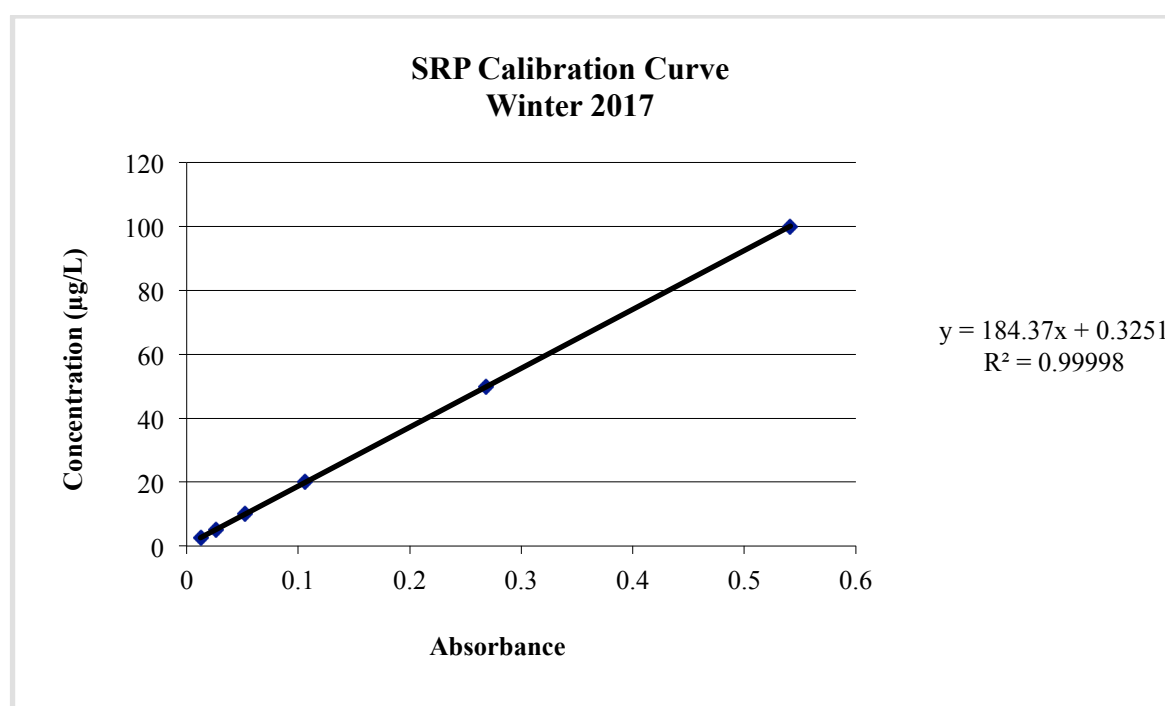
TDP IC Results Winter 2017			
Sample ID	Sample Date	Absorbance	Corrected Concentration (µg/L)
Well 11	11/8/17	0.0114	1.64
Well 11	11/29/17	0.0162	2.55
Well 11	12/1/17	0.0113	0.7296
Well 11	1/26/18	0.0091	0.3474
Well 12	11/8/17	0.0229	3.83
Well 12	11/29/17	0.0116	1.67
Well 12	12/1/17	0.0113	0.7296
Well 12	1/26/18	0.0173	1.77
Well 13	11/8/17	0.0122	1.79
Well 13	11/29/17	0.0118	1.71
Well 13	12/1/17	0.0122	1.79
Well 13	1/26/18	0.0199	2.22

PHREEQC Files

Input file: C:\Users\madeline.salo\Desktop\WK11 12_22_18

Output file: C:\Users\madeline.salo\Desktop\WK11 12_22_18.pqo
Database file: C:\Program Files (x86)\USGS\Phreeqc Interactive 3.4.0-
12927\database\phreeqc.dat

Reading data base.

        SOLUTION_MASTER_SPECIES
        SOLUTION_SPECIES
        PHASES
        EXCHANGE_MASTER_SPECIES
        EXCHANGE_SPECIES
        SURFACE_MASTER_SPECIES
        SURFACE_SPECIES
        RATES
        END

Reading input data for simulation 1.

        DATABASE C:\Program Files (x86)\USGS\Phreeqc Interactive 3.4.0-
12927\database\phreeqc.dat
        SOLUTION_MASTER_SPECIES
          Acetate   Acetate-   1.0   Acetate   59.
        SOLUTION_SPECIES
        Acetate- = Acetate-
          log_k   0.0
              analytical_expression   -0.96597E+02   -0.34535E-01   0.19753E+04
0.38593E+02   0.30850E+02
        Acetate- + H+ = AcetateH
          log_k   4.76
          delta_h   116.1 kcal/mol   #from llnl.dat
        END

End of simulation.

Reading input data for simulation 2.

        SOLUTION 1 #WK11 collected on 2/28/17 through 1/26/18
          Temp   10.42
          pH   6.98
          pe
          redox   pe

145

```
            units        mg/L
            density      1
            Ca           93.12
            Mg           54.93
            Na           101.43
            K            3.3
            Fe(+2)       0.1
            Alkalinity   420.68
            Cl           218.48
            S(6)         64.11
            S(-2)        0.1
            N(5)         1.49
            N(3)         0.05
            N(-3)        0.001
            P            0.002
            H(0)         0.002 umol/L
            O(0)         0.182
            C(-4)        0.007 umol/L
            Acetate      1.2
            water        1 # kg
         END
```

Beginning of initial solution calculations.

Initial solution 1.

----------------------------Solution composition----------------------------

Elements	Molality	Moles
Acetate	2.036e-05	2.036e-05
Alkalinity	8.414e-03	8.414e-03
C(-4)	7.007e-09	7.007e-09
Ca	2.326e-03	2.326e-03
Cl	6.168e-03	6.168e-03
Fe(2)	1.792e-06	1.792e-06
H(0)	2.002e-09	2.002e-09
K	8.448e-05	8.448e-05
Mg	2.262e-03	2.262e-03
N(-3)	7.146e-08	7.146e-08
N(3)	3.573e-06	3.573e-06
N(5)	1.065e-04	1.065e-04
Na	4.416e-03	4.416e-03
O(0)	1.139e-05	1.139e-05
P	6.463e-08	6.463e-08

S(-2)   3.122e-06   3.122e-06

S(6)   6.680e-04   6.680e-04

---------------------------Description of solution---------------------------
$$pH = 6.980$$
$$pe = 6.980$$
Specific Conductance (μS/cm, $10\infty C$) = 1006
Density (g/cm≥) = 1.00052
Volume (L) = 1.00063
Activity of water = 1.000
Ionic strength (mol/kgw) = 1.912e-02
Mass of water (kg) = 1.000e+00
Total carbon (mol/kg) = 1.053e-02
Total CO2 (mol/kg) = 1.053e-02
Temperature (∞C) = 10.42
Electrical balance (eq) = -2.350e-03
Percent error, 100*(Cat-|An|)/(Cat+|An|) = -8.19
Iterations = 10
Total H = 1.110208e+02
Total O = 5.553868e+01

--------------------------------Redox couples--------------------------------

Redox couple	pe	Eh (volts)
C(-4)/C(4)	-2.9904	-0.1682
H(0)/H(1)	-4.0230	-0.2263
N(-3)/N(3)	6.9617	0.3917
N(-3)/N(5)	7.4380	0.4185
N(3)/N(5)	8.8668	0.4989
O(-2)/O(0)	14.4994	0.8158
S(-2)/S(6)	-3.0590	-0.1721

--------------------------Distribution of species--------------------------

Species	Molality	Activity	Log Molality	Log Activity	Log Gamma	mole V cm≥/mol
H+	1.172e-07	1.047e-07	-6.931	-6.980	-0.049	0.00
OH-	3.343e-08	2.915e-08	-7.476	-7.535	-0.059	-4.87
H2O	5.551e+01	9.996e-01	1.744	-0.000	0.000	18.02
Acetate	2.036e-05					
Acetate-	2.036e-05	1.783e-05	-4.691	-4.749	-0.058	(0)
AcetateH	4.505e-12	4.525e-12	-11.346	-11.344	0.002	(0)
C(-4)	7.007e-09					
CH4	7.007e-09	7.038e-09	-8.154	-8.153	0.002	34.03

147

C(4)	1.053e-02					
HCO3-	8.140e-03	7.165e-03	-2.089	-2.145	-0.055	23.34
CO2	2.152e-03	2.161e-03	-2.667	-2.665	0.002	33.68
MgHCO3+	1.161e-04	1.015e-04	-3.935	-3.993	-0.058	5.00
CaHCO3+	9.884e-05	8.724e-05	-4.005	-4.059	-0.054	9.03
NaHCO3	1.687e-05	1.695e-05	-4.773	-4.771	0.002	1.80
CaCO3	3.980e-06	3.997e-06	-5.400	-5.398	0.002	-14.65
CO3-2	3.751e-06	2.252e-06	-5.426	-5.647	-0.222	-6.90
MgCO3	2.159e-06	2.169e-06	-5.666	-5.664	0.002	-17.07
FeHCO3+	5.700e-07	4.991e-07	-6.244	-6.302	-0.058	(0)
NaCO3-	8.523e-08	7.464e-08	-7.069	-7.127	-0.058	-2.79
(CO2)2	5.056e-08	5.078e-08	-7.296	-7.294	0.002	67.37
FeCO3	3.747e-08	3.763e-08	-7.426	-7.424	0.002	(0)
Ca	2.326e-03					
Ca+2	2.158e-03	1.295e-03	-2.666	-2.888	-0.222	-18.15
CaHCO3+	9.884e-05	8.724e-05	-4.005	-4.059	-0.054	9.03
CaSO4	6.488e-05	6.517e-05	-4.188	-4.186	0.002	6.81
CaCO3	3.980e-06	3.997e-06	-5.400	-5.398	0.002	-14.65
CaHPO4	6.666e-09	6.695e-09	-8.176	-8.174	0.002	(0)
CaOH+	2.343e-09	2.052e-09	-8.630	-8.688	-0.058	(0)
CaH2PO4+	6.467e-10	5.693e-10	-9.189	-9.245	-0.055	(0)
CaPO4-	1.287e-10	1.133e-10	-9.890	-9.946	-0.055	(0)
CaHSO4+	4.266e-11	3.735e-11	-10.370	-10.428	-0.058	(0)
Cl	6.168e-03					
Cl-	6.168e-03	5.386e-03	-2.210	-2.269	-0.059	17.49
FeCl+	5.915e-09	5.179e-09	-8.228	-8.286	-0.058	(0)
Fe(2)	1.792e-06					
Fe+2	1.148e-06	6.966e-07	-5.940	-6.157	-0.217	-23.00
FeHCO3+	5.700e-07	4.991e-07	-6.244	-6.302	-0.058	(0)
FeCO3	3.747e-08	3.763e-08	-7.426	-7.424	0.002	(0)
FeSO4	2.958e-08	2.971e-08	-7.529	-7.527	0.002	38.22
FeCl+	5.915e-09	5.179e-09	-8.228	-8.286	-0.058	(0)
Fe(HS)2	8.561e-10	8.598e-10	-9.067	-9.066	0.002	(0)
FeOH+	7.612e-10	6.688e-10	-9.118	-9.175	-0.056	(0)
FeHPO4	3.466e-11	3.482e-11	-10.460	-10.458	0.002	(0)
FeH2PO4+	9.151e-12	8.055e-12	-11.039	-11.094	-0.055	(0)
Fe(HS)3-	1.258e-13	1.102e-13	-12.900	-12.958	-0.058	(0)
FeHSO4+	2.294e-14	2.009e-14	-13.639	-13.697	-0.058	(0)
Fe(OH)2	1.426e-14	1.432e-14	-13.846	-13.844	0.002	(0)
Fe(OH)3-	4.974e-18	4.370e-18	-17.303	-17.360	-0.056	(0)
H(0)	2.002e-09					
H2	1.001e-09	1.005e-09	-9.000	-8.998	0.002	28.62
K	8.448e-05					
K+	8.433e-05	7.358e-05	-4.074	-4.133	-0.059	8.50
KSO4-	1.427e-07	1.256e-07	-6.846	-6.901	-0.055	33.64
KHPO4-	2.046e-12	1.801e-12	-11.689	-11.744	-0.055	39.47

Mg	2.262e-03					
Mg+2	2.080e-03	1.262e-03	-2.682	-2.899	-0.217	-20.98
MgHCO3+	1.161e-04	1.015e-04	-3.935	-3.993	-0.058	5.00
MgSO4	6.301e-05	6.328e-05	-4.201	-4.199	0.002	5.14
MgCO3	2.159e-06	2.169e-06	-5.666	-5.664	0.002	-17.07
MgOH+	1.239e-08	1.096e-08	-7.907	-7.960	-0.053	(0)
MgHPO4	8.784e-09	8.822e-09	-8.056	-8.054	0.002	(0)
MgH2PO4+	8.027e-10	7.065e-10	-9.095	-9.151	-0.055	(0)
MgPO4-	1.692e-10	1.490e-10	-9.772	-9.827	-0.055	(0)
N(-3)	7.146e-08					
NH4+	7.106e-08	6.162e-08	-7.148	-7.210	-0.062	17.40
NH4SO4-	2.878e-10	2.520e-10	-9.541	-9.599	-0.058	32.27
NH3	1.128e-10	1.133e-10	-9.948	-9.946	0.002	23.54
N(3)	3.573e-06					
NO2-	3.573e-06	3.107e-06	-5.447	-5.508	-0.061	24.02
N(5)	1.065e-04					
NO3-	1.065e-04	9.260e-05	-3.973	-4.033	-0.061	27.81
Na	4.416e-03					
Na+	4.393e-03	3.856e-03	-2.357	-2.414	-0.057	-2.29
NaHCO3	1.687e-05	1.695e-05	-4.773	-4.771	0.002	1.80
NaSO4-	6.323e-06	5.566e-06	-5.199	-5.254	-0.055	14.83
NaCO3-	8.523e-08	7.464e-08	-7.069	-7.127	-0.058	-2.79
NaHPO4-	1.072e-10	9.439e-11	-9.970	-10.025	-0.055	34.98
NaOH	1.119e-20	1.124e-20	-19.951	-19.949	0.002	(0)
O(0)	1.139e-05					
O2	5.693e-06	5.718e-06	-5.245	-5.243	0.002	29.00
P	6.463e-08					
H2PO4-	2.621e-08	2.307e-08	-7.581	-7.637	-0.055	33.62
HPO4-2	2.107e-08	1.255e-08	-7.676	-7.901	-0.225	7.36
MgHPO4	8.784e-09	8.822e-09	-8.056	-8.054	0.002	(0)
CaHPO4	6.666e-09	6.695e-09	-8.176	-8.174	0.002	(0)
MgH2PO4+	8.027e-10	7.065e-10	-9.095	-9.151	-0.055	(0)
CaH2PO4+	6.467e-10	5.693e-10	-9.189	-9.245	-0.055	(0)
MgPO4-	1.692e-10	1.490e-10	-9.772	-9.827	-0.055	(0)
CaPO4-	1.287e-10	1.133e-10	-9.890	-9.946	-0.055	(0)
NaHPO4-	1.072e-10	9.439e-11	-9.970	-10.025	-0.055	34.98
FeHPO4	3.466e-11	3.482e-11	-10.460	-10.458	0.002	(0)
FeH2PO4+	9.151e-12	8.055e-12	-11.039	-11.094	-0.055	(0)
KHPO4-	2.046e-12	1.801e-12	-11.689	-11.744	-0.055	39.47
H3PO4	2.950e-13	2.963e-13	-12.530	-12.528	0.002	46.41
PO4-3	1.334e-13	3.979e-14	-12.875	-13.400	-0.525	-21.32
S(-2)	3.122e-06					
H2S	1.770e-06	1.778e-06	-5.752	-5.750	0.002	37.09
HS-	1.350e-06	1.177e-06	-5.870	-5.929	-0.059	19.73
Fe(HS)2	8.561e-10	8.598e-10	-9.067	-9.066	0.002	(0)
S-2	7.972e-13	4.750e-13	-12.098	-12.323	-0.225	(0)

Fe(HS)3-	1.258e-13	1.102e-13	-12.900	-12.958	-0.058	(0)

S(6)   6.680e-04

SO4-2	5.336e-04	3.174e-04	-3.273	-3.498	-0.226	12.20
CaSO4	6.488e-05	6.517e-05	-4.188	-4.186	0.002	6.81
MgSO4	6.301e-05	6.328e-05	-4.201	-4.199	0.002	5.14
NaSO4-	6.323e-06	5.566e-06	-5.199	-5.254	-0.055	14.83
KSO4-	1.427e-07	1.256e-07	-6.846	-6.901	-0.055	33.64
FeSO4	2.958e-08	2.971e-08	-7.529	-7.527	0.002	38.22
HSO4-	2.740e-09	2.399e-09	-8.562	-8.620	-0.058	39.03
NH4SO4-	2.878e-10	2.520e-10	-9.541	-9.599	-0.058	32.27
CaHSO4+	4.266e-11	3.735e-11	-10.370	-10.428	-0.058	(0)
FeHSO4+	2.294e-14	2.009e-14	-13.639	-13.697	-0.058	(0)

---------------------------Saturation indices-----------------------------

Phase	SI**	log IAP	log K(283 K, 1 atm)	
Anhydrite	-2.26	-6.39	-4.13	CaSO4
Aragonite	-0.28	-8.54	-8.26	CaCO3
Calcite	-0.12	-8.54	-8.41	CaCO3
CH4(g)	-5.52	-8.15	-2.64	CH4
CO2(g)	-1.39	-2.67	-1.28	CO2
Dolomite	-0.35	-17.08	-16.73	CaMg(CO3)2
FeS(ppt)	-1.19	-5.11	-3.92	FeS
Gypsum	-1.79	-6.39	-4.60	CaSO4:2H2O
H2(g)	-5.94	-9.00	-3.06	H2
H2O(g)	-1.90	-0.00	1.90	H2O
H2S(g)	-4.88	-12.91	-8.03	H2S
Halite	-6.24	-4.68	1.56	NaCl
Hydroxyapatite	-8.16	-10.22	-2.06	Ca5(PO4)3OH
Mackinawite	-0.46	-5.11	-4.65	FeS
Melanterite	-7.25	-9.66	-2.40	FeSO4:7H2O
NH3(g)	-12.06	-9.95	2.12	NH3
O2(g)	-2.47	-5.24	-2.77	O2
Pyrite	28.81	9.90	-18.90	FeS2
Siderite	-1.01	-11.80	-10.80	FeCO3
Sulfur	16.93	22.17	5.24	S
Sylvite	-7.23	-6.40	0.82	KCl
Vivianite	-9.27	-45.27	-36.00	Fe3(PO4)2:8H2O

**For a gas, SI = log10(fugacity). Fugacity = pressure * phi / 1 atm.

For ideal gases, phi = 1.

End of simulation.

Reading input data for simulation 3.

End of Run after 0.049 Seconds.

Input file: C:\Users\madeline.salo\Desktop\WK12 12_22_18

Output file: C:\Users\madeline.salo\Desktop\WK12 12_22_18.pqo

Database file: C:\Program Files (x86)\USGS\Phreeqc Interactive 3.4.0-12927\database\wateq4f.dat

----
Reading data base.

        SOLUTION_MASTER_SPECIES
        SOLUTION_SPECIES
        PHASES
        EXCHANGE_MASTER_SPECIES
        EXCHANGE_SPECIES
        SURFACE_MASTER_SPECIES
        SURFACE_SPECIES
        RATES
        END

Reading input data for simulation 1.

        DATABASE C:\Program Files (x86)\USGS\Phreeqc Interactive 3.4.0-12927\database\wateq4f.dat
        SOLUTION_MASTER_SPECIES
          Acetate   Acetate- 1.0   Acetate   59.
        SOLUTION_SPECIES
        Acetate- = Acetate-
           log_k 0.0
              analytical_expression   -0.96597E+02   -0.34535E-01   0.19753E+04
0.38593E+02   0.30850E+02
        Acetate- + H+ = AcetateH
           log_k   4.76
           delta_h   116.1 kcal/mol   #from llnl.dat
        END

End of simulation.

Reading input data for simulation 2.

        SOLUTION 1 #WK11 collected on 2/28/17 through 12/1/17
           Temp   10.61
           pH   6.99

```
        pe
        redox       pe
        units       mg/L
        density     1
        Ca          90.48
        Mg          53.32
        Na          81.1
        K           3.16
        Fe(+2)      0.1
        Alkalinity  462.25
        Cl          201.28
        S(6)        68.17
        S(-2)       0.1
        N(5)        0.3
        N(3)        0.003
        N(-3)       0.07
        P           0.004
        H(0)        0.005 umol/L
        O(0)        0.1475
        C(-4)       0.417 umol/L
        Acetate     2.27
        water       1 # kg
     END
--------------------------------------------------
Beginning of initial solution calculations.
--------------------------------------------------

Initial solution 1.

----------------------------Solution composition----------------------------

     Elements      Molality      Moles

     Acetate       3.851e-05     3.851e-05
     Alkalinity    9.245e-03     9.245e-03
     C(-4)         4.174e-07     4.174e-07
     Ca            2.260e-03     2.260e-03
     Cl            5.683e-03     5.683e-03
     Fe(2)         1.792e-06     1.792e-06
     H(0)          5.005e-09     5.005e-09
     K             8.089e-05     8.089e-05
     Mg            2.195e-03     2.195e-03
     N(-3)         5.002e-06     5.002e-06
     N(3)          2.144e-07     2.144e-07
     N(5)          2.144e-05     2.144e-05
     Na            3.531e-03     3.531e-03
```

O(0)	9.228e-06	9.228e-06	
P	1.293e-07	1.293e-07	
S(-2)	3.122e-06	3.122e-06	
S(6)	7.103e-04	7.103e-04	

--------------------------Description of solution--------------------------

pH	=	6.990
pe	=	6.990
Activity of water	=	1.000
Ionic strength (mol/kgw)	=	1.856e-02
Mass of water (kg)	=	1.000e+00
Total carbon (mol/kg)	=	1.150e-02
Total CO2 (mol/kg)	=	1.150e-02
Temperature (∞C)	=	10.61
Electrical balance (eq)	=	-3.840e-03
Percent error, 100*(Cat-|An|)/(Cat+|An|)	=	-13.80
Iterations	=	10
Total H	=	1.110216e+02
Total O	=	5.554132e+01

------------------------------Redox couples------------------------------

Redox couple	pe	Eh (volts)
C(-4)/C(4)	-3.2220	-0.1814
H(0)/H(1)	-4.2324	-0.2383
N(-3)/N(3)	6.4247	0.3617
N(-3)/N(5)	7.0953	0.3995
N(3)/N(5)	9.1069	0.5127
O(-2)/O(0)	14.4491	0.8135
S(-2)/S(6)	-3.0667	-0.1727

--------------------------Distribution of species--------------------------

Species	Molality	Activity	Log Molality	Log Activity	Log Gamma	mole V cm≥/mol
H+	1.144e-07	1.023e-07	-6.942	-6.990	-0.048	0.00
OH-	3.453e-08	3.016e-08	-7.462	-7.521	-0.059	(0)
H2O	5.551e+01	9.996e-01	1.744	-0.000	0.000	18.02
Acetate	3.851e-05					
Acetate-	3.851e-05	3.378e-05	-4.414	-4.471	-0.057	(0)
AcetateH	9.577e-12	9.618e-12	-11.019	-11.017	0.002	(0)
C(-4)	4.174e-07					
CH4	4.174e-07	4.192e-07	-6.379	-6.378	0.002	(0)

154

C(4)	1.150e-02					
HCO3-	8.939e-03	7.880e-03	-2.049	-2.103	-0.055	(0)
CO2	2.303e-03	2.313e-03	-2.638	-2.636	0.002	(0)
MgHCO3+	1.236e-04	1.082e-04	-3.908	-3.966	-0.058	(0)
CaHCO3+	1.056e-04	9.334e-05	-3.976	-4.030	-0.054	(0)
NaHCO3	1.361e-05	1.367e-05	-4.866	-4.864	0.002	(0)
CaCO3	4.354e-06	4.373e-06	-5.361	-5.359	0.002	(0)
CO3-2	4.220e-06	2.549e-06	-5.375	-5.594	-0.219	(0)
MgCO3	2.374e-06	2.384e-06	-5.625	-5.623	0.002	(0)
FeHCO3+	6.069e-07	5.323e-07	-6.217	-6.274	-0.057	(0)
NaCO3-	7.747e-08	6.830e-08	-7.111	-7.166	-0.055	(0)
FeCO3	4.112e-08	4.129e-08	-7.386	-7.384	0.002	(0)
Ca	2.260e-03					
Ca+2	2.076e-03	1.254e-03	-2.683	-2.902	-0.219	(0)
CaHCO3+	1.056e-04	9.334e-05	-3.976	-4.030	-0.054	(0)
CaSO4	7.326e-05	7.357e-05	-4.135	-4.133	0.002	(0)
CaCO3	4.354e-06	4.373e-06	-5.361	-5.359	0.002	(0)
CaHPO4	1.323e-08	1.328e-08	-7.879	-7.877	0.002	(0)
CaOH+	2.299e-09	2.032e-09	-8.638	-8.692	-0.054	(0)
CaH2PO4+	1.251e-09	1.103e-09	-8.903	-8.958	-0.055	(0)
CaPO4-	2.620e-10	2.310e-10	-9.582	-9.636	-0.055	(0)
CaHSO4+	4.315e-11	3.785e-11	-10.365	-10.422	-0.057	(0)
Cl	5.683e-03					
Cl-	5.683e-03	4.967e-03	-2.245	-2.304	-0.058	(0)
FeCl+	5.263e-09	4.631e-09	-8.279	-8.334	-0.056	(0)
Fe(2)	1.792e-06					
Fe+2	1.107e-06	6.755e-07	-5.956	-6.170	-0.214	(0)
FeHCO3+	6.069e-07	5.323e-07	-6.217	-6.274	-0.057	(0)
FeCO3	4.112e-08	4.129e-08	-7.386	-7.384	0.002	(0)
FeSO4	3.073e-08	3.086e-08	-7.512	-7.511	0.002	(0)
FeCl+	5.263e-09	4.631e-09	-8.279	-8.334	-0.056	(0)
Fe(HS)2	8.449e-10	8.486e-10	-9.073	-9.071	0.002	(0)
FeOH+	7.661e-10	6.741e-10	-9.116	-9.171	-0.056	(0)
FeHPO4	6.864e-11	6.893e-11	-10.163	-10.162	0.002	(0)
FeH2PO4+	1.766e-11	1.557e-11	-10.753	-10.808	-0.055	(0)
Fe(HS)3-	1.251e-13	1.097e-13	-12.903	-12.960	-0.057	(0)
FeHSO4+	2.325e-14	2.039e-14	-13.634	-13.691	-0.057	(0)
Fe(OH)2	1.498e-14	1.505e-14	-13.824	-13.823	0.002	(0)
Fe(OH)3-	5.349e-18	4.707e-18	-17.272	-17.327	-0.056	(0)
H(0)	5.005e-09					
H2	2.502e-09	2.513e-09	-8.602	-8.600	0.002	(0)
K	8.089e-05					
K+	8.075e-05	7.057e-05	-4.093	-4.151	-0.058	(0)
KSO4-	1.464e-07	1.290e-07	-6.835	-6.889	-0.055	(0)
KHPO4-	4.001e-12	3.527e-12	-11.398	-11.453	-0.055	(0)
Mg	2.195e-03					

Mg+2	2.004e-03	1.223e-03	-2.698	-2.913	-0.215	(0)
MgHCO3+	1.236e-04	1.082e-04	-3.908	-3.966	-0.058	(0)
MgSO4	6.550e-05	6.578e-05	-4.184	-4.182	0.002	(0)
MgCO3	2.374e-06	2.384e-06	-5.625	-5.623	0.002	(0)
MgHPO4	1.744e-08	1.752e-08	-7.758	-7.757	0.002	(0)
MgOH+	1.250e-08	1.107e-08	-7.903	-7.956	-0.053	(0)
MgH2PO4+	1.554e-09	1.370e-09	-8.809	-8.863	-0.055	(0)
MgPO4-	3.447e-10	3.039e-10	-9.463	-9.517	-0.055	(0)
N(-3)	5.002e-06					
NH4+	4.972e-06	4.361e-06	-5.303	-5.360	-0.057	(0)
NH4SO4-	2.163e-08	1.903e-08	-7.665	-7.721	-0.056	(0)
NH3	8.331e-09	8.331e-09	-8.079	-8.079	0.000	(0)
N(3)	2.144e-07					
NO2-	2.144e-07	1.880e-07	-6.669	-6.726	-0.057	(0)
N(5)	2.144e-05					
NO3-	2.144e-05	1.868e-05	-4.669	-4.729	-0.060	(0)
Na	3.531e-03					
Na+	3.512e-03	3.085e-03	-2.454	-2.511	-0.056	(0)
NaHCO3	1.361e-05	1.367e-05	-4.866	-4.864	0.002	(0)
NaSO4-	5.399e-06	4.759e-06	-5.268	-5.322	-0.055	(0)
NaCO3-	7.747e-08	6.830e-08	-7.111	-7.166	-0.055	(0)
NaHPO4-	1.749e-10	1.542e-10	-9.757	-9.812	-0.055	(0)
O(0)	9.228e-06					
O2	4.614e-06	4.634e-06	-5.336	-5.334	0.002	(0)
P	1.293e-07					
H2PO4-	5.216e-08	4.598e-08	-7.283	-7.337	-0.055	(0)
HPO4-2	4.276e-08	2.563e-08	-7.369	-7.591	-0.222	(0)
MgHPO4	1.744e-08	1.752e-08	-7.758	-7.757	0.002	(0)
CaHPO4	1.323e-08	1.328e-08	-7.879	-7.877	0.002	(0)
MgH2PO4+	1.554e-09	1.370e-09	-8.809	-8.863	-0.055	(0)
CaH2PO4+	1.251e-09	1.103e-09	-8.903	-8.958	-0.055	(0)
MgPO4-	3.447e-10	3.039e-10	-9.463	-9.517	-0.055	(0)
CaPO4-	2.620e-10	2.310e-10	-9.582	-9.636	-0.055	(0)
NaHPO4-	1.749e-10	1.542e-10	-9.757	-9.812	-0.055	(0)
FeHPO4	6.864e-11	6.893e-11	-10.163	-10.162	0.002	(0)
FeH2PO4+	1.766e-11	1.557e-11	-10.753	-10.808	-0.055	(0)
KHPO4-	4.001e-12	3.527e-12	-11.398	-11.453	-0.055	(0)
PO4-3	2.639e-13	8.348e-14	-12.578	-13.078	-0.500	(0)
S(-2)	3.122e-06					
H2S	1.733e-06	1.740e-06	-5.761	-5.759	0.002	(0)
HS-	1.359e-06	1.187e-06	-5.867	-5.925	-0.059	(0)
S6-2	2.244e-09	1.526e-09	-8.649	-8.816	-0.167	(0)
S5-2	2.000e-09	1.330e-09	-8.699	-8.876	-0.177	(0)
S4-2	1.156e-09	7.499e-10	-8.937	-9.125	-0.188	(0)
Fe(HS)2	8.449e-10	8.486e-10	-9.073	-9.071	0.002	(0)
S-2	8.298e-13	4.975e-13	-12.081	-12.303	-0.222	(0)

S3-2	3.947e-13	2.489e-13	-12.404	-12.604	-0.200	(0)
Fe(HS)3-	1.251e-13	1.097e-13	-12.903	-12.960	-0.057	(0)
S2-2	2.106e-14	1.297e-14	-13.677	-13.887	-0.211	(0)
S(6)	7.103e-04					
SO4-2	5.660e-04	3.387e-04	-3.247	-3.470	-0.223	(0)
CaSO4	7.326e-05	7.357e-05	-4.135	-4.133	0.002	(0)
MgSO4	6.550e-05	6.578e-05	-4.184	-4.182	0.002	(0)
NaSO4-	5.399e-06	4.759e-06	-5.268	-5.322	-0.055	(0)
KSO4-	1.464e-07	1.290e-07	-6.835	-6.889	-0.055	(0)
FeSO4	3.073e-08	3.086e-08	-7.512	-7.511	0.002	(0)
NH4SO4-	2.163e-08	1.903e-08	-7.665	-7.721	-0.056	(0)
HSO4-	2.860e-09	2.511e-09	-8.544	-8.600	-0.057	(0)
CaHSO4+	4.315e-11	3.785e-11	-10.365	-10.422	-0.057	(0)
FeHSO4+	2.325e-14	2.039e-14	-13.634	-13.691	-0.057	(0)

----------------------------Saturation indices----------------------------

Phase	SI** log	IAP	log K(283 K, 1 atm)	
Anhydrite	-2.04	-6.37	-4.34	CaSO4
Aragonite	-0.24	-8.50	-8.26	CaCO3
Artinite	-8.11	2.56	10.67	MgCO3:Mg(OH)2:3H2O
Brucite	-6.78	11.07	17.85	Mg(OH)2
Calcite	-0.08	-8.50	-8.41	CaCO3
CH4(g)	-3.64	-6.38	-2.73	CH4
CO2(g)	-1.36	-2.64	-1.28	CO2
Dolomite	-0.26	-17.00	-16.74	CaMg(CO3)2
Dolomite(d)	-0.87	-17.00	-16.13	CaMg(CO3)2
Epsomite	-4.14	-6.38	-2.24	MgSO4:7H2O
FeS(ppt)	-1.19	-5.11	-3.92	FeS
Gypsum	-1.78	-6.37	-4.59	CaSO4:2H2O
H2(g)	-5.52	-8.60	-3.08	H2
H2O(g)	-1.90	-0.00	1.90	H2O
H2S(g)	-4.93	-5.76	-0.83	H2S
Halite	-6.36	-4.81	1.55	NaCl
Huntite	-5.00	-34.01	-29.01	CaMg3(CO3)4
Hydromagnesite	-16.14	-22.96	-6.82	Mg5(CO3)4(OH)2:4H2O
Hydroxyapatite	-7.25	-9.32	-2.08	Ca5(PO4)3OH
Mackinawite	-0.46	-5.11	-4.65	FeS
Magnesite	-0.71	-8.51	-7.80	MgCO3
Melanterite	-7.24	-9.64	-2.40	FeSO4:7H2O
Mirabilite	-6.67	-8.49	-1.82	Na2SO4:10H2O
Nahcolite	-3.93	-4.61	-0.69	NaHCO3
Natron	-8.72	-10.62	-1.90	Na2CO3:10H2O
Nesquehonite	-3.10	-8.51	-5.41	MgCO3:3H2O
NH3(g)	-10.15	-8.08	2.07	NH3

O2(g)	-2.56	-5.33	-2.77	O2
Portlandite	-12.87	11.08	23.95	Ca(OH)2
Pyrite	28.84	9.94	-18.90	FeS2
Siderite	-0.97	-11.76	-10.80	FeCO3
Siderite(d)(3)	-1.31	-11.76	-10.45	FeCO3
Sulfur	17.00	1.68	-15.32	S
Thenardite	-8.33	-8.49	-0.16	Na2SO4
Thermonatrite	-10.84	-10.62	0.23	Na2CO3:H2O
Trona	-15.10	-15.23	-0.13	NaHCO3:Na2CO3:2H2O
Vivianite	-8.67	-44.67	-36.00	Fe3(PO4)2:8H2O

**For a gas, SI = log10(fugacity). Fugacity = pressure * phi / 1 atm.

 For ideal gases, phi = 1.

End of simulation.

Reading input data for simulation 3.

End of Run after 0.225 Seconds.

Input file: C:\Users\madeline.salo\Desktop\WK13 12_22_18
Output file: C:\Users\madeline.salo\Desktop\WK13 12_22_18.pqo
Database file: C:\Program Files (x86)\USGS\Phreeqc Interactive 3.4.0-
12927\database\wateq4f.dat

Reading data base.

        SOLUTION_MASTER_SPECIES
        SOLUTION_SPECIES
        PHASES
        EXCHANGE_MASTER_SPECIES
        EXCHANGE_SPECIES
        SURFACE_MASTER_SPECIES
        SURFACE_SPECIES
        RATES
        END

Reading input data for simulation 1.

        DATABASE C:\Program Files (x86)\USGS\Phreeqc Interactive 3.4.0-
12927\database\wateq4f.dat
        SOLUTION_MASTER_SPECIES
          Acetate   Acetate-   1.0   Acetate   59.
        SOLUTION_SPECIES
        Acetate- = Acetate-
           log_k 0.0
             analytical_expression   -0.96597E+02   -0.34535E-01   0.19753E+04
0.38593E+02   0.30850E+02
        Acetate- + H+ = AcetateH
           log_k   4.76
           delta_h   116.1 kcal/mol   #from llnl.dat
        END

End of simulation.

Reading input data for simulation 2.

        SOLUTION 1 #WK11 collected on 6/29/17 through 1/26/18
          Temp   10.5
          pH   7.06
          pe
          redox   pe

```
        units       mg/L
        density     1
        Ca          83.71
        Mg          56.71
        Na          39.79
        K           2.56
        Fe(+2)      0.1
        Alkalinity  411.26
        Cl          97.24
        S(6)        96.9
        S(-2)       0.1
        N(5)        1.74
        N(3)        0.04
        N(-3)       0.03
        P           0.003
        H(0)        0.004 umol/L
        O(0)        0.14375
        C(-4)       0.043 umol/L
        Acetate     1.59
        water       1 # kg
    END
-------------------------------------------------
Beginning of initial solution calculations.
-------------------------------------------------

Initial solution 1.

----------------------------Solution composition----------------------------

        Elements    Molality        Moles

        Acetate     2.697e-05       2.697e-05
        Alkalinity  8.223e-03       8.223e-03
        C(-4)       4.303e-08       4.303e-08
        Ca          2.090e-03       2.090e-03
        Cl          2.745e-03       2.745e-03
        Fe(2)       1.792e-06       1.792e-06
        H(0)        4.003e-09       4.003e-09
        K           6.552e-05       6.552e-05
        Mg          2.334e-03       2.334e-03
        N(-3)       2.144e-06       2.144e-06
        N(3)        2.858e-06       2.858e-06
        N(5)        1.243e-04       1.243e-04
        Na          1.732e-03       1.732e-03
        O(0)        8.991e-06       8.991e-06
        P           9.693e-08       9.693e-08
```

```
S(-2)           3.121e-06      3.121e-06
S(6)            1.010e-03      1.010e-03
```

----------------------------Description of solution--------------------------

$$
\begin{aligned}
\text{pH} &= 7.060 \\
\text{pe} &= 7.060 \\
\text{Activity of water} &= 1.000 \\
\text{Ionic strength (mol/kgw)} &= 1.606\text{e-}02 \\
\text{Mass of water (kg)} &= 1.000\text{e+}00 \\
\text{Total carbon (mol/kg)} &= 9.947\text{e-}03 \\
\text{Total CO2 (mol/kg)} &= 9.947\text{e-}03 \\
\text{Temperature (}\infty\text{C)} &= 10.50 \\
\text{Electrical balance (eq)} &= -2.462\text{e-}03 \\
\text{Percent error, } 100*(\text{Cat-}|\text{An}|)/(\text{Cat+}|\text{An}|) &= -10.95 \\
\text{Iterations} &= 10 \\
\text{Total H} &= 1.110206\text{e+}02 \\
\text{Total O} &= 5.553872\text{e+}01
\end{aligned}
$$

-------------------------------Redox couples-------------------------------

Redox couple	pe	Eh (volts)
C(-4)/C(4)	-3.1812	-0.1790
H(0)/H(1)	-4.2535	-0.2394
N(-3)/N(3)	6.5875	0.3707
N(-3)/N(5)	7.1564	0.4028
N(3)/N(5)	8.8629	0.4988
O(-2)/O(0)	14.3863	0.8096
S(-2)/S(6)	-3.1274	-0.1760

--------------------------Distribution of species--------------------------

Species	Molality	Activity	Log Molality	Log Activity	Log Gamma	mole V cm≥/mol
H+	9.683e-08	8.710e-08	-7.014	-7.060	-0.046	0.00
OH-	3.985e-08	3.510e-08	-7.400	-7.455	-0.055	(0)
H2O	5.551e+01	9.997e-01	1.744	-0.000	0.000	18.02
Acetate	2.697e-05					
Acetate-	2.697e-05	2.384e-05	-4.569	-4.623	-0.054	(0)
AcetateH	5.314e-12	5.334e-12	-11.275	-11.273	0.002	(0)
C(-4)	4.303e-08					
CH4	4.303e-08	4.319e-08	-7.366	-7.365	0.002	(0)
C(4)	9.947e-03					
HCO3-	7.959e-03	7.067e-03	-2.099	-2.151	-0.052	(0)

CO2	1.763e-03	1.770e-03	-2.754	-2.752	0.002	(0)
MgHCO3+	1.189e-04	1.050e-04	-3.925	-3.979	-0.054	(0)
CaHCO3+	8.816e-05	7.847e-05	-4.055	-4.105	-0.051	(0)
NaHCO3	6.036e-06	6.058e-06	-5.219	-5.218	0.002	(0)
CO3-2	4.306e-06	2.677e-06	-5.366	-5.572	-0.206	(0)
CaCO3	4.299e-06	4.315e-06	-5.367	-5.365	0.002	(0)
MgCO3	2.695e-06	2.705e-06	-5.569	-5.568	0.002	(0)
FeHCO3+	5.663e-07	5.005e-07	-6.247	-6.301	-0.054	(0)
FeCO3	4.531e-08	4.548e-08	-7.344	-7.342	0.002	(0)
NaCO3-	3.967e-08	3.522e-08	-7.402	-7.453	-0.052	(0)

Ca   2.090e-03

Ca+2	1.897e-03	1.179e-03	-2.722	-2.929	-0.207	(0)
CaSO4	1.005e-04	1.009e-04	-3.998	-3.996	0.002	(0)
CaHCO3+	8.816e-05	7.847e-05	-4.055	-4.105	-0.051	(0)
CaCO3	4.299e-06	4.315e-06	-5.367	-5.365	0.002	(0)
CaHPO4	1.002e-08	1.005e-08	-7.999	-7.998	0.002	(0)
CaOH+	2.523e-09	2.246e-09	-8.598	-8.649	-0.051	(0)
CaH2PO4+	8.003e-10	7.106e-10	-9.097	-9.148	-0.052	(0)
CaPO4-	2.307e-10	2.049e-10	-9.637	-9.689	-0.052	(0)
CaHSO4+	4.992e-11	4.412e-11	-10.302	-10.355	-0.054	(0)

Cl   2.745e-03

Cl-	2.745e-03	2.419e-03	-2.561	-2.616	-0.055	(0)
FeCl+	2.668e-09	2.365e-09	-8.574	-8.626	-0.052	(0)

Fe(2)   1.792e-06

Fe+2	1.129e-06	7.083e-07	-5.947	-6.150	-0.202	(0)
FeHCO3+	5.663e-07	5.005e-07	-6.247	-6.301	-0.054	(0)
FeSO4	4.696e-08	4.713e-08	-7.328	-7.327	0.002	(0)
FeCO3	4.531e-08	4.548e-08	-7.344	-7.342	0.002	(0)
FeCl+	2.668e-09	2.365e-09	-8.574	-8.626	-0.052	(0)
Fe(HS)2	1.053e-09	1.057e-09	-8.978	-8.976	0.002	(0)
FeOH+	9.285e-10	8.231e-10	-9.032	-9.085	-0.052	(0)
FeHPO4	5.808e-11	5.830e-11	-10.236	-10.234	0.002	(0)
FeH2PO4+	1.263e-11	1.121e-11	-10.899	-10.950	-0.052	(0)
Fe(HS)3-	1.684e-13	1.489e-13	-12.774	-12.827	-0.054	(0)
FeHSO4+	2.999e-14	2.651e-14	-13.523	-13.577	-0.054	(0)
Fe(OH)2	2.128e-14	2.136e-14	-13.672	-13.670	0.002	(0)
Fe(OH)3-	8.847e-18	7.842e-18	-17.053	-17.106	-0.052	(0)

H(0)   4.003e-09

H2	2.002e-09	2.009e-09	-8.699	-8.697	0.002	(0)

K   6.552e-05

K+	6.535e-05	5.759e-05	-4.185	-4.240	-0.055	(0)
KSO4-	1.727e-07	1.533e-07	-6.763	-6.814	-0.052	(0)
KHPO4-	2.614e-12	2.321e-12	-11.583	-11.634	-0.052	(0)

Mg   2.334e-03

Mg+2	2.110e-03	1.323e-03	-2.676	-2.878	-0.203	(0)
MgHCO3+	1.189e-04	1.050e-04	-3.925	-3.979	-0.054	(0)

MgSO4	1.032e-04	1.036e-04	-3.986	-3.985	0.002	(0)
MgCO3	2.695e-06	2.705e-06	-5.569	-5.568	0.002	(0)
MgOH+	1.562e-08	1.392e-08	-7.806	-7.856	-0.050	(0)
MgHPO4	1.520e-08	1.526e-08	-7.818	-7.817	0.002	(0)
MgH2PO4+	1.144e-09	1.016e-09	-8.942	-8.993	-0.052	(0)
MgPO4-	3.494e-10	3.102e-10	-9.457	-9.508	-0.052	(0)
N(-3)	2.144e-06					
NH4+	2.126e-06	1.879e-06	-5.672	-5.726	-0.054	(0)
NH4SO4-	1.350e-08	1.197e-08	-7.870	-7.922	-0.052	(0)
NH3	4.181e-09	4.181e-09	-8.379	-8.379	0.000	(0)
N(3)	2.858e-06					
NO2-	2.858e-06	2.526e-06	-5.544	-5.598	-0.054	(0)
N(5)	1.243e-04					
NO3-	1.243e-04	1.092e-04	-3.905	-3.962	-0.056	(0)
Na	1.732e-03					
Na+	1.722e-03	1.524e-03	-2.764	-2.817	-0.053	(0)
NaHCO3	6.036e-06	6.058e-06	-5.219	-5.218	0.002	(0)
NaSO4-	3.862e-06	3.430e-06	-5.413	-5.465	-0.052	(0)
NaCO3-	3.967e-08	3.522e-08	-7.402	-7.453	-0.052	(0)
NaHPO4-	6.921e-11	6.145e-11	-10.160	-10.211	-0.052	(0)
O(0)	8.991e-06					
O2	4.496e-06	4.512e-06	-5.347	-5.346	0.002	(0)
P	9.693e-08					
H2PO4-	3.558e-08	3.159e-08	-7.449	-7.500	-0.052	(0)
HPO4-2	3.348e-08	2.067e-08	-7.475	-7.685	-0.209	(0)
MgHPO4	1.520e-08	1.526e-08	-7.818	-7.817	0.002	(0)
CaHPO4	1.002e-08	1.005e-08	-7.999	-7.998	0.002	(0)
MgH2PO4+	1.144e-09	1.016e-09	-8.942	-8.993	-0.052	(0)
CaH2PO4+	8.003e-10	7.106e-10	-9.097	-9.148	-0.052	(0)
MgPO4-	3.494e-10	3.102e-10	-9.457	-9.508	-0.052	(0)
CaPO4-	2.307e-10	2.049e-10	-9.637	-9.689	-0.052	(0)
NaHPO4-	6.921e-11	6.145e-11	-10.160	-10.211	-0.052	(0)
FeHPO4	5.808e-11	5.830e-11	-10.236	-10.234	0.002	(0)
FeH2PO4+	1.263e-11	1.121e-11	-10.899	-10.950	-0.052	(0)
KHPO4-	2.614e-12	2.321e-12	-11.583	-11.634	-0.052	(0)
PO4-3	2.334e-13	7.892e-14	-12.632	-13.103	-0.471	(0)
S(-2)	3.121e-06					
H2S	1.615e-06	1.621e-06	-5.792	-5.790	0.002	(0)
HS-	1.469e-06	1.294e-06	-5.833	-5.888	-0.055	(0)
S6-2	2.824e-09	1.954e-09	-8.549	-8.709	-0.160	(0)
S5-2	2.496e-09	1.692e-09	-8.603	-8.772	-0.169	(0)
S4-2	1.439e-09	9.537e-10	-8.842	-9.021	-0.179	(0)
Fe(HS)2	1.053e-09	1.057e-09	-8.978	-8.976	0.002	(0)
S-2	1.023e-12	6.316e-13	-11.990	-12.200	-0.209	(0)
S3-2	4.897e-13	3.164e-13	-12.310	-12.500	-0.190	(0)
Fe(HS)3-	1.684e-13	1.489e-13	-12.774	-12.827	-0.054	(0)

163

S2-2	2.605e-14	1.647e-14	-13.584	-13.783	-0.199	(0)
S(6)	1.010e-03					
SO4-2	8.017e-04	4.944e-04	-3.096	-3.306	-0.210	(0)
MgSO4	1.032e-04	1.036e-04	-3.986	-3.985	0.002	(0)
CaSO4	1.005e-04	1.009e-04	-3.998	-3.996	0.002	(0)
NaSO4-	3.862e-06	3.430e-06	-5.413	-5.465	-0.052	(0)
KSO4-	1.727e-07	1.533e-07	-6.763	-6.814	-0.052	(0)
FeSO4	4.696e-08	4.713e-08	-7.328	-7.327	0.002	(0)
NH4SO4-	1.350e-08	1.197e-08	-7.870	-7.922	-0.052	(0)
HSO4-	3.519e-09	3.113e-09	-8.454	-8.507	-0.053	(0)
CaHSO4+	4.992e-11	4.412e-11	-10.302	-10.355	-0.054	(0)
FeHSO4+	2.999e-14	2.651e-14	-13.523	-13.577	-0.054	(0)

-----------------------------Saturation indices-----------------------------

Phase	SI** log	IAP	log K(283 K, 1 atm)	
Anhydrite	-1.90	-6.23	-4.34	CaSO4
Aragonite	-0.24	-8.50	-8.26	CaCO3
Artinite	-7.89	2.79	10.68	MgCO3:Mg(OH)2:3H2O
Brucite	-6.61	11.24	17.86	Mg(OH)2
Calcite	-0.09	-8.50	-8.41	CaCO3
CH4(g)	-4.63	-7.36	-2.73	CH4
CO2(g)	-1.48	-2.75	-1.28	CO2
Dolomite	-0.22	-16.95	-16.74	CaMg(CO3)2
Dolomite(d)	-0.83	-16.95	-16.12	CaMg(CO3)2
Epsomite	-3.94	-6.19	-2.25	MgSO4:7H2O
FeS(ppt)	-1.06	-4.98	-3.92	FeS
Gypsum	-1.64	-6.23	-4.59	CaSO4:2H2O
H2(g)	-5.61	-8.70	-3.08	H2
H2O(g)	-1.90	-0.00	1.90	H2O
H2S(g)	-4.96	-5.79	-0.83	H2S
Halite	-6.98	-5.43	1.55	NaCl
Huntite	-4.85	-33.85	-29.00	CaMg3(CO3)4
Hydromagnesite	-15.76	-22.56	-6.80	Mg5(CO3)4(OH)2:4H2O
Hydroxyapatite	-7.39	-9.46	-2.07	Ca5(PO4)3OH
Mackinawite	-0.33	-4.98	-4.65	FeS
Magnesite	-0.65	-8.45	-7.80	MgCO3
Melanterite	-7.05	-9.46	-2.40	FeSO4:7H2O
Mirabilite	-7.12	-8.94	-1.83	Na2SO4:10H2O
Nahcolite	-4.28	-4.97	-0.69	NaHCO3
Natron	-9.31	-11.21	-1.90	Na2CO3:10H2O
Nesquehonite	-3.05	-8.45	-5.40	MgCO3:3H2O
NH3(g)	-10.45	-8.38	2.08	NH3
O2(g)	-2.57	-5.35	-2.77	O2
Portlandite	-12.77	11.19	23.96	Ca(OH)2

Pyrite	29.22	10.31	-18.90	FeS2
Siderite	-0.93	-11.72	-10.80	FeCO3
Siderite(d)(3)	-1.27	-11.72	-10.45	FeCO3
Sulfur	17.24	1.92	-15.32	S
Thenardite	-8.78	-8.94	-0.16	Na2SO4
Thermonatrite	-11.44	-11.21	0.23	Na2CO3:H2O
Trona	-16.05	-16.17	-0.12	NaHCO3:Na2CO3:2H2O
Vivianite	-8.66	-44.66	-36.00	Fe3(PO4)2:8H2O

**For a gas, SI = log10(fugacity). Fugacity = pressure * phi / 1 atm.

  For ideal gases, phi = 1.

End of simulation.

Reading input data for simulation 3.

End of Run after 0.23 Seconds.